

Facile and Universal Synthesis of Polyrotaxane Based Stimuli Sensitive Sliding Polymer Gels and Their Characterizations

Abu Bin Imran

Facile and Universal Synthesis of Polyrotaxane Based Stimuli Sensitive Sliding Polymer Gels and Their Characterizations

A Dissertation Submitted to Nagoya University for the Partial Fulfillment of the Requirements of the Degree of Doctor of Engineering in the Department of Molecular Design and Engineering

Abu Bin Imran
Department of Molecular Design and Engineering
Graduate School of Engineering
Nagoya University, Nagoya, Japan

March, 2009

To
My elder brother (Dadabhai)
Dr. Md. Abu Bin Hasan Susan

Acknowledgement

My very sincere thanks first goes to Almighty Allah, who has generously gifted me the ability to conduct the research work and knowledge to understand Chemistry for writing this dissertation.

I would like to express my sincere gratitude and appreciation to my academic supervisor Professor **Yukikazu Takeoka**, Department of Molecular Design and Engineering, Graduate School of Engineering, Nagoya University, Nagoya, for his friendly co-operation, meticulous attention, productive suggestions and continual guidance during the course of this work. I gratefully acknowledge his assiduous effort, perseverance, enthusiasm and kindness to continue this work without which the present achievement might not have been materialized. I am fortunate enough to have been influenced by his approach to research, which embodies all the best of collegiality and the true spirit of scientific endeavor. I would next like to express my cordial thanks to Professor **Takahiro Seki**, Department of Molecular Design and Engineering, Graduate School of Engineering, Nagoya University, Nagoya, for his valuable comments, constructive criticisms and noteworthy inspiration during the course of experiments which helped to resolve many critical points related to this work. I am also indebted to Assistant Professor **Shusaku Nagano**, Department of Molecular Design and Engineering, Graduate School of Engineering, Nagoya University, Nagoya, for his very helpful co-operation not only in my research work but also any type of problems which I faced in daily life.

I would like to extend my very sincere appreciation to Professor **Kohzo Ito**, and Assistant Professor **Masatoshi Kidowaki** of Department of Advanced Materials Science, Graduate School of Frontier Sciences, the University of Tokyo, Kashiwa, Japan, for allowing me to use the resources of the Ito laboratory for my research work. I passed very nice time there with excellent research facilities and hospitality. I will remain grateful to former student of Ito Laboratory **Dr. Toshiyuki Kataoka** for his valuable instructions during various measurements.

I express my gratitude to former students of Seki laboratory **Mr. Shuichi Shinohara, Ms. Harumi Murayama, Mr. Akiyuki Ueda and Mr. Masaki Honda** for their very initial co-operation during the course of the work. I am indebted to all of my former and present lab mates for their amazing complaisance and co-operation not only in my research work, but also to the every span of my life in Japan. They have tied me for ever in life with unforgettable sweet memories. I do not have the courage to further mention some by names for the fear of perplexing omission.

Cordial thanks to all of my well-wishers for their amicable co-operation and incentive.

Finally, a standing ovation is due to all my family members for their continuous support and encouragement.

(Abu Bin Imran)

Contents

Chapter 1

General Introduction

1.1. Polymer gel.....	2
<i>1.1.1. Definition</i>	
<i>1.1.2. Classification of gels</i>	
<i>1.1.2.1. Physical gel</i>	
<i>1.1.2.2. Chemical gel</i>	
1.2. Stimuli responsive polymer gel.....	4
<i>1.2.1. Thermo- and pH-sensitive polymers and gels</i>	
1.3. Volume phase transition of polymer gel	8
1.4. Polyrotaxane.....	9
1.5. Some well known polymer gels exhibiting higher mechanical strength.....	12
<i>1.5.1. Double network gel</i>	
<i>1.5.2. Nanocomposite gel</i>	
<i>1.5.3. Slide ring gel</i>	
1.6. Application of polymer gels.....	17
1.7. Objectives of this study.....	17
1.8. Present work.....	18
References.....	19

Chapter 2

Preparation of soft and mechanically improved hydrogels using a vinyl modified polyrotaxane as a Cross-linker

Abstract.....	25
2.1. Introduction.....	27
2.2. Experimental.....	30
2.2.1. Materials	
2.2.2. Preparation of hydrophobic polyrotaxane cross-linker, MPR	
2.2.3. Preparation of hydrophobic polyrotaxane based rotaxane-NIPA, $R_{wi}N$ gels	
2.2.4. Preparation of typical NIPA, TNx gels	
2.2.5. Mechanical strength test	
2.2.6. Swelling ratio measurement	
2.2.7. Scanning Electron Microscope (SEM)	
2.3. Results and Discussion.....	37
2.3.1. Preparation and characterizations of hydrophobic polyrotaxane cross-linker, MPR	
2.3.2. Transmission spectra of gels	
2.3.3. Swelling behaviors of gels in DMSO and water	
2.3.4. Effect of 0.1M NaOH on the swelling ratio $R_{wi}N3$ gel	
2.3.5. Sampling for the measurements of shrinking kinetics and rheological studies	
2.3.6. Morphological changes of $R_{wi}N$ and TN hydrogels after a temperature jump	
2.3.7. Shrinking kinetics of $R_{wi}N$ and TN gels after a temperature jump	

2.3.8. Rheological studies of $R_{wi}N$ and TN gels	
2.4. Conclusion.....	58
References.....	59
Chapter 3	
Anomalous shrinking and swelling behavior of poly(NIPA) gels prepared by hydrophilic polyrotaxane based movable cross-linkers	
Abstract.....	65
3.1. Introduction.....	67
3.2. Experimental	70
3.2.1. Materials	
3.2.2. Preparation of MPR and MHPR	
3.2.3. Preparation of Rotaxane-NIPA, RN gel	
3.2.4. Preparation of typical poly(NIPA), TN gel	
3.2.5. 1H -NMR spectra	
3.2.6. Setup for shrinking and swelling kinetics	
3.2.7. Transmittance spectra of gels	
3.2.8. Thermo Gravimetric / Differential Thermal Analysis, TG/DTA	
3.2.9. Scanning Electron Microscope, SEM	
3.2.10. Rheometric Solids Analyzer, RSA	
3.3. Results and Discussion.....	79
3.3.1. Preparations and characterizations of polyrotaxane cross-linkers and their gels	
3.3.2. Transparency tests of RN gels	

3.3.3. Swelling behaviors of RN gels	
3.3.4. Morphological changes of hydrogels after a temperature jump	
3.3.5. Shrinking kinetics of RN gels	
3.3.6. Mechanical properties	
3.3.7. Kinetics of swelling	
3.3.8. Thermo Gravimetric / Differential Thermal Analysis (TG /DTA)	
3.4. Conclusion.....	102
References.....	105
 Chapter 4	
Synthesis of super absorbent and highly elastic novel polyelectrolyte gel using polyrotaxane based cross-linker	
Abstract.....	111
4.1. Introduction.....	113
4.2. Experimental.....	115
4.2.1. Materials	
4.2.2. Preparation of Rotaxane-NIPA-Sodium acrylate, $R_{ws}N$ -S gels	
4.2.3. Preparation of BIS- NIPA-Sodium acrylate, TN-S gels	
4.2.4. Preparation of polyelectrolyte buffer solutions	
4.2.5. Measurements of swelling ratio	
4.2.6. Gel Permeation Chromatography, GPC	
4.2.7. Thermo Gravimetric / Differential Thermal Analysis, TG/DTA	
4.2.8. Scanning Electron Microscope (SEM)	
4.2.9. Mechanical Strength tests	

4.3. Results and Discussion.....	123
4.3.1. Preparation of water soluble polyrotaxane cross-linker, MHPR	
4.3.2. Effect of salt on the swelling behaviors of ionic gels	
4.3.3. Swelling behavior at pH 5.5	
4.3.4. Swelling behavior at pH 9.5	
4.3.5. Shrinking Kinetics of TN-S and $R_{ws}N$ -S gel at pH 5.5	
4.3.6. Super absorbency of $R_{ws}N$ -S gels	
4.3.7. TG/DTA analysis of $R_{ws}N$ -S gel	
4.3.8. SEM	
4.3.9. Mechanical properties of polyelectrolyte gels	
4.4. Scopes and future prospects of $R_{ws}N$-S gel.....	149
4.5. Conclusion.....	151
References.....	153

Chapter 5

Appendix: Chromic Slide-Ring Gel Based on Reflection from Photonic Bandgap

Abstract.....	157
5.1. Introduction.....	159
5.2. Experimental Section.....	162
5.2.1. Materials	
5.2.2. Preparation of a Colloidal Crystal	
5.2.3. Preparation of Gels	
5.2.4. Sample Characterizations	

5.3. Results and Discussion.....	170
5.3.1. <i>Preparation of Slide-Ring Gels</i>	
5.3.2. <i>Properties of Slide-Ring Gels. Rheometric Analysis</i>	
5.3.3. <i>Equilibrium Swelling Degree of Slide-Ring Gel</i>	
5.3.4. <i>Kinetics of Swelling Degree of Slide-Ring Gel</i>	
5.3.5. <i>Properties of Colloidal Crystal</i>	
5.3.6. <i>Properties of Structural Colored Slide-Ring Gel</i>	
5.4. Conclusion.....	182
References	183
 Chapter 6	
 General Conclusions and Outlook	
<i>General Conclusions and Outlook</i>	185
List of publications.....	191
List of attended conferences.....	193

CHAPTER

1

General Introduction

1.1. Polymer gel

1.1.1. Definition

A polymer gel consists of an cross-linked polymer network with a fluid filling the interstitial space of the network but insoluble in any solvents. Gels swollen in solvents have unique properties in that they show both liquid-like and solid-like behavior. This is in contrast with most industrial materials, such as metals, ceramics, and plastics, which are dry and hard. Living organisms are highly aqueous gel materials that are largely composed of protein and polysaccharide networks in which the water contents range up to 90% (blood plasma). This makes it easier for the organism to effectively transport ions and molecules while keeping its solidity.

1.1.2. Classification of gels

There are a variety of ways to classify gels, such as according to the source: natural gel, synthetic gel, and hybrid gel; according to the liquid medium in the polymer network: hydrogel , liogel, xerogel, aerogel, organogel etc; and according to their cross-linkage: chemical gel or physical gel.

1.1.2.1. Physical gel

Physical gels are formed by the non-covalent cross-linked among the polymer chains. When the polymer networks held together by molecular entanglements, or secondary forces including ionic interaction, van der waals forces, H-bonding or hydrophobic forces are called physical gel.^{1,2} These gels are not homogeneous in nature, since clusters of molecular entanglements, or hydrophobically- or ionically-associated domains create inhomogeneities in the gel network. A network structure that uses secondary forces is easy to create, but it generally lacks stability due to sol-gel transitions caused by changing temperature, ionic strength, or pH etc.

1.1.2.2. Chemical gel

In the chemical gels polymer chains are cross-linked chemically by fixed covalent bonds. The gels may be generated by cross-linking of water-soluble polymers, or by conversion of hydrophobic polymers to hydrophilic polymers plus cross-linking to form a gel network. A first approach to gel synthesis uses additive polymerization. For example, in the free radical polymerization, the double bond of a vinyl monomer may react with other to form linear polymer chains. However, if a small fraction of a di-vinyl derivative is added to the mixture, the two double bonds will participate in the construction of two distinct chains, and will form a cross-linking bridge in the structure. A second method of gel preparation is based on the condensation of polyfunctional units. A typical example would be the condensation reaction between a triol and diisocyanate. Due to the presence of fixed covalent bonds among the polymer chains, chemical gel always exhibits poor mechanical strength.

1.2. Stimuli responsive polymer gel

Polymers that can change their properties or structures in response to environmental stimuli are called stimuli-responsive polymers and the gels prepared from these polymers are called stimuli responsive polymer gels. Polymer and gels are found to respond in the effects of following stimuli. Such as temperature, pH, electric field, light, magnetic field, ionic strength, solvent composition, glucose, antigen, self oscillating gels etc. Some polymeric gels have a unique ability to undergo abrupt changes in their volume in response to environmental changes. This unique property is known as volume phase transition. After the innovation of volume phase transition in polymer gel, many researchers have focused on gels as stimuli-responsive materials. The fascinating properties of stimuli-responsive polymers and gels suggest that they have potential as suitable intelligent materials for mimicking biomolecules and smart

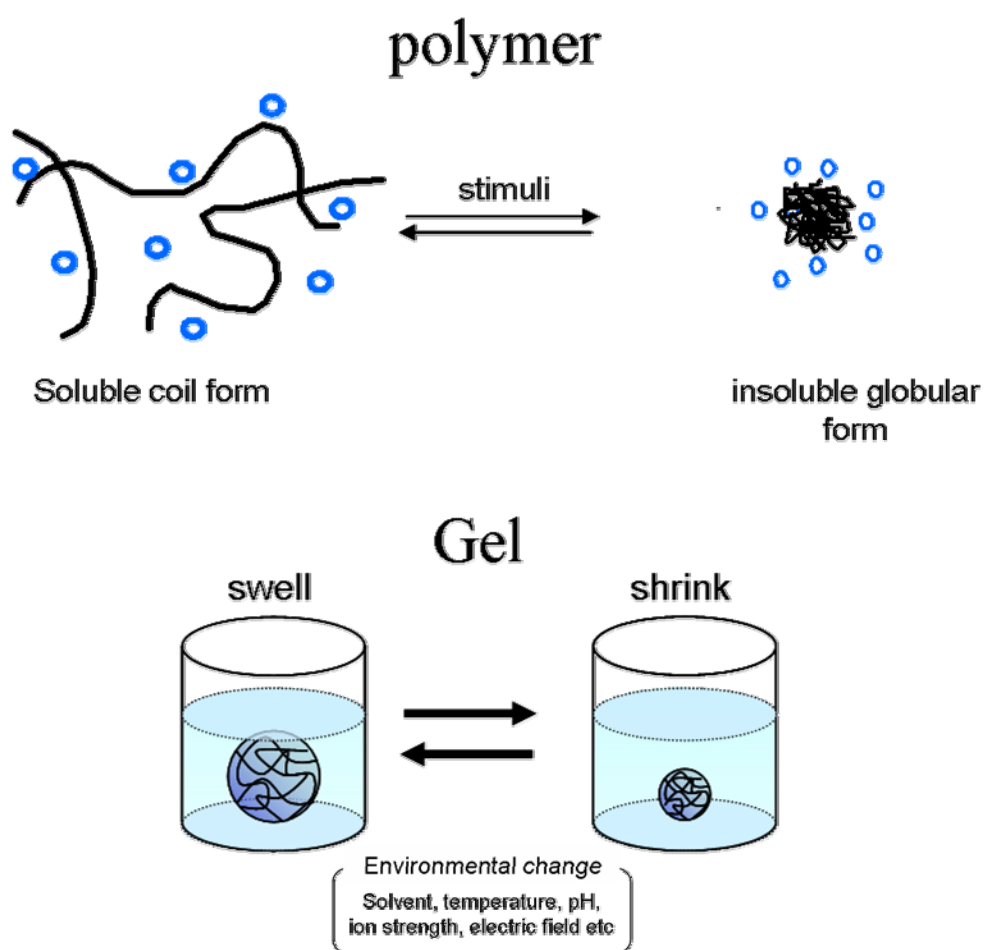


Figure 1.1. Schematic representation of stimuli-responsive polymer and their gel.

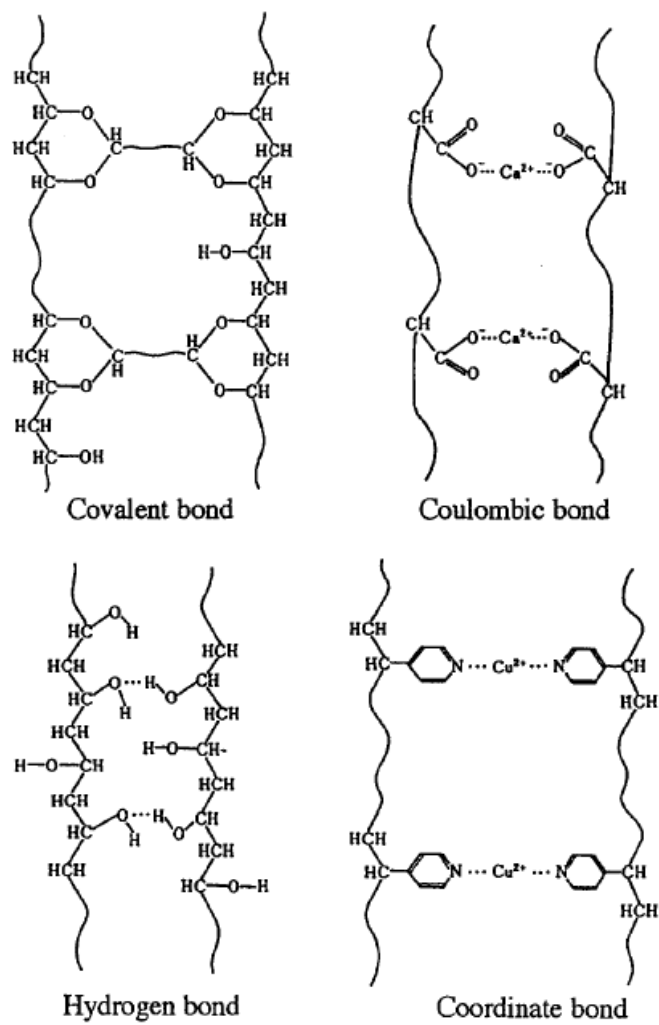


Figure 1.2. Schematic representation showing the chemical and physical cross-linking

systems in the bio-chemical and bio-medical fields. They have been used to construct switches, sensors, actuators, bio-reactors, separation systems, and drug delivery systems etc.

1.2.1. Thermo- and pH-sensitive polymers and gels

Most temperature responsive polymers and gels are based on poly(N-alkylacrylamide),³⁻⁵ poly(vinylmethylether),⁶ poly(ethyleneoxide)-poly(propyleneoxide)-poly(ethyleneoxide),⁷ and poly(N-vinylisobutylamide).⁸ Thermosensitive polymer gels Poly(*N*-isopropylacrylamide) (PNIPA) is known for its novel thermal behavior in aqueous media.^{23, 24} The poly(*N*-isopropylacrylamide) (PNIPA) of a representative temperature-responsive polymer is very unique in that its solubility in water changes abruptly at a lower critical solution temperature(LCST). It is soluble in water at temperatures below LCST (about 32° C),but becomes insoluble above LCST due to strong intermolecular interaction between the hydrophobic groups. A PNIPA gel can be obtained by the addition of a cross-linking agent to the polymerization recipe. *N,N'*-Methylene-bisacrylamide (BIS) is the major choice for this component, which is probably a consequence of its structural similarity to PNIPA. Temperature-responsive polymers and gels containing PNIPA are currently of great interest in biochemical and biomedical fields.

Poly(vinyl methyl ether) (PVME) also has a LCST of about 37°C in aqueous media and is a thermo-sensitive polymer. Hirasa and co-workers prepared PVME gels using γ -ray irradiation methods and studied the thermo-mechanical response of PVME hydrogels in detail.^{25, 26} Irradiation with γ -rays of an aqueous PVME solution brings about gelation. The gel shows thermo-sensitivity similar to the solution.²⁷ Swelling occurs below 37 °C and shrinks above this temperature.

Polymers with ionizable groups are promising candidates as pH- responsive polymers. Since an environmental change in pH as a stimulus induces their conformational changes due to ionization of the polymer chains. Many studies on pH-responsive polymers and gels based on polymers with ionizable groups, such as carboxyl, sulfonic, and amino groups have been reported. Tanaka et al ⁹⁻¹⁰ found that ionized poly(acrylamide)(PAAm) gels undergo a discrete phase transition in equilibrium volume upon varying the salt concentration in the solution. The ionized PAAm gels were collapse in response to the varying pH. Hoffman et al ^{11,12} proposed a novel approach for preparation of pH-responsive polymers and gels by introducing temperature-responsive NIPA. Their gels were sensitive to both temperature and pH, and responded to the pH change to a much greater extent than normal gels with carboxyl groups, as they were composed of pH- responsive PAAc and temperature-responsive PNIPA. The studies by Peppas et. al. ⁹⁻¹⁰ also revealed that random copolymer or IPN gels of MAAC and NIPA showed sharp swelling transition with small changes in pH. Besides, Kim et al.^{13, 14.} also synthesized copolymer gels composed of PNIPA as the temperature-responsive component, (diethylamino)ethyl methacrylate as the pH-responsive component, and BMA as a hydrophobic component to improve the mechanical properties of the gels. The pH-responsive swelling behavior of the copolymer gels can be controlled by temperature because the ionization of pH-responsive components is influenced by temperature-responsive PNIPA.

1.3. Volume phase transition of polymer gel

The volume of a gel swollen in a solvent is strongly dependent upon its constituent polymer chains and cross-linking structure. Some gels are found to undergo drastic changes in volume in response to environmental changes such as solvent composition, temperature, pH, etc. Reversible and discontinuous volume

changes of gels are envisaged as volume phase transitions,^{15, 16-19} The balance of the repulsion and attraction forces of polymer chains in gels plays an important role in volume phase transition. When the repulsion between polymer chains is more dominant than the attraction, the gel swells. The strong attraction between polymer chains causes shrinking of the gel. Such repulsion and attraction between polymer chains are mainly generated from four fundamental molecular interactions: van der waals interaction, hydrophobic interaction, hydrogen bonding, and electrostatic interaction. Phase transitions in polymer gels were theoretically predicted on the basis of coil–globule transitions that were observed in solution by Dusek²⁰ and later experimentally confirmed by Tanaka.²¹ The equilibrium state of the gel can be expressed from the Flory–Huggins derivation:²²

$$\tau = 1 - \frac{\Delta F}{kT} = -\frac{v\nu}{N\phi^2} \left[(2f+1)\left(\frac{\phi}{\phi_0}\right) - 2\left(\frac{\phi}{\phi_0}\right)^{1/3} \right] + 1 + \frac{2}{\phi} + \frac{2\ln(1-\phi)}{\phi^2}$$

where τ is the reduced temperature; N is the Avogadro's number; k is the Boltzmann constant; T is the absolute temperature; v is the molar volume of the solvent; ϕ is the volume fraction of the polymer network; ΔF is the free-energy decrease associated with the formation of a contact between polymer segments; ϕ_0 is the network volume fraction at the condition that the constituent polymer chains have random configurations; ν is the number of constituent chains per unit volume at $\phi = \phi_0$; and f is the number of dissociated counter ions per effective polymer chain. Thus, the equilibrium network volume fraction is determined as a function of the reduced temperature.

1.4. Polyrotaxane

Supramolecules and their intriguing topological characteristics have attracted considerable interest.²⁸⁻³⁰ A typical example is that of rotaxanes, in which cyclic

molecules are threaded on a single polymer chain and trapped by capping the chain with bulky end groups.^{31–35} Ogino reported the first rotaxane using cyclodextrin (CD) as the ring molecule.³⁶ CDs are cyclic oligosaccharides consisting of six, seven, or eight glucose units with inner diameter of 0.44, 0.58, or 0.74 nm, respectively, that are called α -, β -, or γ -CDs respectively.^{28, 37, 38} As compared to other cyclic molecules, CDs are readily available in both high purities and large quantities and can be modified by various functional groups. The most important feature of CDs is their amphiphilic property: CDs have hydrophobic inside cavity and hydrophilic outside. Therefore, water-soluble CDs tend to include small hydrophobic molecules in their cavities, which is called the inclusion complex formation. Harada and Kamachi reported the first synthesis of pseudo-polyrotaxane in which many α -CD molecules are threaded on a single polymer chain of polyethylene glycol (PEG).³⁹ CDs mixed with PEG in water were threaded onto a PEG by self-assembly. Subsequently, both the ends of the pseudo-polyrotaxane were capped with bulky groups to form polyrotaxane.⁴⁰ In recent years, this novel architecture in supramolecular chemistry has attracted great attention as a new technique for developing functional polymeric materials.^{31–35, 41–50} The first report of a physical gel based on the polyrotaxane architecture was also presented by Harada et al.⁴¹ When α -CDs were mixed with long PEG chains at a high concentration in water, sol-gel transition occurred due to hydrogen bonding between the α -CDs threaded on the PEG chains in different pseudo-polyrotaxanes. In addition, Yui and co-workers formed some hydrogels using biodegradable CD based polyrotaxane⁴³ as the cross-linker for use in regenerative medicine.⁵¹ The biodegradable polyrotaxane has a hydrolysis part, namely, an ester bond between a bulky end group and the polymer axis. Consequently, the erosion time of the biodegradable hydrogel strongly depends on its polyrotaxane content.

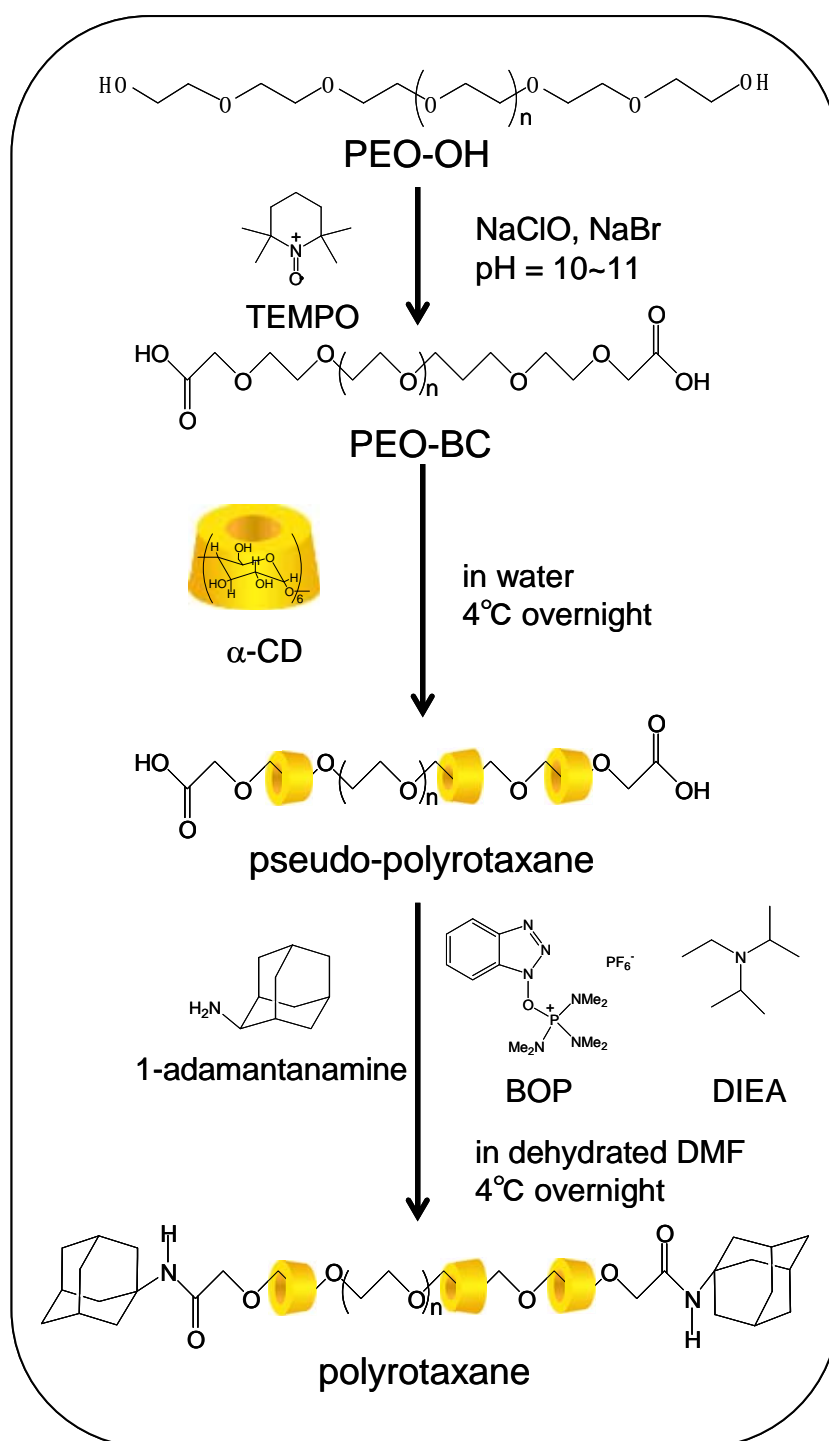


Figure 1.3. One pot synthesis of Polyrotaxane from Poly(ethyleneglycol), α -Cyclodextrin, and 1-Adamantanamine

Furthermore, Takata et al. synthesized recyclable cross-linked polyrotaxane gels: topologically networked polyrotaxane capable of undergoing reversible assembly and disassembly based on the concept of dynamic covalent bond chemistry.^{32,35} They cross-linked poly(crown ether)s with dumb-bell-shaped axle molecules, which show a reversible cleavage of the disulfide bond. As a result, a novel reversible cross-linking or decross-linking system that could recycle networked polymeric materials was realized.

1.5. Some well known polymer gels exhibiting higher mechanical strength

1.5.1. Double network gel

Gong and Osada developed a double network gel having a high modulus up to the sub mega Pascal range with a failure compressive stress as high as 20 MPa.⁶¹⁻⁶⁶ The double network gel has both soft and hard components so as to avoid fracture as in the case of biomaterials.

1.5.2. Nanocomposite gel

Haraguchi et al. have recently developed a novel type of gel called the nano-composite gel, which has clay as the cross-linking junction.^{67,68} Polymer chains of *N*-isopropyl acrylamide strongly absorb onto the clay surface at both ends, thus bridging different clays. Surprisingly, the nano-composite gel shows high tensile strength up to 10 times of its original length.

1.5.3. Slide ring gel

Slide ring gels have figure-of-eight cross-links that can slide along polymer chains. A typical example is the polyrotaxane gel synthesized by a technique of supramolecular chemistry by Okumura and Ito⁶⁹; a polyrotaxane molecule consists of

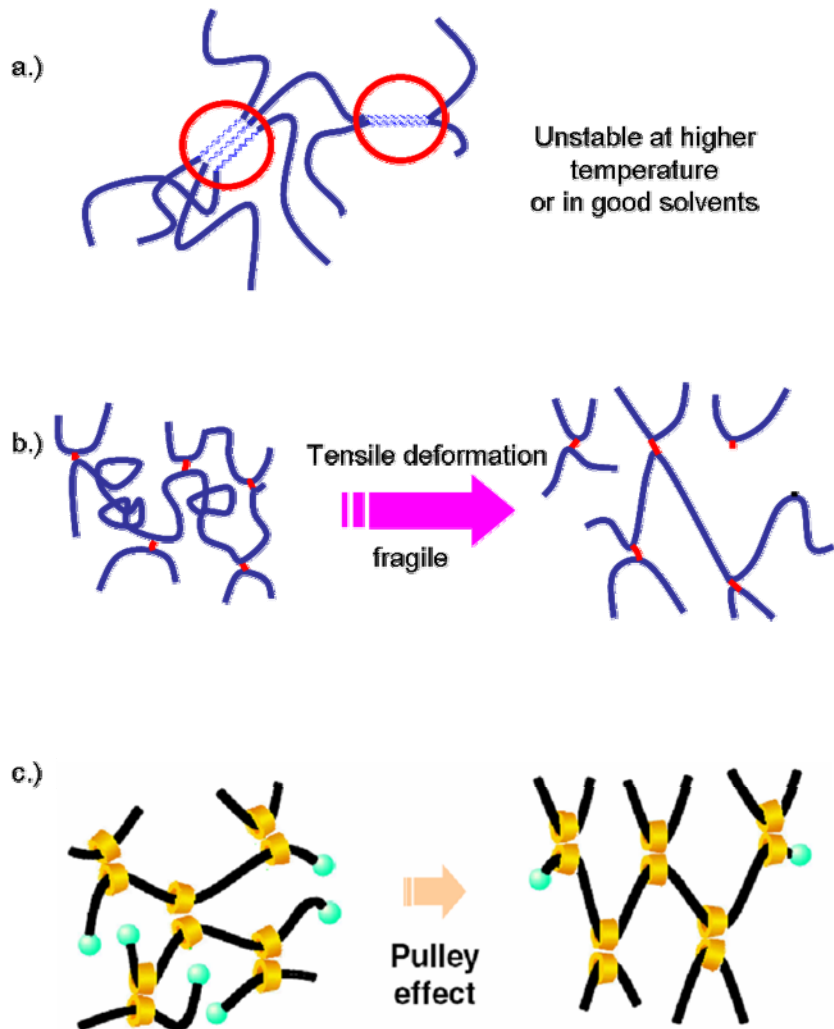


Figure 1.4. Schematic comparison between a.) physical gel b.) chemical gel and c.) slide ring gel. Physical gel is unstable at higher temperature or in good solvent. The pulley effect in the slide-ring gel can disperses the tension in the polymer chains under tensile deformation while the tensile stress concentrates on short polymer chains in the chemical gel.

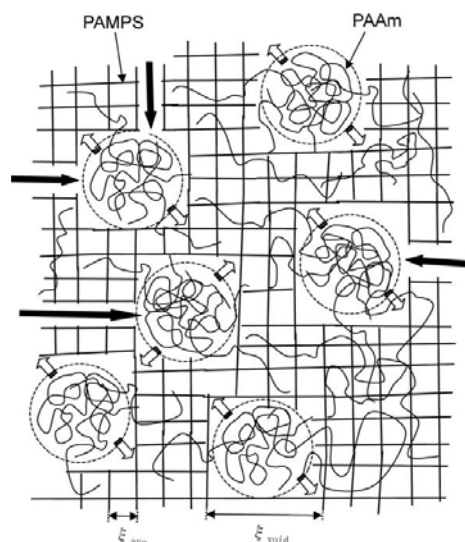


Figure 1.5.a). Structural model and mechanism to prevent crack development in PAMPS/PAAm DN gels

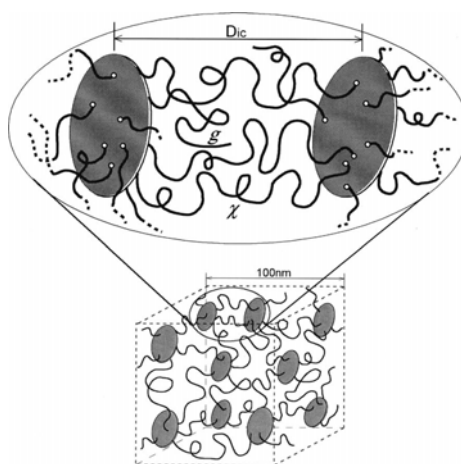


Figure 1.5.b). Structural model for the nanocomposite gels.

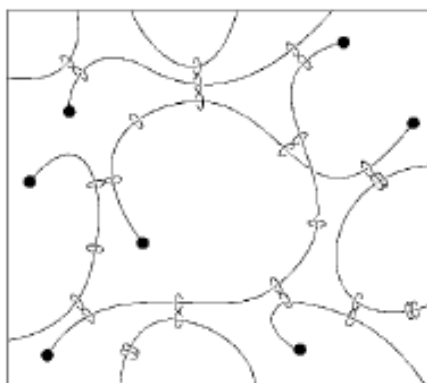


Figure 1.5.c). Structural model for the slide-ring gels.

a poly(ethylene glycol) (PEG) chain, α -cyclodextrin (CD) rings threaded on the PEG chain and bulky end groups trapping the α -CD macro-cycles. Chemically cross-links of the α -CD in an aqueous solution of polyrotaxane results in the polyrotaxane gel or slide ring gel. The slide ring gels are highly water absorbent and stretchable. The gel swells to about 500 times of its original (as-prepared) weight. A Slide ring gel can be stretched to about 20 times of its original length. Another unique nature of the slide ring gels appears in macroscopic and equilibrium mechanical behavior when the cross-linking density is low: stress-strain (S-S) curve of the slide ring gels under uniaxial elongation exhibit low convexity in all ranges of strain. This is quite different from the usual chemical gels, for which the S-S curve exhibits upper convexity in the small strain regime. The sliding motion of the figure-of-eight cross-links accounts for the special feature of the slide ring gels that distinguish the gels from the usual chemical and physical gels. In the chemical gel, the tension is distributed unevenly among the polymer chains; scission of the polymer chains gradually occurs. On the other hand, in a slide ring gel, the relative sliding of the polymer chains by figure-of-eight cross-links occurs to equalize the experienced tension among the polymer chains. Okumura and Ito refer to such an adjustment of the tensions by sliding as the ‘pulley effect’. The sliding mode (pulley effect) is obviously related to the large water absorbance mentioned above. Dynamic light scattering measurements have been performed to clarify dynamics of the sliding mode: in the spectrum of the relaxation time, a peak corresponding with the sliding mode was observed in between the peaks of the usual cooperative and self diffusion modes.

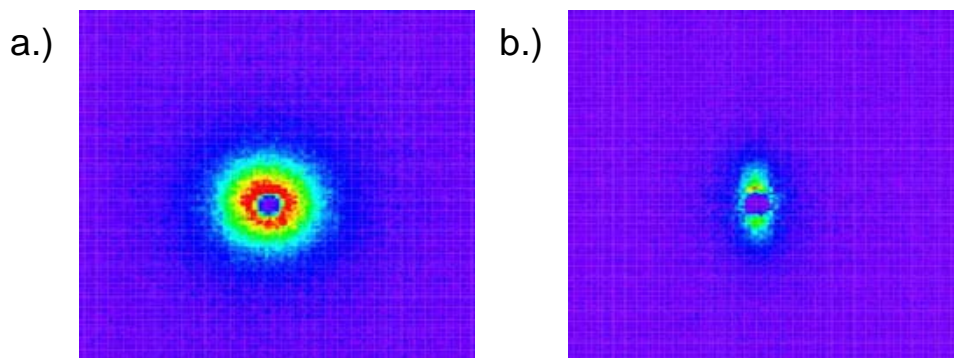


Figure 1.6. SANS patterns of the slide-ring gel before (a) and after (b) uniaxial deformation 1.8 times in length in the horizontal axis. The normal butterfly pattern perpendicular to the deformed direction is clearly observed and the scattering intensity decreases with increasing extension ratio.

1.6. Application of polymer gels

Polymer gels can easily be deformed by external physical and chemical stimuli and can generate a force or execute work to the exterior. If such responses can be translated from the microscopic level into a macroscopic scale, a conversion of chemical free energy into mechanical work should be realized. These energy-conversion systems have great potential that may be applied to actuators, sensors, chemical valves, delivery controllers, and permselective separators. Hydrogels can be used in the following bio-medical applications- artificial organs, catheters, contact lenses, drug delivery systems, artificial corneas, sensors (electrodes), burn dressings cell culture, synthetic cartilages, breast or other soft-tissue substrates etc. A polymer gel can absorb solvent up to several thousands times its original weight, depending on the chemical structure of the gel. Diapers, feminine napkins, and perfumes, used in everyday life are typical examples of this highly water-absorbing property of hydrogels.

1.7. Objectives of this study:

To successfully exploit the slide ring gels for a particular polymer, the polymer chain needs to be tailored with polyrotaxane like architecture in which the macro cycles together with active cross-link points can slide or rotate through that template polymer chains and the macro cycles need to be trapped in polymer chains using stable capping agent to prevent dethreading. However, the complicated and protracted process is not applicable for most of the polymer chains and a widespread use for a variety of polymer chains still remains an elusive goal. The present work was initiated to accomplish the following objectives:

To prepare stimuli sensitive slide-ring gel by facile and universal way.

To fabricate polymer gel having fast stimuli sensitivity and isotropic volume change during shrinking.

To synthesize polymer gel consisting of reversible, soft and flexible gel networks.

To prepare polymer gels which have higher mechanical strength and exhibits non-linear elasticity.

To fabricate the polymer gel which can uptake huge amount of solvent molecules.

1.8. Present work

A novel type of stimuli responsive slide ring gels have been synthesized using supramolecular polyrotaxane architecture as cross-linkers. A sparsely dispersed α -CDs or derivatives threaded into the long polyethylene glycol axle (MW=35000) and trapped these macro cycles by a stable capping agent, 1-adamantanamine of polyrotaxane unit was used as starting materials. The hydroxyl groups of α -CDs or derivatives of polyrotaxanes were modified by vinyl monomer through the formation of stable carbamate bond to have the hydrophobic and hydrophilic polyrotaxane cross-linkers. Polymer gels were fabricated by free radical polymerization of different types of stimuli sensitive monomers or co-monomers in presence of polyrotaxane cross-linkers.

References

1. Campoccia, D.; Doherty, P.; Radice, M.; Brun, P.; Abatangelo, G.; Williams, D.F. *Biomaterials*. **1998**, 19, 2101–2127.
2. Prestwich, G.D.; Marecak, D.M.; Marecak, J.F.; Ver- cruysse, K.P.; Ziebell, M.R. *J. Controlled Release*. **1998**, 53, 93–103.
3. Hirokawa, Y.; Tanaka, T. *J. Chem. Phys.* **1984**, 81, 6379.
4. Amiya, T. *J. Chem. Phys.* **1987**, 86, 2375.
5. Fujishige, S.; Kubota, K.; Ando, I. *J. Phys. Chem.* **1989**, 93, 3311.
6. Kabra, B.G.; Akhtar, M.K.; Gehrke, S.H. *Polymer*. **1992**, 33, 990.
7. Malstom, M.; Lindman, B. *Macromolecules*. **1992**, 25, 5440,
8. Akashi, M.; Nakano, S.; Kishida, A. *J. Polym. Sci., Part A Polym. Chem. Ed* **1996**, 34, 301.
9. Brazel, C.S.; and Peppas, N.A. *Macromolecules*. **1995**, 28, 8016.
10. Zhang, J.; Peppas, N.A. **2000**, 33, 102.
11. Dong, L-C.; Hoffman, A.S.; *J. Controlled release*. **1991**, 15, 141.
12. Chen, G.; Hoffman, A.S. *Nature*, **1995**, 373, 49.
13. Kim, Y.H.; Bae, Y.H.; Kim, S.W. *J. Controlled Release*. **1994**, 28, 143.
14. Feil, H. *Macromolecules*. **1992**, 25, 5528.
15. Tanaka, T. *Phys. Rev. Lett.* **1978**, 40, 820
16. Tanaka, T.; *Phys. Rev. Lett.* **1980**, 45, 1636
17. Hirokawa, Y.; Tanaka, T.; Sato, E. *Macromolecules*. **1985**, 18, 2782.
18. Hirokawa, Y.; Tanaka, T. *J. Chem. Phys.* **1984**, 81, 6379.
19. Hirotsu, S.; Hirokawa, Y.; Tanaka, T. *J. Chem. Phys.* **1987**, 87, 1392.
20. Dusek, K.; Patterson, D. *J. Polym. Sci. Part 2*, **1968**, 6, 1209.

21. Tanaka, T. *Phys. Rev. Lett.* **1978**, 40, 820.
22. Tanaka, T.; Fillmore, D.J.; Sun, S.T.; Nishio, I.; Swislow, G.; Shah, A. *Phys. Rev. Lett.* **1980**, 45, 1636.
23. Heskins, M.; Guillet, J.E. *J. Macromol. Sci. Chem.* **1968**, A2, 1441.
24. Schild, H.G. *Prog. Polym. Sci.* **1992**, 17, 163.
25. Hirasa, O.; Ito, S.; Yamauchi, A.; Fujishige, S.; Ichijo, H. In *Polymer Gels*; De Rossi, D., et al., Eds.; Plenum: New York, **1991**, 247 pp.
26. Suzuki, M.; Hirasa, O. *Adv. Polym. Sci.* **1993**, 110, 253.
27. Ichijo, H.; Kishi, R.; Hirasa, O.; Takiguchi, Y. *Polym. Gels Networks.* **1994**, 2, 315.
28. Wenz, G. *Angew. Chem., Int. Ed.* **1994**, 33, 803.
29. H. W. Gibson., H. Marand. *Adv. Mater.* **1993**, 5, 11.
30. Philp, D.; Stoddart, J. F. *Angew. Chem., Int. Ed.* **1996**, 35, 1155.
31. Harada, A. *Acc. Chem., Res.* **2001**, 34, 456.
32. Takata, T.; Kihara, N.; Furusho, Y. *Adv. Polym. Sci.* **2004**, 171, 1.
33. Huang, F. H.; Gibson, H. W. *Prog. Polym. Sci.* **2005**, 30, 982..
34. Wenz, G.; Han, B. H.; Muller, A. *Chem. Rev.* **2006**, 106, 782.
35. Takata, T. *Polym. J.* **2006**, 38, 1.
36. Ogino, H. *J. Am. Chem. Soc.* **1981**, 103, 1303.
37. *Comprehensive Supramolecular Chemistry Vol. 3: Cyclodextrins*, Szejtli, J. Osa, T. Ed., Pergamon, Elsevier, Oxford, **1996**.
38. *Cyclodextrins and Their Complexes: Chemistry, Analytical Methods, Applications*, Dodziuk, H. Ed., Wiley-VCH, New York, **2006**.
39. Harada, A.; Kamachi, M. *Macromolecules.* **1990**, 23, 2821.
40. Harada, A.; Li, J.; Kamachi, M. *Nature.* **1992**, 356, 325.

41. Li, J.; Harada, A.; Kamachi, M. *Polym. J.* **1994**, 26, 1019.
42. Okumura, Y.; Ito, K.; Hayakawa, R. *Phys. Rev. Lett.* **1998**, 80, 5003.
43. Ooya, T.; Yui, N.; *Macromol. Chem.* **1998**, Phys. 199, 2311.
44. Okumura, Y.; Ito, K. Hayakawa, R. *Phys. Rev. E: Stat., Nonlinear, Soft Matter Phys.* **1999**, 59, 3823.
45. Yoshida, K.; Shimomura, T.; Ito, K.; Hayakawa, R. *Langmuir*. **1999**, 15, 910.
46. Fujita, H.; Ooya, T.; Yui, N. *Macromolecules*. **1999**, 32, 2534.
47. Ikeda, T.; Ooya, T.; Yui, N. *Macromol. Rapid Commun.* **2000**, 21, 1257.
48. Watanabe, J.; Ooya, T.; Yui, N. *J. Artif. Organs*. **2000**, 3, 136.
49. Okumura, Y.; Ito, K.; Hayakawa, R. Nishi, T. *Langmuir*, **2000**, 16, 10278 .
50. Ikeda, E.; Okumura, Y.; Shimomura, T.; Ito, K.; Hayakawa, R. *J. Chem. Phys.* **2000**, 112, 4321.
51. Shimomura, T.; Yoshida, K.; Ito, K.; Hayakawa, R. *Polym. Adv. Technol.* **2000**, 11, 837.
52. Okumura, Y.; Ito, K.; Hayakawa, R. *Polym. Adv. Technol.* **2000**, 11, 815.
53. Saito, M.; Shimomura, T.; Okumura, Y.; Ito, K.; Hayakawa, R. *J. Chem. Phys.* **2001**, 114, 1.
54. Ichi, T.; Watanabe, J.; Ooya, T.; Yui, N. *Biomacromolecules*. **2001**, 2, 204.
55. Okumura, Y.; Ito, K. *Adv. Mater.* **2001**, 13, 485.
56. Shimomura, T. Akai, T.; Abe, T.; Ito, K. *J. Chem. Phys.* **2002**, 116, 1753.
57. Oya, T.; Noguchi, M.; Yui, N. *J. Am. Chem. Soc.* **2003**, 125, 13016.
58. Oku, T.; Furusho, Y.; Takata, T. *Angew. Chem., Int. Ed.* **2004**, 43, 966 .
59. Oya, T.; Utsunomiya, H. Noguchi, M.; Yui, N. *Bioconjugate Chem.* **2005**, 16, 62 .
60. Kihara, N.; Hinoue, K.; Takata, T. *Macromolecules*, **2005**, 38, 223.
61. Gong, J. P.; Katsuyama, Y.; Kurokawa, T.; Osada, Y. *Adv. Mater.* **2003**, 15, 1155.

62. Tanaka, Y.; Gong, J. P.; Osada, Y. *Prog. Polym. Sci.* **2005**, 30, 1.
63. Kaneko, D.; Tada, T.; Kurokawa, T.; Gong, J. P.; Osada, Y. *Adv. Mater.*, **2005**, 17, 535.
64. Yasuda, K.; Gong, J. P.; Katsuyama, Y.; Nakayama, O.; Tanab, Y.; Kondo, E.; Ueno, M.; Osada, Y. *Biomaterials*. **2005**, 26, 4468.
65. Tanaka, Y.; Kuwabara, R.; Na, Y.-H.; Kurokawa, T.; Gong, J. P.; Osada, Y. *J. Phys. Chem. B*. **2005**, 109, 11559.
66. Tsukeshiba, H.; Huang, M.; Na, Y.-H.; Kurokawa, T. Kuwabara, R.; Tanaka, Y.; Furukawa, H.; Osada, Y.; Gong, J. P. *J. Phys. Chem.* **2005**, 109, 16304.
67. Haraguchi, K.; Li, H.-J. *Angew. Chem., Int. Ed.* **2005**, 44, 6500.
68. Haraguchi, K.; Li, H.-J. *Macromolecules*. **2006**, 39, 1898.
69. Okumura, Y.; Ito, K. *Adv Mater.* **2001**, 13, 485–7.

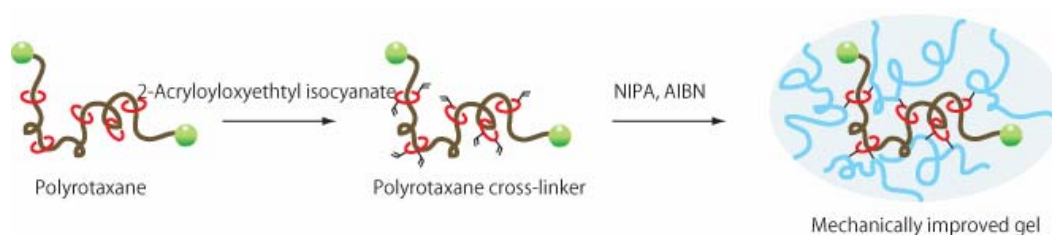
CHAPTER

2

Preparation of soft and mechanically improved hydrogels using a vinyl modified polyrotaxane as a Cross-linker

Abstract

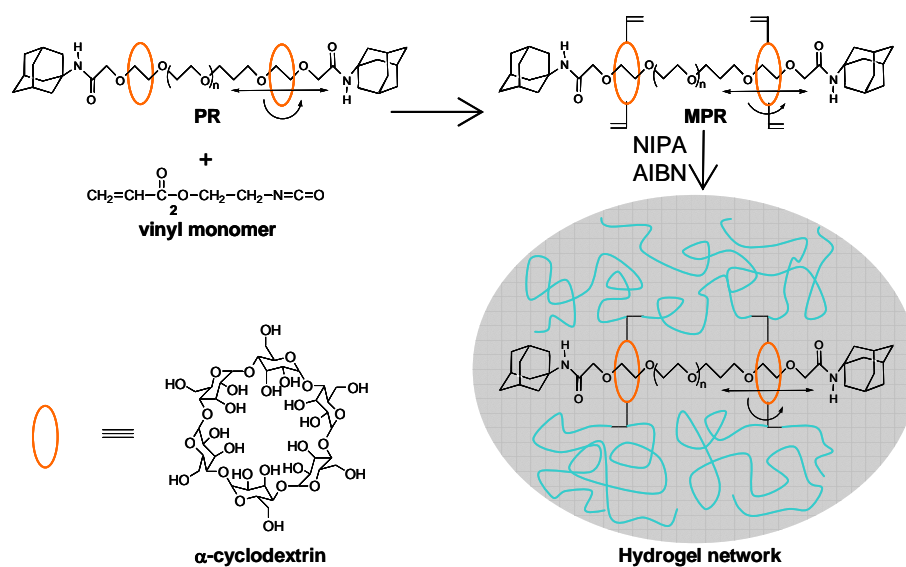
A novel hydrogel using a supramolecular polyrotaxane as the starting material has been synthesized. Sparsely dispersed α -CDs threaded into long polyethylene glycol axle (MW=35000) were trapped with a stable capping agent, 1-adamantanamine of polyrotaxane (PR) unit was used for this purpose. To obtain the hydrophobic polyrotaxane cross-linker, MPR, the hydroxyl groups of α -CDs of the PR were modified by a vinyl monomer, having active isocyanate group at one end which forms a stable carbamate bond. Polymer gels were designed by using MPR as a cross-linker and *N*-isopropylacrylamide, NIPA as a monomer, which yielded transparent, very soft, flexible and mechanically improved polymer gels. In the gel network, the polymer chains can slide and rotate about the movable cross-linker, which potentially improves the mechanical properties of the gels over conventional chemically cross-linked polymer gel. The gel shows an abrupt volume changes in water above the lower critical solution temperature (LCST) of NIPA and exhibit homothetic deformation after a temperature jump. The deswelling rate of the gel is much faster than conventional poly(NIPA) gel. The softness and mechanical stability of the gel were established by analyzing the data of rheometric solid analyses.



2.1. Introduction

Stimuli responsive polymers have a high potential for diverse areas, especially for biomedical applications. Polymers of this variety, responds interestingly to an infinitesimal change in the environment, such as, change in temperature, pH, solvent, ionic composition, electric field and light etc and brings about a discrete change in the gel volume.¹ Among the polymers studied, temperature responsive polymers, have proved to be of great interest due to their interesting phase transition behavior and till to date poly(*N*-isopropylacrylamide), poly(NIPA) has been the mostly studied representative of polymer of this kind. Poly(NIPA) chains in water have a Lower Critical Solution Temperature (LCST) at 31~34 °C . Below the LCST, poly(NIPA) chains have hydrated long flexible coil conformation, which renders into a dehydrated aggregated globular conformation above the LCST. This results in an abrupt volume change of the poly(NIPA) gel around LCST temperature of NIPA. Tanaka et. al² were the first to report such volume phase transition temperature of poly(NIPA) gel in water. Based on the cross-linking points, stimuli responsive polymer gels may be grouped into two distinct categories: physical gels and chemical gels.³ While physical interactions, such as ionic, hydrophilic, and hydrophobic interactions and formation of micro-domains, helices, and microcrystallines are responsible for physical gels, fixed covalent bonds between cross-linker and the polymer chains lead to the formation of chemical gels. The ability of physical gels to reorient non-covalent cross-link points at the deformed state brings about change in the original network structure under deformation. In contrast, as deformation is brought into the network, the fixed cross-links can not avoid the localization of the stress and the chemical gel soon loses its mechanical integrity. Innovation of novel gels, which would be able to exhibit reversible stress relaxation via the reorientation

of non-covalent cross-link points without loss of original network structure, properties and mechanical integrity under deformation, has long been the dream of gel scientists. The concept of movable cross-links was first proposed by Edwards et. al.⁴ and used for synthesis by Gibson et.al.⁵ Recently Ito et. al.⁶ have successfully realized the concept to materialize sliding gels. Supramolecular architecture of polyrotaxane⁷ has been used as a polymer for the preparation of sliding gels. A sparsely dispersed cyclodextrin containing polyrotaxane solution has cooperative, self, and sliding diffusion and the mode of sliding diffusion is observable even after gelation.⁸ This focused eyes on polyrotaxane for their use not only for the preparation of sliding gels but also in syntheses of various smart materials, for instance, molecular tubes⁹, insulated molecular wires¹⁰, drug delivery systems¹¹, light-induced energy transfer systems¹² etc. The threaded cyclic molecules of different polyrotaxanes, which are terminally-capped to linear polymer chain, were covalently cross-linked by a bi-functional cross-linker. The rotating and sliding ability of the cross-linked cyclic molecules along the polymer chain permits to average the length and to equalize the experienced tension of the polymer chains under deformation in the gel network like a pulley. The gel of this kind can be regarded as an intermediate between two well known gels, where the gel network is formed by fixed covalent bonds like chemical gels and cross-link points can reorient under deformation like physical gels. Sliding gels bring radical improvements in physical properties of polymer gels such as, non-linear elasticity, reversibility of the structural changes, softness, large swelling ability, and higher mechanical strength etc. Consequently, for the first time a normal butterfly pattern could be observed in a sliding gel.¹³ The pulley effects of the sliding gel suppress the spatial inhomogeneities of the gel network under deformation. Under stretching the sliding gel maintains its uniformity by the movement of the sliding



Scheme 2.1. Schematic representation of the formation of movable cross linker and its gelation. For the sake of clarity only a few cross-link points are depicted in the scheme.

cross-link points about the polymer chain and exhibits normal butterfly patterns. With a view to introducing sliding phenomenon into the polymer gel networks for a wide variety of polymers, the polymer chains need to act like polyethylene glycol of polyrotaxane where cyclic molecules together with covalently cross-link points can slide or rotate through that template polymer chains. The long and complicated processes are, however, not always suited for achieving such polymer gels. Even the difference in host-guest relationships for different polymers and macro cycles places blocks in realizing polyrotaxane architecture for a variety of polymer chains to synthesize sliding gels.

In this study, we aim at introducing sliding phenomenon into the conventional stimuli responsive polymer gel networks to have the mechanically intriguing polymer gels by using facile and universal synthesis. Polyrotaxane architecture has been used as a movable cross-linker for this purpose where the active vinyl modified cyclic molecules are capable of sliding and rotating about the polymer axle in the free state and with the covalently cross-linked polymer chains even in the gel state. The superiority of the novel gel has been established and compared with conventional chemical gels.

2.2. Experimental

2.2.1. Materials

Polyrotaxane, PR (Advanced Soft Materials Inc., Japan), BIS (Acros Organics, Geel, Belgium), 2,2'-azobisisobutyronitrile, AIBN (Kanto Chemical Co., Japan), Dibutyl tin dilaurate, DBTDL and butylhydroxyltoluene (Tokyo Kasei Kogyo Co., Japan) were used without further purifications. The isocyanate monomer, 2-acryloyloxyethylisocyanate was purchased from Showa Denko K.K. NIPA from Kohjin Co., Tokyo, Japan was purified by recrystallization from toluene/ n-hexane.

Table 2.1. Sample codes of R_{wi}N_x and TN_x gels

Sample codes	NIPA Monomer (M)	MPR (wt%)	BIS (mM)	AIBN (mM)
R _{wi} N1	2	4.0	×	8.13
R _{wi} N2	2	2.7	×	8.13
R _{wi} N3	2	1.4	×	8.13
R _{wi} N4	2	0.8	×	8.13
TN1	2	×	100.0	8.13
TN2	2	×	66.7	8.13
TN3	2	×	33.4	8.13
TN4	2	×	20.0	8.13

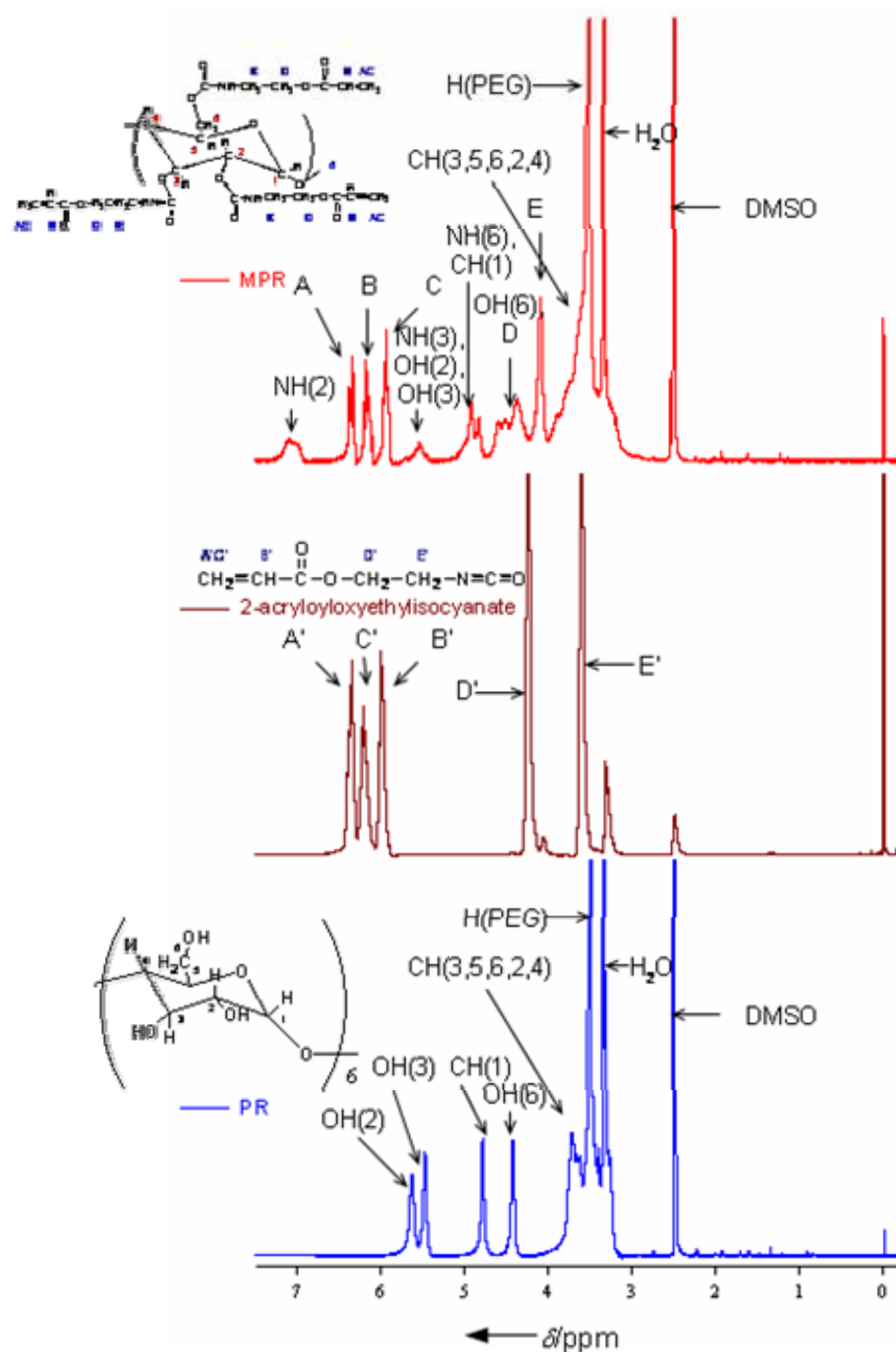


Figure 2. 1. ^1H -NMR spectra of PR, 2-acryloyloxyethyl isocyanate and MPR in DMSO- d_6 with 1% TMS. All of the characteristics peaks of PR and MPR come from the α -cyclodextrin and modified α -cyclodextrin groups. (The number inside the parentheses depicts the carbon position of 1,4 linked α -D-glucopyranoside unit of α -cyclodextrin).

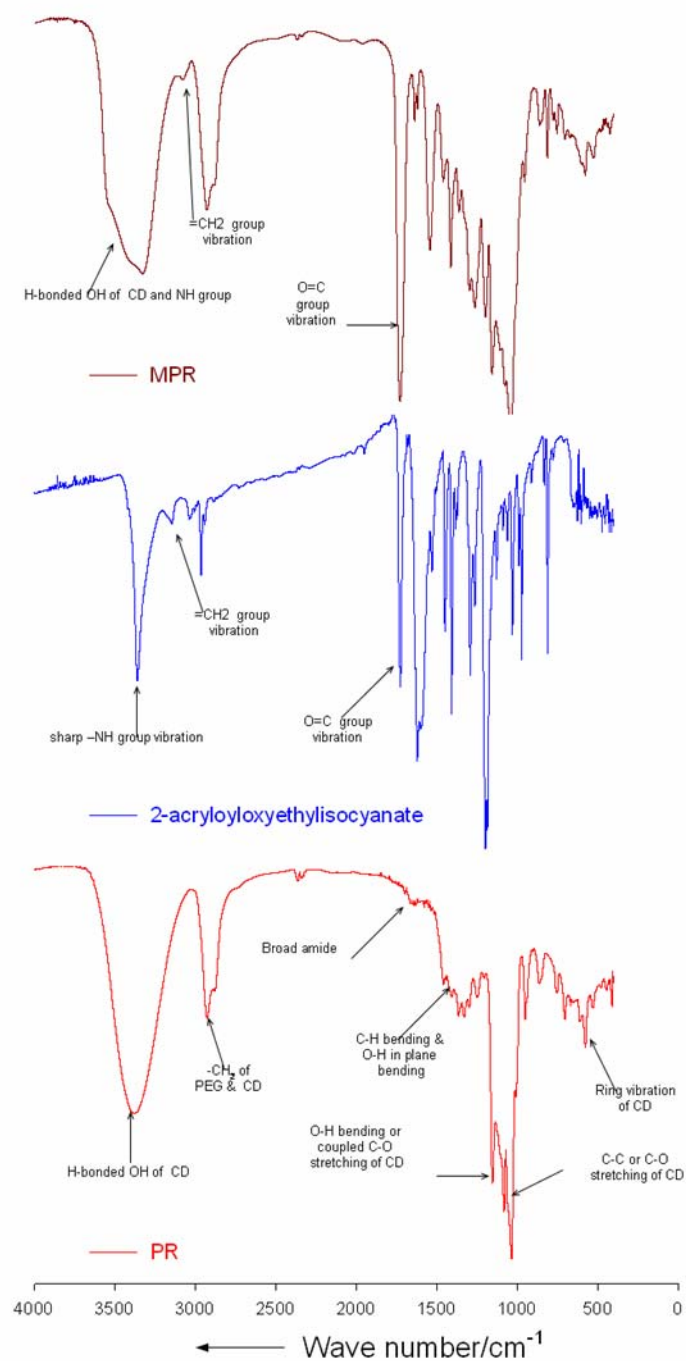


Figure 2.2. FT-IR spectra of PR, 2-acryloyloxyethyl isocyanate and MPR.

All other chemicals were reagent-grade and were used as received. Milli-Q ultra pure water was used throughout the experiments.

2.2.2. Preparation of hydrophobic polyrotaxane cross-linker, MPR

A solution of 2-acryloyloxyethyl isocyanate 2.7 mmol (379 mg) dissolved in 10 ml of DMSO was added drop wise to a mixture of PR (500 mg), DBTDL (catalyst, 1 drop), and butylhydroxytoluene 0.017 mmol (inhibitor, 3.79 mg) dissolved in 30 mL of anhydrous DMSO with vigorous stirring for a period of 45 m in the dark. The mixture was continuously stirred overnight at 40 °C. MPR was collected from the reaction mixture using excess methanol followed by storage in a refrigerator. The yield of the product upon washing several times with methanol and vacuum drying was 700 mg which is ca. 80%.

2.2.3. Preparation of hydrophobic polyrotaxane based rotaxane-NIPA, $R_{wi}N$ gels

The $R_{wi}N$ gels were prepared by free radical polymerization of NIPA monomer in presence of hydrophobic polyrotaxane cross-linker, MPR. The gel precursors, NIPA, MPR, and AIBN were dissolved in oxygen-free anhydrous DMSO and were infused to glass slides separated by Teflon spacers and glass micro-capillary tubes with an inner diameter of 270 μm to obtain slab and cylindrical gels, respectively. The gelation was carried out at 60°C for 24 h, and the gels were thoroughly washed with DMSO followed by water to remove any reaction residues.

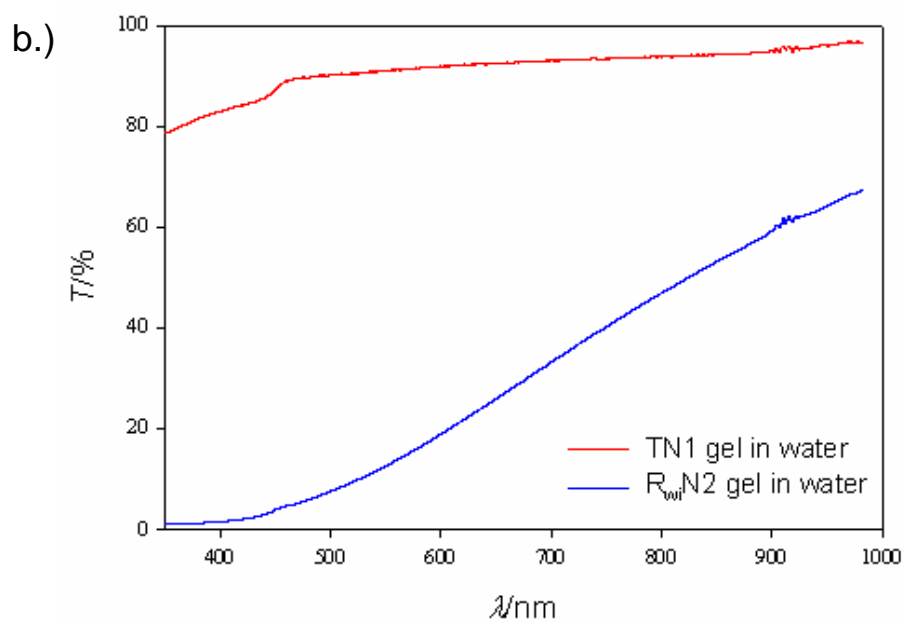
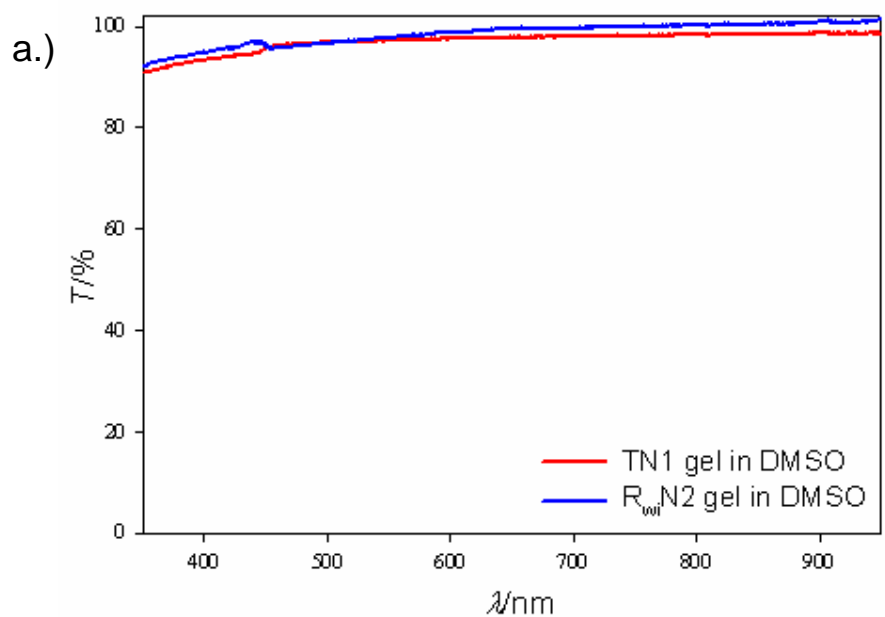


Figure 2.3. Transmittance spectra of TN1 and $R_{wt}N2$ gels at room temperature a.) in DMSO and b.) in water (thickness of the slab gels were 2 mm).

2.2.4. Preparation of typical NIPA, TNx gels

A series of TNx gels were also prepared by free radical polymerization method. The concentrations of NIPA monomer were maintained as 2.0 M and the cross-linker, BIS, was varied from 20 to 100 mM such that the molar ratio of NIPA/BIS = 100, 60, 30, 20. The pre-gel solution containing NIPA, BIS, and 8.13 mM AIBN (initiator) in dehydrated DMSO were bubbled with N₂ gas for 30 m. The gelation was carried out at 60 °C for 24 h. The gels were immersed in DMSO and water, respectively to wash away any reaction residues.

2.2.5. Mechanical strength test

The viscoelastic properties of the gels were measured with a Rheometric Solid Analyzer, RSA III of Rheometric Scientific, Inc. The rheometer consists of one normal force transducer (1kFRT) that can detect normal forces within up to 35 N (3500 g) and a motor having frequency range between 6.28×10^{-6} to 502 rad sec⁻¹, amplitude range ± 1.5 mm, response time <5 msec to 90% of final value, and strain resolution of 0.00005 mm. Prior to measurements, 4 mm thick slab gel samples were immersed in a suitable solvent. After reaching equilibrium swelling states, the gels were cut into rectangular shapes (10 mm \times 10 mm). The deswelling of gels was avoided throughout the experiments by immersing the gels in the solvent used. The temperature inside the sample chamber was controlled by an air oven equipped with N₂ cooling unit. The proper input of the volume change of the gel was performed for rheometric analysis to avoid the volume effect to its modulus values. The gel samples were under compression with a constant pre-strain of 5 % during experiments to ensure the sample was always under compression. The strain controlled dynamic frequency sweep test was used as a test setup and the selected 3% strain was in the

region of the linear viscoelastic region of the sample. The change of E' and E'' were observed in the frequency range 0.01 to 100 rad sec⁻¹.

2.2.6. Swelling ratio measurement

To take the optical micrograph of the kinetics of the volume change of the R_{wi}N and the TN gels, the cylindrical gels (270 mm) were kept in a cell with enough solvent and the temperature was controlled by circulator. Two temperature controllers were connected to the cell so that the temperature of the water can be quickly switched from one temperature to another. The temperature was stable to ± 0.1 °C over a few hours. The volume change of the cylindrical gels was monitored under an inverse microscope (Olympus CKX41) equipped with a color measuring unit (Flovel MC-70).

2.2.7. Scanning Electron Microscope (SEM)

The equilibrium swollen hydrogel samples in water at room temperature were quickly frozen in liquid nitrogen and then fractured carefully there. Samples were then freeze dried under vacuum at -52 °C for 3 days. The internal morphology of the samples was studied by a scanning electron microscope (SEM, JEOL JSM-5600). Samples were coated with Au prior to the SEM observation.

2.3. Results and Discussion

2.3.1. Preparation and characterizations of hydrophobic polyrotaxane cross-linker, MPR

The polyrotaxane (PR), consisting of α -cyclodextrin (α -CD), poly(ethylene glycol) carboxylic acid (PEG), and a capping agent, 1-adamantanamine was purchased from Advanced Soft materials Inc., Tokyo, Japan and was used throughout this work without further purifications. The polyrotaxane with a sliding motion of macro cycles through the PEG chain was designed with sparsely dispersed α -CD. Long PEG chain

having the MW of 35000 gmol⁻¹ was used for the preparation of PR. α -CDs formed inclusion complexes with PEG and the inclusion ratio, calculated from the consideration that stoichiometrically two ethylene glycol repeating units fit in one CD, was 26%.¹⁴ The total number of threaded α -CDs per molecule of PR unit was *ca.* 103, which was estimated from the ¹H-NMR spectrum by the comparison of the integration of PEG and that of α -CD. The detail synthetic route of PR is reported in the literature.¹⁵ Polyrotaxane of this kind has several intriguing features such as sliding and rotating ability of amphiphilic α -CDs through the PEG chain, facile synthesis, bio-compatibility and importantly, the ability of 18 hydroxyl groups per α -CD to be easily modified by various functional groups. The 2-Acryloyloxyethyl isocyanate (AOI) having both isocyanate and vinyl end groups in its parent structure was used as a modifier. The isocyanate groups of AOI react with the hydroxyl group of the α -CD of the PR through the formation of stable carbamate bond to yield the hydrophobic polyrotaxane cross-linker, which we denote as MPR. The degree of substitution, (DS) ($0 \leq DS \leq 18$), i.e., the average number of substituted hydroxyl groups per α -CD unit of the MPR was determined from the ¹H-NMR spectra and was found to be 8.4 (Figure 2.1.). In the FT-IR spectrum(Figure 2.2.), the broad peak of hydrogen bonded –NH vibration at ~ 3500 cm⁻¹ and a sharp peak of –CO vibration at ~ 1725 cm⁻¹ of attached AOI groups to the PR provide the structural confirmation of MPR.¹⁶

Poly(NIPA) gels using MPR as a cross-linker (R_{wi}N_x gels) were prepared by conventional free radical polymerizations. In the pre gel solutions the concentrations of NIPA monomer were kept as constant at 2.0 M, but the quantity of MPR were varied from 0.80 to 4 wt% (Table 2.1.). Typical NIPA gels (TN_x gels) were also prepared under identical conditions using only varying amount of *N, N'*-methylene-

bis-acrylamide, (BIS) (20 mM to 100 mM) as a cross-linker instead of MPR and used as references against the $R_{wi}N_x$ gels (Table 2.1).

2.3.2. *Transmission spectra of gels*

Figure 2.3. represents the transmission spectra of $R_{wi}N_2$ and TN1 gels in dimethylsulfoxide, DMSO. Both gels are highly transparent. The transparency of the $R_{wi}N_x$ gels indicates that the formation of homogeneous gel network and no aggregated clusters was formed in the network which is greater than the wavelength of visible light.

2.3.3. *Swelling behaviors of gels in DMSO and water*

Figure 2.4.a. shows the swelling behaviors of $R_{wi}N_x$ gels in water with change in temperatures. A sharp volume change of the gels are observed around 32°C in water. In analogous to TN $_x$ gels (Figure 2.5.), the volume of the $R_{wi}N_x$ gels can precisely be controlled by the initial amounts of the cross-linker, MPR. The volume of the gels below the LCST temperatures increases gradually with decrease in MPR amounts. In other words, the gel networks of $R_{wi}N_x$ gels are formed only by the reaction between cross-linker and polymer chains, no other aggregation or physical interactions are involved to form the gel networks.

No abrupt volume changes with temperature are observed for any of the $R_{wi}N_x$ gel in DMSO (Figure 2.4.b). Apparently, the gels maintain its volume throughout the temperatures range. In addition, in DMSO, the volume of the $R_{wi}N_x$ gels decrease with increase in cross-linker amount. With increase in cross-linking density, the gel networks can not imbibe much amount of DMSO molecules.

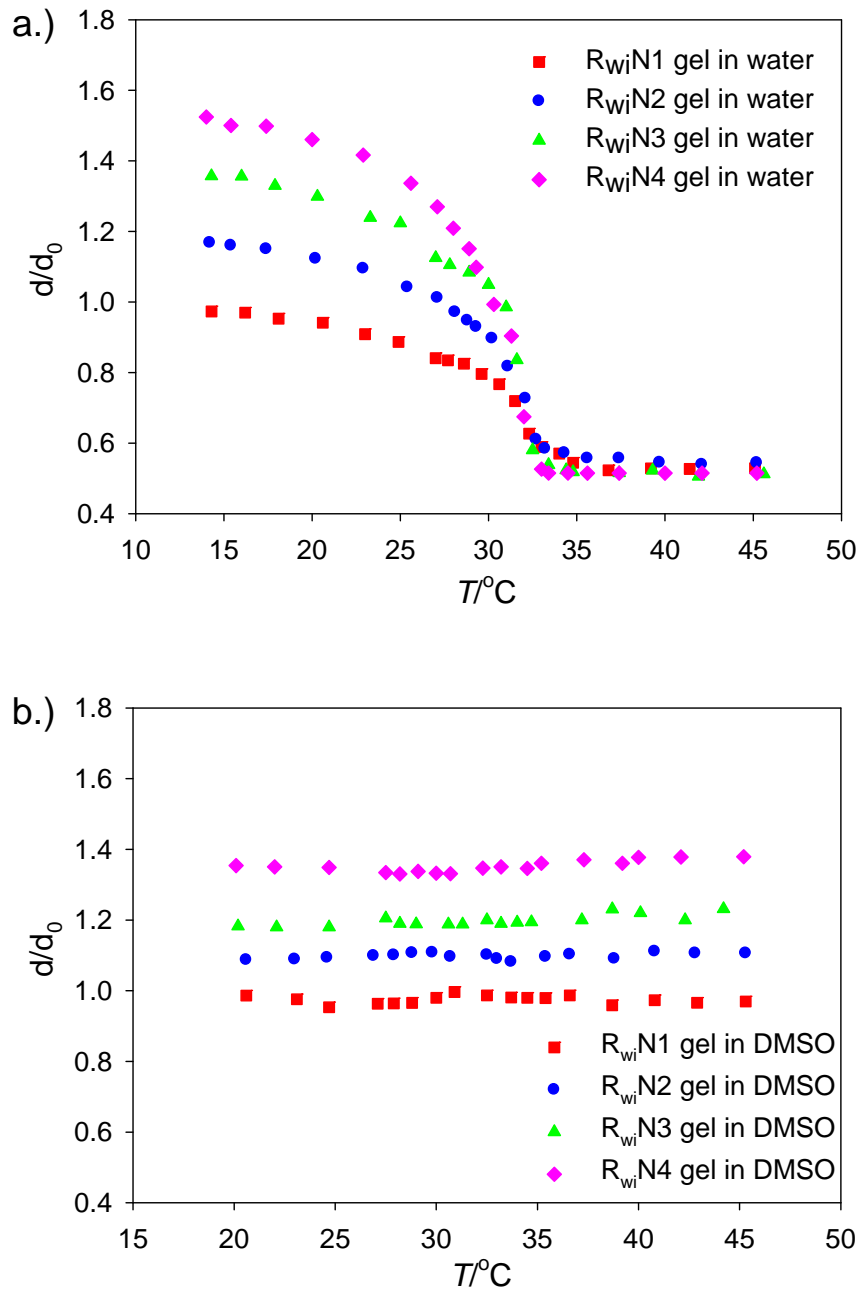


Figure 2.4. Static temperature dependencies on equilibrium degree of swelling of $R_{wi}N1$, $R_{wi}N2$, $R_{wi}N3$, and $R_{wi}N4$ gels a) in water and b) in DMSO.

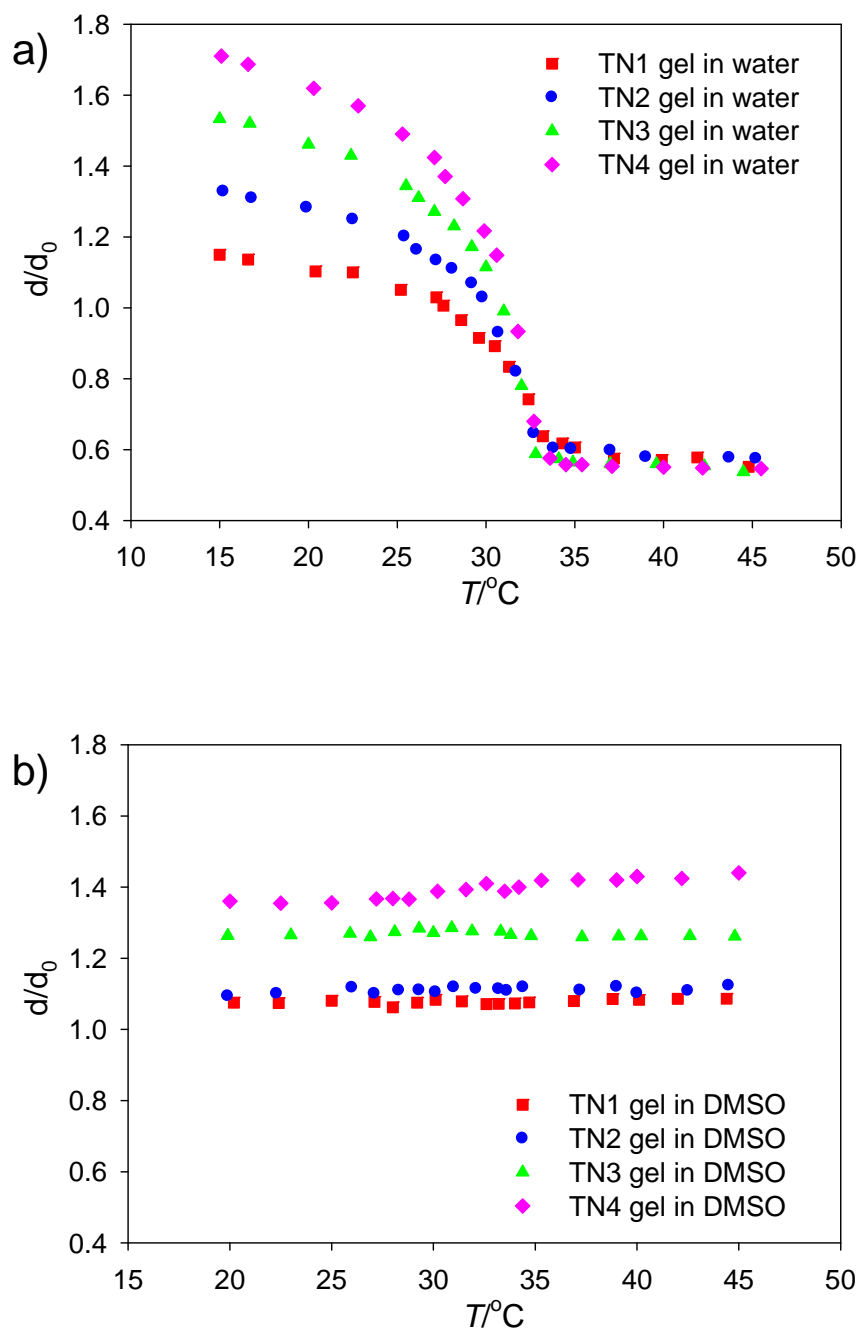


Figure 2.5. Static Temperature dependencies on equilibrium degree of swelling of TN1, TN2, TN3, and TN4 gels a) in water and b) in DMSO.

2.3.4. Effect of 0.1M NaOH on the swelling ratio $R_{wi}N3$ gel

Figure 2.6 shows the effect of 0.1M NaOH on the swelling ratio of $R_{wi}N3$ gel. To measure the effect of NaOH on the swelling ratio, the $R_{wi}N3$ hydrogel was immersed in 0.1M NaOH aqueous solution. After reaching the equilibrium swollen states in NaOH, the gel sample was taken out and washed by water. The swelling ratio of the gel was then measured in water at different temperatures. The figure clearly depicts that, at low temperature the gel exhibits higher swelling ratio than the $R_{wi}N3$ hydrogel and the volume phase transition temperature also shifts to the higher temperature. In NaOH aq. solution, the unmodified hydroxyl groups of the cross-linker MPR are exchanged by sodium ions. These sodium ions increase the electrostatic repulsion and thereby increases the dispersity of the macro-cycles. Since in the gel networks, polymer chains are attached to these macro-cycles, so the gel shows higher swelling ratio at low temperatures (below the LCST of NIPA). The presence of strong electrostatic interaction inside the gel increases the Donnan osmotic pressure and reduces the hydrophobic interactions of the $R_{wi}N3$ gel networks. Hence the volume phase transition temperature occurs at relatively higher temperature region.

2.3.5. Sampling for the measurements of shrinking kinetics and rheological studies

The TN1 and the $R_{wi}N2$ gels show the identical degree of swelling behaviors in DMSO and water and used them as references for rheological studies and kinetic processes of shrinking in water. The effect of the novel cross-linker MPR on the kinetic process of shrinking and the mechanical properties of the $R_{wi}N_x$ gel over the TN x gel can be realized easily using these gels.

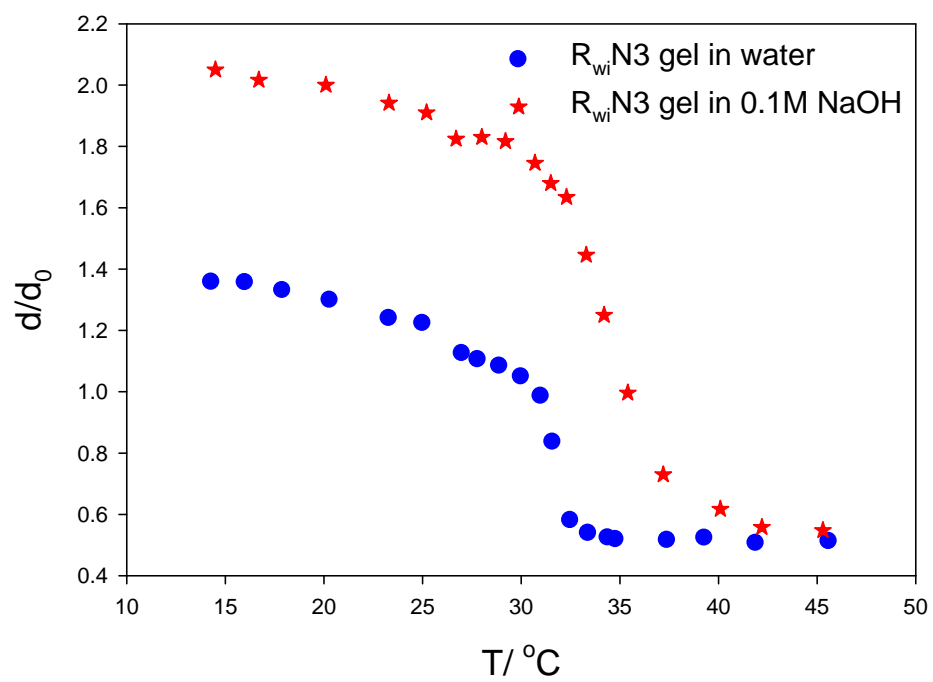


Figure 2.6. Effect of 0.1M NaOH on the equilibrium degree of swelling behavior of $R_{wi}N3$ gel in water as a function of temperatures.

2.3.6. Morphological changes of $R_{wi}N$ and TN hydrogels after a temperature jump

Figure 2.7. represents the optical micrographs of the morphological changes of $R_{wi}N2$ and TN1 gels after a temperature jump from 20 to 40 °C in water. The $R_{wi}N2$ gel shrinks isotropically; while the TN1 gel shrinks anisotropically. When the temperature of the gel suddenly rises above the LCST of poly(NIPA) chains, the $R_{wi}N2$ gel changes its volume homogeneously without any bubble formation on the surface of the gel. Similar behavior is observed for all of the $R_{wi}Nx$ gel series. In contrast, the TN1 gel changes its volume with quite irregular basis by the formation of bubble on the gel surface. The number of bubbles is inversely proportional to the amount of the cross-linker. The gelation of either gels proceed by the free radical polymerization of NIPA monomer and simultaneously the formation of fixed cross-linked polymer networks with cross-linker. The discrete nature of gelation method divides the polymer networks into lightly and heavily cross-linked polymer rich regions and brings spatial inhomogeneities in the gel networks. After a temperature jump, due to the presence of covalently bonded fixed cross-linked points in TNx gels, the gel networks cannot disperse the experienced tension to the whole networks and exhibit an anisotropic volume changes during shrinking. In contrast, the micro and macro level spatial inhomogeneities and local stresses inside the $R_{wi}Nx$ polymer gels network can automatically be homogenized and relaxed by a movement of the mobile cross-links points. This results in a homogeneous change in the volume after a sudden temperature jump.

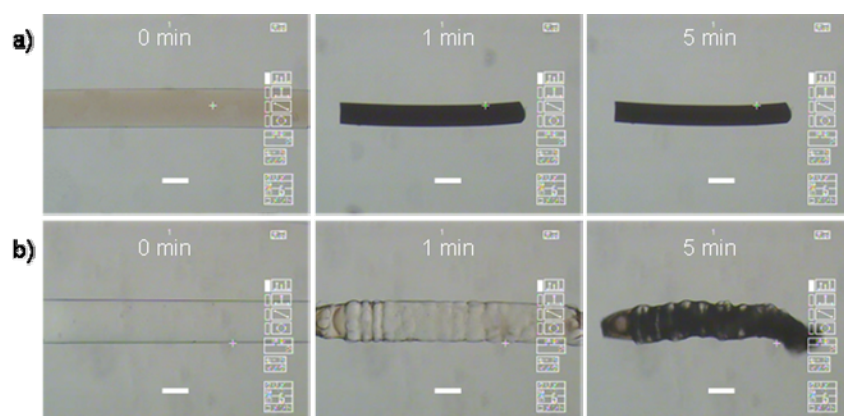


Figure 2.7. Optical micrographs of morphological change of cylindrical a) $R_{wi}N\ 2$ and b) TN1 gels in water after a temperature jump from 20 °C to 40 °C. (white bar line = 200 μm)

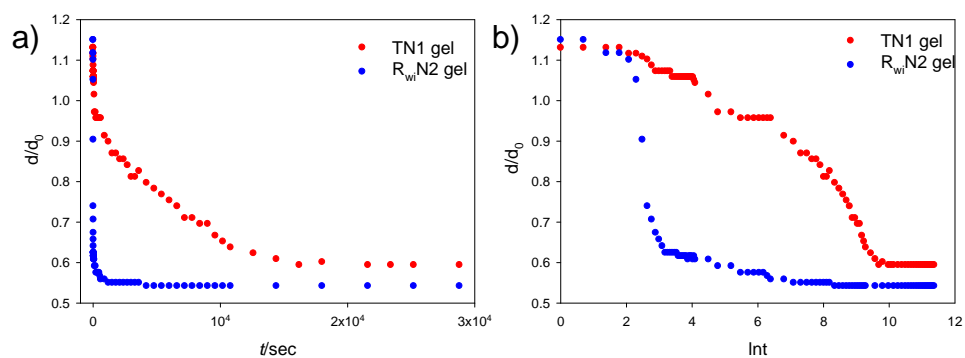


Figure 2.8. Shrinking kinetics of sub-micrometer sized cylindrical TN1 and $R_{wi}N\ 2$ gels in water after a temperature jump from 20 °C to 40 °C
a) d/d_0 vs time in sec b) d/d_0 vs $\ln t$

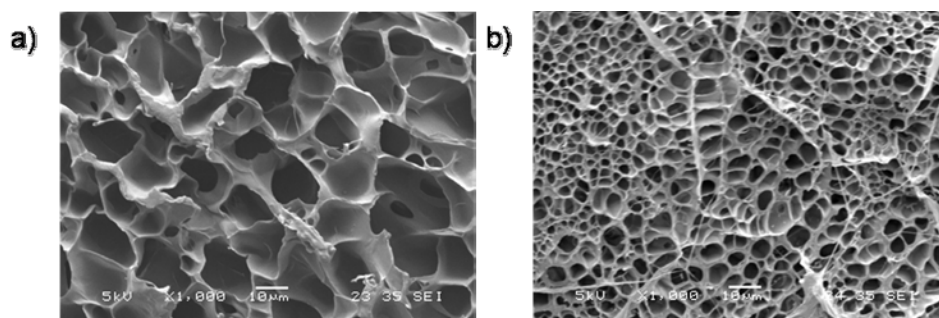


Figure 2.9. SEM images of the a) TN1 gel and b) R_{wi}N 2 gel after reaching to equilibrium swollen states in water

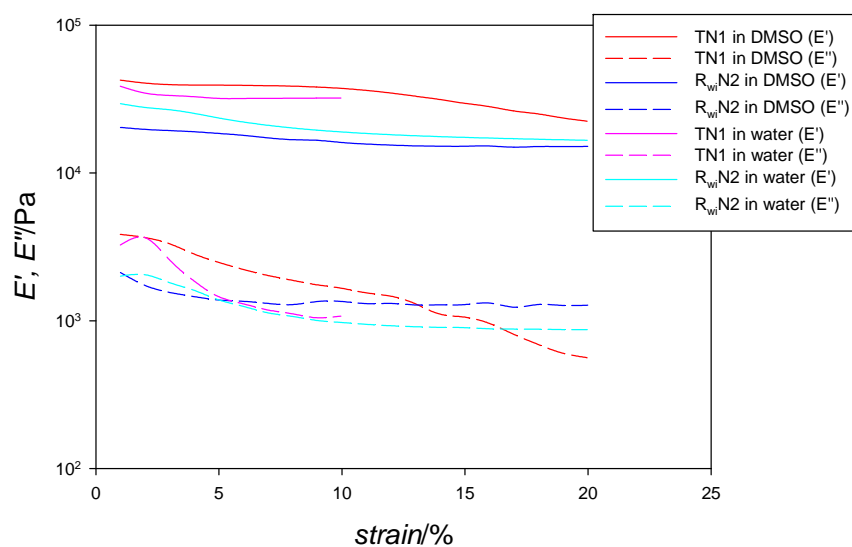


Figure 2.10. Frequency controlled (1 radsec^{-1}) dynamic strain sweep test of TN1 and R_{wi}N 2 gels in DMSO and water.

2.3.7. Shrinking kinetics of $R_{wi}N$ and TN gels after a temperature jump

Figure 2.8.a. shows the deswelling rate of the $R_{wi}N2$ and the TN1 gels in water after a temperature jump. The $R_{wi}N2$ gel soon reaches to an equilibrium shrunken state, but complete collapsed state of the TN1 gel requires prolonged period. Above the LCST, the cross-linked poly(NIPA) chains of TN1 gel forms a phase separated insoluble globular structure. In the TN1 gel, the fixed cross-linking facilitates to form an insoluble skin layer on the surface. Water molecules can not come outside through this impermeable skin layer and several relaxation points appear during shrinking (Figure 2.8.b.). On the other hand, the average pore sizes to imbibe water molecules for $R_{wi}N2$ gel are smaller than the TN1 gel and the wall of the pores is also thin (Figure 2.9.). Hence after a temperature jump, water molecules can quickly come outside from the $R_{wi}N2$ gel networks through these thin and well oriented pores. In addition in the $R_{wi}N2$ gel, the movability of the cross-links points helps to aggregate polymer networks to reach a complete collapsed state before forming any impermeable skin layer on the surface of the gel which bringing about faster shrinking of the $R_{wi}N2$ gel.

2.3.8. Rheological studies of $R_{wi}N$ and TN gels

For the rheological measurements, every gel samples were placed between parallel plates and measured at a frequency range of 0.01 to 100 Hz with a constant pre-strain of 5% to ensure that the samples are always in contact with the instrument. Strain sweeps were run on all of the samples to confirm that the measurements were consistently collected in the linear viscoelastic regime. The storage and loss moduli as a function of strain amplitude ranging from 0.01 to 20% at room temperature was carried out at a fixed frequency, $\omega = 1 \text{ rad sec}^{-1}$ (Figure 2.10.). Two distinct regions were observed in the amplitude of measurements: linear viscoelastic and non-linear

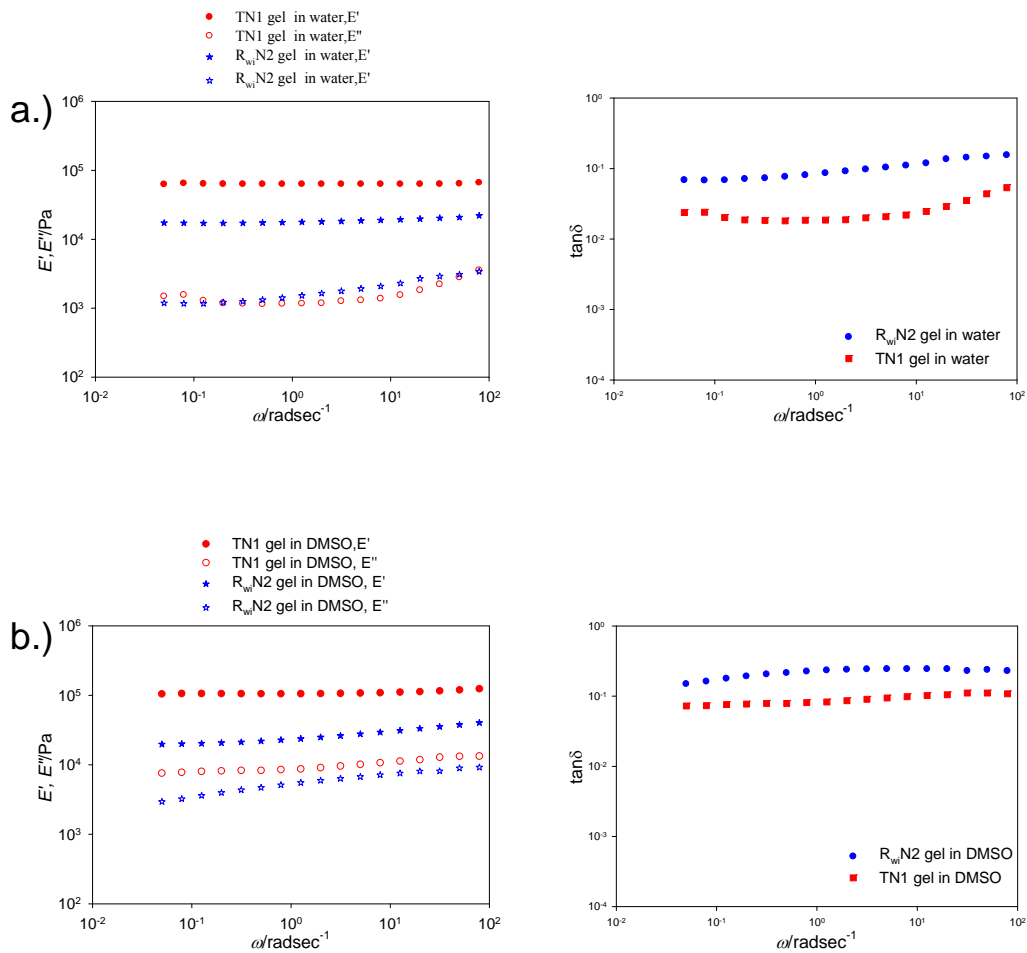


Figure 2.11. Strain-controlled dynamic frequency sweep test of storage moduli, E' loss moduli, E'' and loss tangent, $\tan\delta$ for TN1 gel and $R_{wi}N2$ gel at 26 °C a) in water (where both gels are in swollen states) and b) in DMSO.

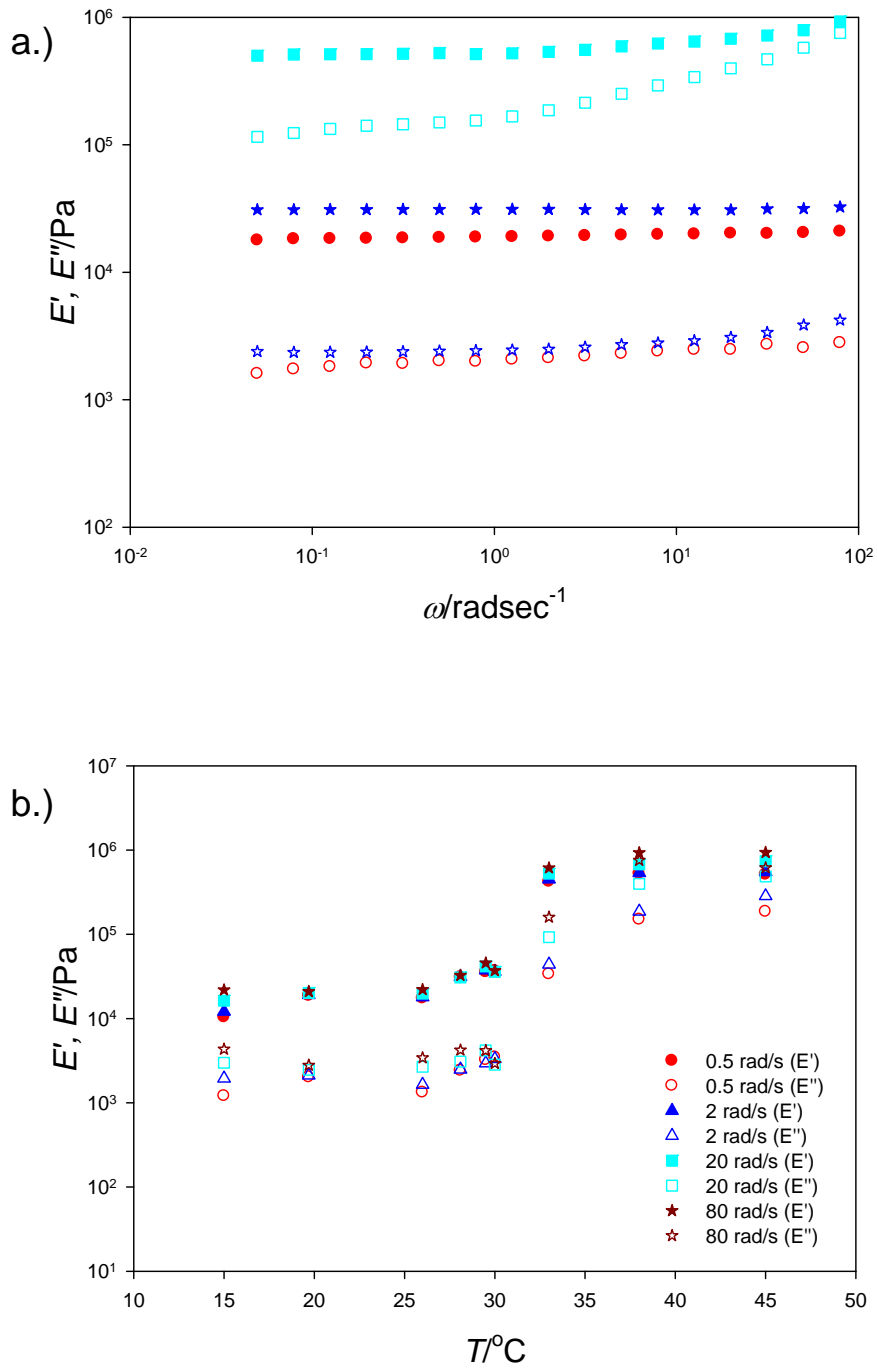


Figure 2.12. Strain-controlled dynamic frequency sweep test of storage moduli (closed symbols) and loss moduli (open symbols) of R_{wi}N 2 gel in water a) at 19.7 °C (circle), 28.1 °C (star), and 38 °C (square) as a function of frequencies and b) at 0.5 rad sec⁻¹ (circle), 2 rad sec⁻¹ (triangle up), 20 rad sec⁻¹ (square), and 80 rad sec⁻¹ (star) as a function of temperatures.

viscoelastic regions. In the linear viscoelastic region, the storage moduli of gel samples were independent of the strain amplitude. Beyond this region, the moduli decrease significantly with increasing strain amplitude. Below the 10% strain, TNx gels respond completely elastically but above it cracking or deformation of the samples were frequently observed. We have chosen 3 % constant strain from the linear viscoelastic region to carry out the strain controlled dynamic frequency sweep tests.

Figure 2.11. clearly shows that the values of E' are always higher than E'' and E' 's are independent of frequency in the entire frequency range for both gels studied in water and DMSO. These are the characteristic behaviors of solid like materials. The higher storage moduli of TNx gels evidently originate from the increasing elastically responded fixed cross-linked polymer chains in the gel network. The larger E' and smaller $\tan\delta$ (Figure 2.12.) values indicate the rigidity of the TNx gel networks compared to the $R_{wi}Nx$ gels. When a strain controlled dynamic frequencies are applied to the gels, the poly(NIPA) chains inside both gels squeeze sufficiently. The sliding and rotating ability of the MPR of the $R_{wi}Nx$ gels can gradually equalize the tension of the polymer chains, but the fixed cross-links of the TNx gels do not permit it. This is why the $R_{wi}N2$ gel is more liquid-like, soft and flexible than the TN1 gel. Identical behaviors (Figure 2.11.b.) could be observed in DMSO, although the E' and E'' values at all frequencies for the $R_{wi}N$ gel are slightly higher than those in water. In DMSO, the MPR chains take up a rigid rod like conformation. DMSO has better affinity to the polyrotaxane strands and also prevents cyclodextrins to aggregate via hydrogen bond. But unmodified -OH groups of α -CDs of MPR in DMSO facilitate the formation of cyclodextrin tube,¹⁷ which to some extent decreases the movability of the cross-linked poly(NIPA) chains through MPR and consequently slightly increases

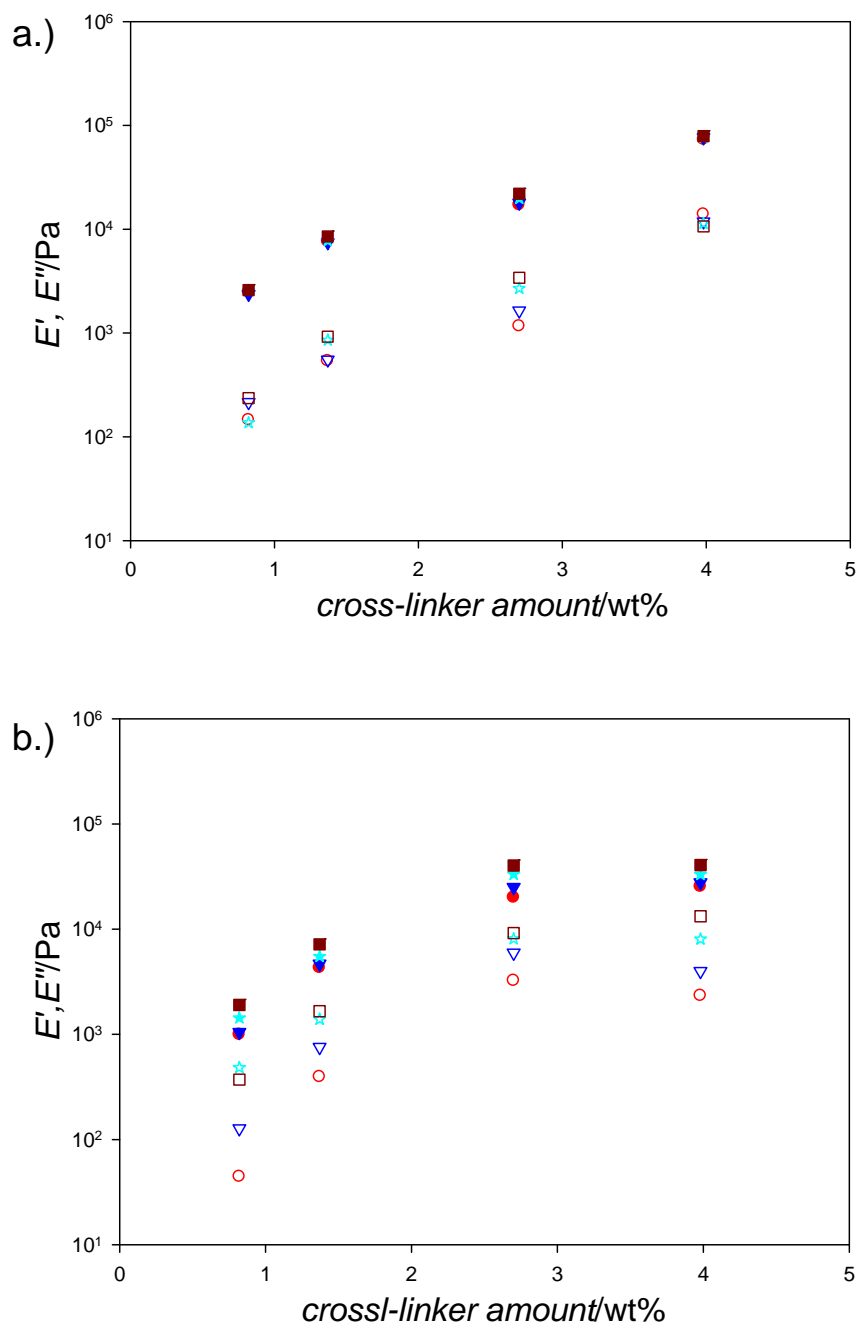


Figure 2.13. Cross-linker amount dependencies on the storage moduli (closed symbols) and loss moduli (open symbols) of $R_{wi}N_x$ gels at 26 °C at the frequencies 0.08 rad sec^{-1} (circle), 2 rad sec^{-1} (triangle down), 20 rad sec^{-1} (star), and 80 rad sec^{-1} (square) a) in water b) in DMSO.

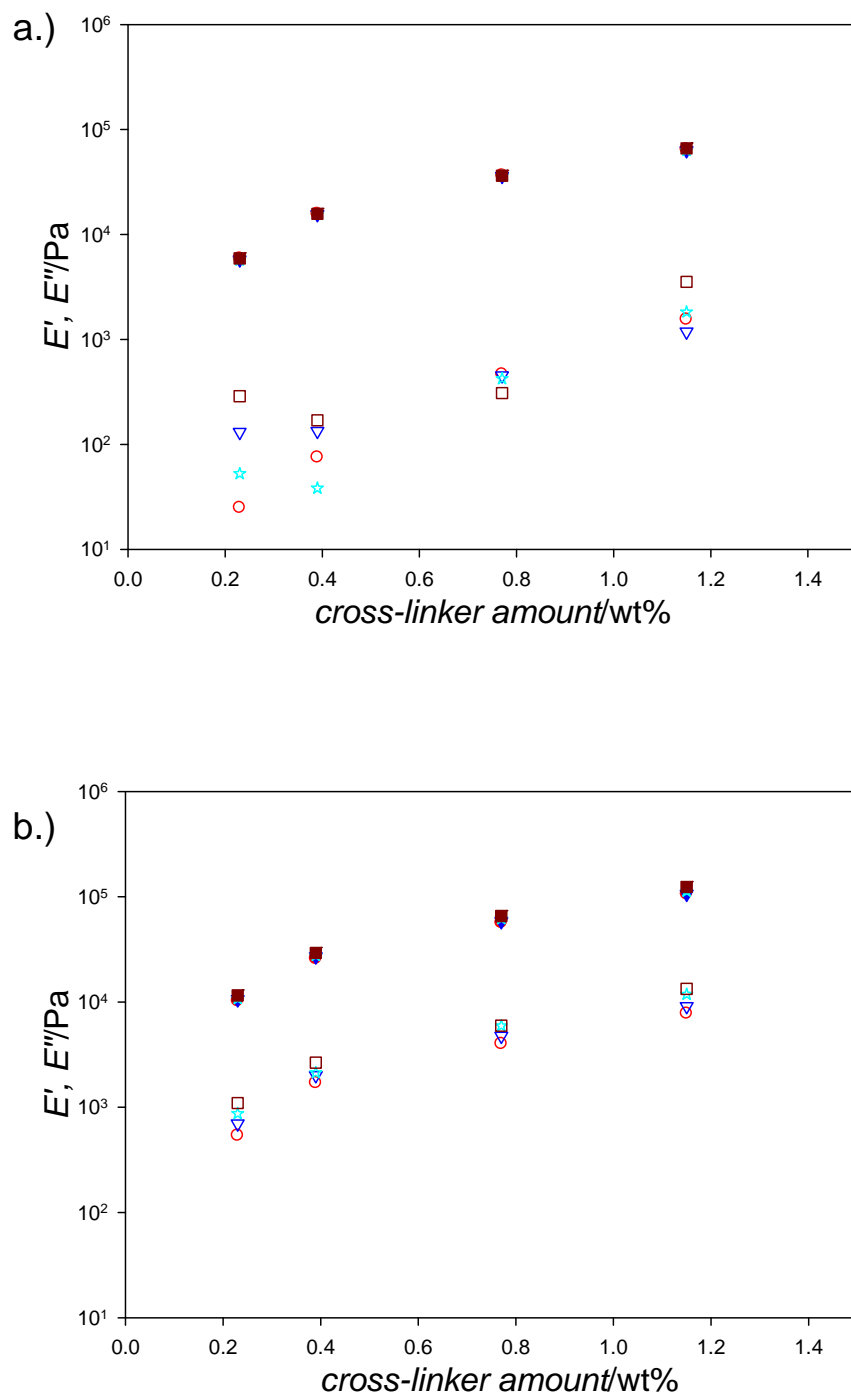


Figure 2.14. Cross-linker amount dependencies on the storage moduli (closed symbols) and loss moduli (open symbols) of TNx gels at 26 °C at the frequencies 0.08 rad sec⁻¹ (circle), 2 rad sec⁻¹ (triangle down), 20 rad sec⁻¹ (star), and 80 rad sec⁻¹ (square) a) in water b) in DMSO.

the values of the modulus. But the storage and loss moduli of the $R_{wi}N_x$ gels in water and DMSO are very small compared to the TN_x gels. That is, in both solvents the sliding and rotating ability of the cross-linked polymer chains prevent them to reach glassy state and provide very soft and flexible nature to the gel networks.

E' and E'' values of the $R_{wi}N_2$ gel increase with rise in temperature in the entire frequency range (Figure 2.12.a.). Above the LCST of NIPA, poly(NIPA) chains turns to collapsed globular form and the sliding ability of the cross-linked poly(NIPA) chains helps the gel networks to reach into complete collapsed state. Water molecules drive out from the gel networks by the evolved squeezing force created from the movement of the polymer networks. The E' and E'' values increase progressively as the temperature is raised below the LCST. A steeper increase in the values is noticed in the volume phase transition temperature above which a steady value is observed.

The values of the moduli of the $R_{wi}N_2$ gel are depended on frequency (Figure 2.12.b.). It is worth mentioning that sliding motion of cross-linked polymer chains occur with ease at low frequencies compared to that at high frequencies. At higher frequency, the cross-link points do not have enough time to counterbalance the experienced tension by the movement of cross-linked polymer networks and soon it starts to respond elastically. We, therefore, observed higher storage and loss modulus values at higher frequencies than that at lower frequencies. Viscoelastic measurements yielded reproducible results with the clear indication that the differences at high to low frequencies are not due to the damage of the gel networks.

E' and E'' are proportional to the cross-linking density in water (Figure 2.13.a.), but in DMSO the feature is slightly different (Figure 2.13.b). In water, an increase in the cross-linker amount results in significant increase in both storage and loss moduli. But in DMSO, at higher cross-linker density, the change in E' and E'' do not follow a

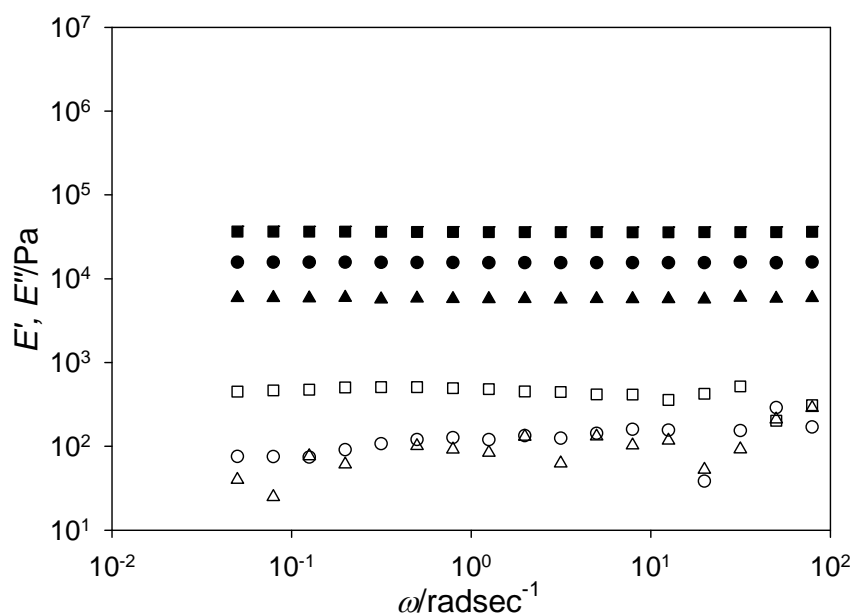


Figure 2.15. Strain-controlled dynamic frequency sweep test of storage moduli (closed symbols) and loss moduli (open symbols) of TN2 (square), TN3 (circle), and TN4 (triangle up) gels in water at 26 °C

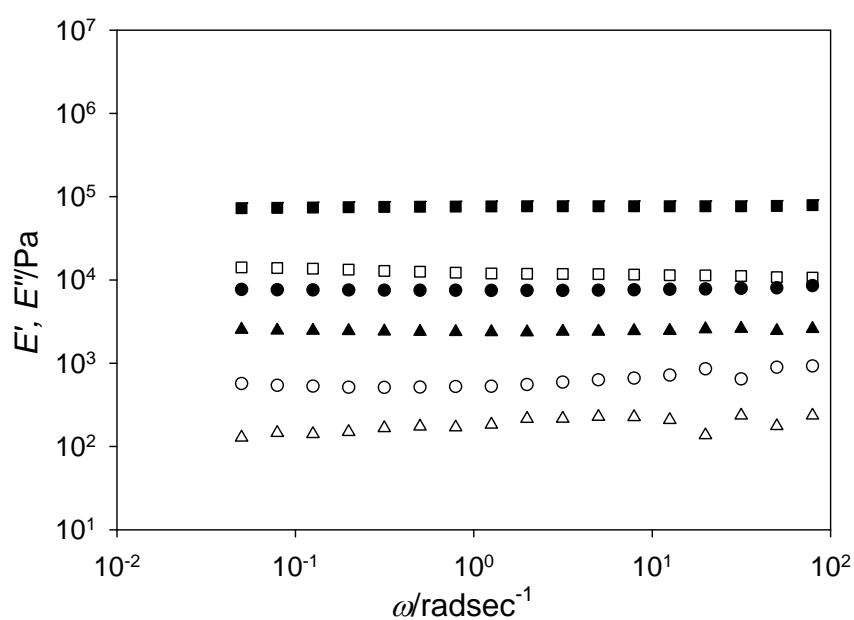


Figure 2.16. Strain-controlled dynamic frequency sweep test of storage moduli (closed symbols) and loss moduli (open symbols) of $R_{wi}N1$ (square), $R_{wi}N3$ (circle), and $R_{wi}N4$ (triangle up) gels in water at 26 °C

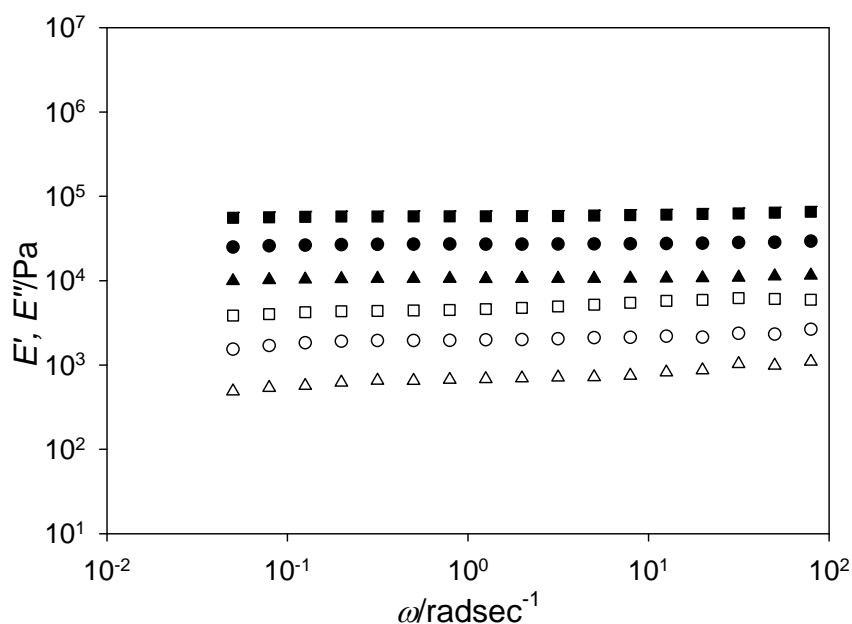


Figure 2.17. Strain-controlled dynamic frequency sweep test of storage moduli (closed symbols) and loss moduli (open symbols) of TN2 (square), TN3 (circle), and TN4 (triangle up) gels in DMSO at 26 °C.

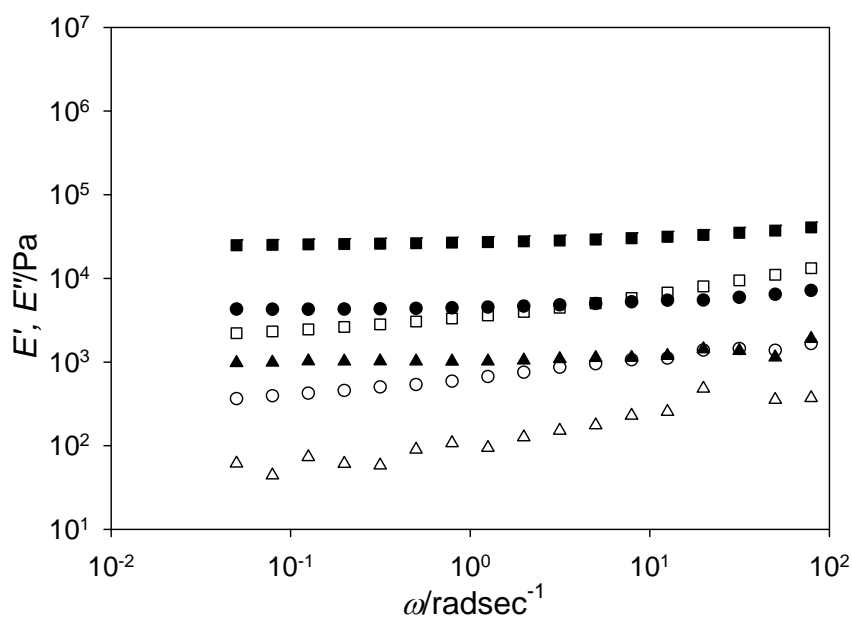


Figure 2.18. Strain-controlled dynamic frequency sweep test of storage moduli (closed symbols) and loss moduli (open symbols) of $R_{wi}N1$ (square), $R_{wi}N3$ (circle), and $R_{wi}N4$ (triangle up) gels in DMSO at 26 °C.

regular trend. As the cross-linker density increases, the average intercross-linking distance decreases suppressing the sliding and rotating ability of cross-link points to some extent. This gives rise to higher modulus values in the rheological plot. It is clear from the rheological behavior that softness or hardness of the $R_{wi}N$ gel may be precisely controlled only by changing the cross-linker density in the pre-gel solution or temperature.

Modification ratio of the cross-linker MPR has a little effect on the swelling ratios of $R_{wi}N2$ gels in water (figure 2.19.). At low temperature, $R_{wi}N2$ (MR = 8.4) gel has been found as higher degree of swelling behavior. In the $R_{wi}N2$ (MR = 11.1) gel networks, one molecule of MPR can attach more polymer chains than $R_{wi}N2$ (MR = 8.4). Hence, the possibilities to form aggregated polymer clusters are high enough which reduces the swelling ratio to some extent. But the mechanical properties of the gels are significantly varied from each other (figure 2.20.). In DMSO it has been found that $R_{wi}N2$ (MR = 8.4) gel has low storage moduli, E' and loss moduli, E'' values than $R_{wi}N2$ (MR = 11.1) gel in the entire frequency ranges. This implies that $R_{wi}N2$ (MR = 8.4) gel formed a soft and flexible gel networks. The presence of low polymer density in the unit space of $R_{wi}N2$ (MR = 8.4) gel networks prevents to form aggregated clusters. Hence the polymer chains in the $R_{wi}N2$ (MR = 8.4) gel possesses more degree of freedom via the movement of the movable cross-links. This gives low moduli value in the strain controlled frequency sweep test.

In our rheological studies, no cracking and breaking were observed for the $R_{wi}Nx$ gels; although the TNx gels exhibited frequent cracking. The $R_{wi}Nx$ gels readily deformed under compression or applied strain and this deformation can gradually alter to its original position when strain is removed from the gel. The characteristic sliding and rotating ability of the cross-linked polymer chains gives a

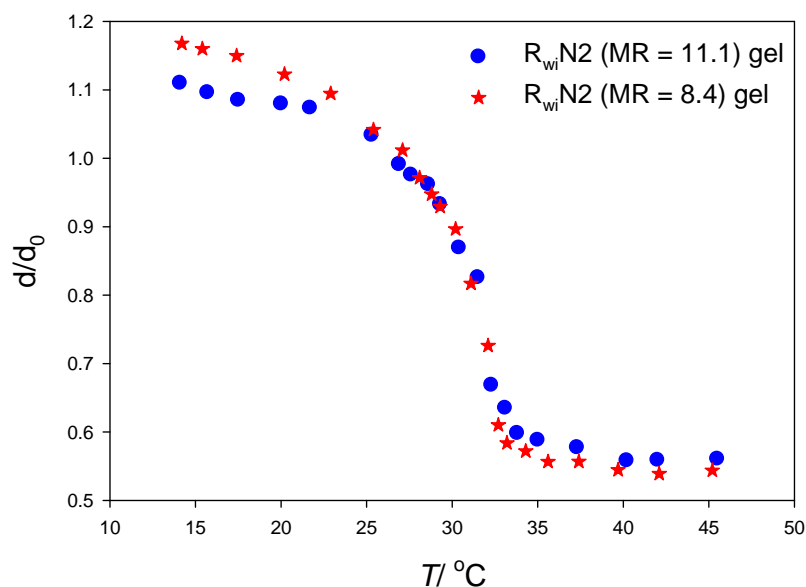


Figure 2.19. Effect of modification ratio of α -CD of the cross-linker MPR on the equilibrium degree of swelling behaviors of $R_{wi}N2$ gels in water.

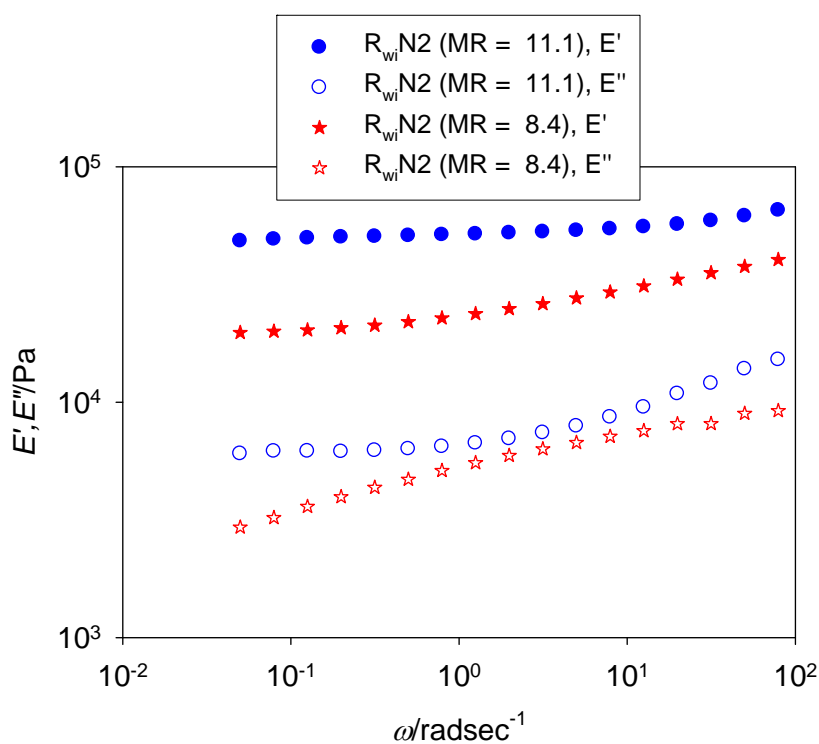


Figure 2.20. Strain-controlled dynamic frequency sweep test of storage moduli, E' and loss moduli, E'' of $R_{wi}N2$ gels prepared by cross-linker, MPR having different modification ratios. The measurements were carried out for the gels swollen in DMSO at 26 °C.

very soft, highly deformable and mechanically stable $R_{wi}N_x$ gels. On the other hand, the covalently bonded fixed cross-links of the TN_x gels divide the long poly(NIPA) chains into short segments. The external tension is, thereby, solely centered on the shortest poly(NIPA) chains and the gel network cannot maintain its mechanical integrity at the micro and macro level.

2.4. Conclusion

In summary, we report here the synthesis of a new movable cross-linker. In the gel network, the cross-link points can slide and rotate with polymer chains, which potentially improve the mechanical properties of the gel over conventional chemically cross-linked polymer gels. The phenomenon of sliding gels may widely be used in the field of biomedical applications.

References

- (1) a) Tanaka, T. *Polymer* **1979**, *20*, 1404. b) Khokhlov, A. R. *Polymer* **1980**, *21*, 376.
c) Tanaka, T. *Sci. Am.* **1981**, *40*, 110. d) Shibayama, M.; Tanaka, T. *Adv. Polym. Sci.* **1993**, *109*, 1. e) Hirotsu, S.; Hirokawa, Y.; Tanaka, T. *J. Chem. Phys.* **1987**, *87*, 1392. f) Tanaka, T.; Nishio, I.; Sun, S-T., Ueno-Nishio, S. *Science* **1982**, *218*, 467-469 g) Mamada, A.; Tanaka, T.; Kungwatchakun, D.; Irie, M. *Macromolecules* **1990**, *23*, 1517-1519.
- (2) a) Tanaka, T. *Phys. Rev. Lett.* **1978**, *40*, 820. b) Suzuki, A.; Tanaka, T. *Nature* **1990**, *346*, 345-347
- (3) Gels Handbook, *vol. 1* (Eds.: Y. Osada.; K. Kajiwara), *Academic press*, San Diego, USA, **2000**.
- (4) Edwards, S.F.; Vilgis, Th. *Polymer* **1986**, *27*, 483
- (5) a) Delaviz, Y.; Gibson, H. W. *Macromolecules.* **1992**, *25*, 4859-4862. b) Gong, C.; Gibson, H. W. *J. Am. Chem. Soc.* **1997**, *119*, 5862-5866. c) Gong, C.; Gibson, H. W. *Macromol. Chem. Phys.* **1998**, *199*, 1801-1806. d) Gibson, H. W.; Nagvekar, D. S.; Yamaguchi, N.; Bhattacharjee, S.; Wang, H.; Vergne, M.; Hercules, D. M. *Macromolecules.* **2004**, *37*, 7514-7529 e) Gong, C.; Gibson, H. W. *J. Am. Chem. Soc.* **1997**, *119*, 8585-8591. f) Gibson, H.W.; Nagvekar, D.; Powell, J.; Gong, C.; Bryant, W. *Tetrahedron* **1997**, *53*, 15197-15207.
- (6) a) Okumura, Y.; Ito, K. *Adv. Mater.* **2001**, *13*, 485-487. b) Oku, T.; Furusho, Y.; Takata, T. *Angew. Chem., Int. Ed.* **2004**, *13*, 966-969. c) de Gennes, P. G. *Physica A.* **1999**, *271*, 231-237. d) Fleury, G.; Schlatter, G.; Brochon, C.; Hadziioannou, G. *Polymer.* **2005**, *46*, 8494–8501 e) Araki, J.; Ito, K. *Soft Matter* , **2007**, *3*, 1456-1473 f) Karaky, K.; Brochon, C.; Schlatter, G.; Hadziioannou, G. *Soft Matter.* **2008**, *4*, 1165-1168

- (7) a) Cantrill, S. J.; Pease, A. R.; Stoddart, J. F. *J. Chem. Soc., Dalton Trans.* **2000**, 3715-3734. b) Huang, F.; Gibson, H. W. *Progr. Polym. Sci.* **2005**, *30*, 982-1018. c) Molecular Catenanes, Rotaxanes and Knots, Sauvage, J.-P.; Dietrich-Buchecker, C. O., eds., *Wiley-VCH*, Weinheim, **1999**. d) Mahan, E.; Gibson, H. W. Rotaxanes, in *Cyclic Polymers*, 2nd ed., Semlyen, A. J.; ed., *Kluwer Publishers*, Dordrecht, **2000**, 415-560. e) Takata, T.; Kihara, N. *Rev. Heteroatom Chem.* **2000**, *22*, 197-218. f) Hubin, T. J.; Busch, D. H. *Coord. Chem. Rev.* **2000**, *200-202*, 5-52. g) Panova, I. G.; Topchieva, I. N. *Russ. Chem. Rev.* **2001**, *70*, 23-44. h) Carlucci, L.; Ciani, G.; Proserpio, D. M. *Coord. Chem. Rev.* **2003**, *246*, 247-289.
- (8) Zhao, C.; Domon, Y.; Okumura, Y.; Okabe, S.; Shibayama, M.; Ito, K. *J. phys.: Condens. Matter.* **2005**, *17*, S2841-S2846.
- (9) Harada, A.; Li, J.; Kamachi, M. *Nature.* **1993**, *364*, 516-518.
- (10) a) Taylor, P. N.; O'Connell, M. J.; McNeill, L. A.; Hall, M. J.; Aplin, R. T.; Anderson, H. L. *Angew. Chem., Int. Ed.* **2000**, *39*, 3456-3460. b) Shimomura, T.; Akai, T.; Abe, T.; Ito, K. *J. Chem. Phys.* **2002**, *116*, 1753-1756. c) Silva, C.; Friend, R. H.; Severin, N.; Samori, P.; Rabe, J. P.; O'Connell, M. J.; Taylor, P. N.; Anderson, H. L. *Nat Mater.* **2002**, *1*, 160-164. d) Taylor, P. N.; Hagan, A. J.; Anderson, H. L.; *Org Biomol Chem.* **2003**, *1*, 3851-3856. e) Michels, J. J.; O'Connell, M. J.; Taylor, P. N.; Wilson, J. S.; Cacialli, F.; Anderson, H. L. *Chem-Eur J.* **2003**, *9*, 6167-6176. f) Frampton, M. J.; Anderson, H. L. *Angew. Chem. Int. Ed.* **2007**, *46*, 1028-1064.
- (11) a) Yui, N.; Ooya, T.; Kumeno, T. *Bioconj. Chem.* **1998**, *9*, 118-125. b) Ooya, T.; Yui, N. *J. Controlled Release.* **2002**, *80*, 219-228. c) Ooya, T.; Arizono, K.; Yui, N. *Polym. Adv. Technol.* **2000**, *11*, 642-651.

- (12) a) Tamura, M.; Ueno, A. *Bull Chem Soc Jpn* **2000**, 73, 147–154. b) Tamura, M.; Gao, D.; Ueno, A. *Chem—Eur J* **2001**, 7, 1390–1397.
- (13). Karino, T.; Shibayama, M.; Okumura, Y.; Ito, K.; *Physica B*. **2006**, 385–386, 807–809
- (14) Harada, A. *Coord. Chem. Rev.* **1996**, 148, 115-133.
- (15) Araki, J.; Zhao, C.; Ito, K. *Macromolecules*. **2005**, 38, 7524-7527.
- (16) Imran, A. B.; Seki, T.; Kataoka, T.; Kidowaki, M.; Ito, K.; and Takeoka, Y.; *Chem. Commun.*, **2008**, 41, 5227-5229
- (17) a) Karino, T.; Okumura, Y.; Ito, K.; Shibayama, M. *Macromolecules*. **2004**, 37, 6177-6182. b) Fleury, G.; Schlatter, G.; Brochon, C.; Travelet, C.; Lapp, A.; Lindner, P.; and Hadziioannou, G. *Macromolecules*. **2007**, 40, 535-543. c) Fleury, G.; Schlatter, G.; Brochon, C.; and Hadziioannou, G.; *Adv. Mater.* **2006**, 18, 2847-2851.

CHAPTER

3

Anomalous shrinking and swelling behavior of poly(NIPA) gels prepared by hydrophilic polyrotaxane based movable cross-linkers

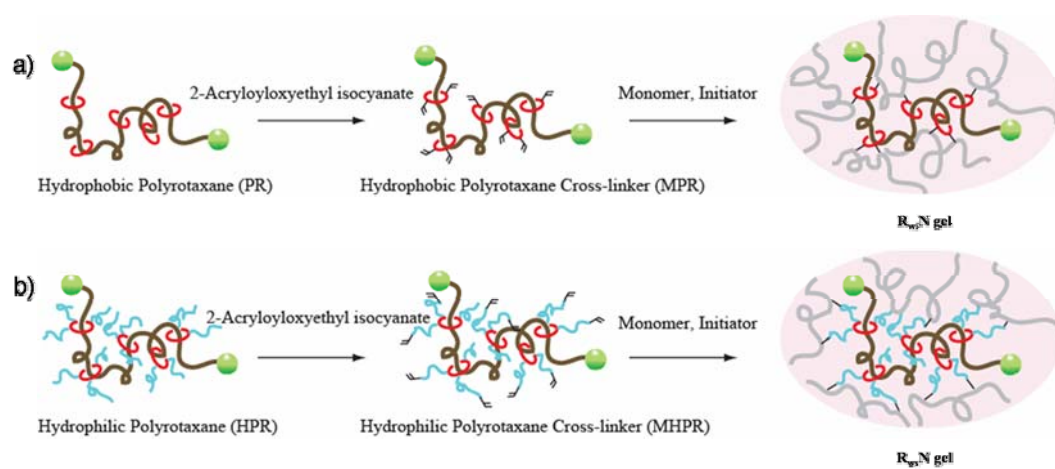
Abstract

The syntheses of novel hydrogels using hydrophilic polyrotaxane as a movable cross-linker have been reported here. A sparsely dispersed α -Cyclodextrins modified by propylene oxide was threaded into the long polyethylene glycol ($M_w = 35000 \text{ g mol}^{-1}$) and capped by bulky 1-adamantanamine molecules of the polyrotaxane (HPR) unit was used. HPR was modified by small amount 2-acryloyloxyethylisocyanate monomer through the formation of stable carbamate bond to obtain polyrotaxane-based multifunctional cross-linker, MHPR. Polymer gels were synthesized by free radical polymerization of thermo-sensitive monomer *N*-isopropylacrylamide (NIPA) and cross-linker MHPR. A transparent, very soft, flexible, mechanically stable and homogeneous gel was obtained. Introduction of hydrophilic moieties to the hydrogel network increase the degree of swelling at low temperatures; but unusually the volume phase transition temperature does not shift to higher temperatures. The shrinking and swelling kinetics of the gel has been found very fast. By a proper control over the monomer to cross-linker ratio, inherent large hysteresis during shrinking of the poly(NIPA) chains inside the gel networks can be ignored completely. The gel changes its volume isotropically and reaches rapidly to the equilibrium shrunken state after a temperature jump. The hydrophilicity of the cross-linker retains the homogeneity of the gel network and restricts the formation of aggregated globules, which permits the poly(NIPA) chains inside the gel network to move or rotate freely through the long polymer axle under deformation. The movability of the cross-linked polymer chains can strongly minimize their localized stress during deformation. The fascinating characteristics behavior of the gel was compared and contrasted with the gel prepared using the multifunctional hydrophobic polyrotaxane cross-linker and bi-functional *N,N'*-methylene-bis-acrylamide cross-linker.

3.1. Introduction

Stimuli sensitive poly(*N*-isopropylacrylamide) hydrogels, due to their fascinating characteristics, *inter alia*, volume change at ambient temperature, change in opacity and in the gel surface from hydrophilic to a hydrophobic one, and adsorption and desorption of solutes, attributable to the phase transition of poly(NIPA) chains at the lower critical solution temperature (LCST), have received a surge of interest for manifold applications, which include: drug delivery systems¹, biosensors², on-off switches³, artificial muscles⁴, bio-catalysts⁵, and immobilization of enzymes⁶. But the inherent weak mechanical properties, such as, critical slowing down during the process of shrinking and less bio-compatibility of the conventional cross-linkers used for gelation restrict the use of hydrogels of this variety for widespread use.

Sliding gels in which the cross-linking points can slide through the polymer axle^(7,8) have recently been introduced to have improved mechanical strengths. The novel polymer gels, are synthesized from polyrotaxane; the latin word “rota” corresponds to a wheel and “axis” to an axle. Polyrotaxane is a supramolecule in which macro cycle rings are threaded onto long polymer axles and trapped by bulky end group moieties. The conceptual model of rotaxane structure was first proposed by Frisch et al⁹ and syntheses realized by Harrison and coworkers¹⁰. α -Cyclodextrin/polyethylene glycol (α -CD/PEG) based polyrotaxane has been the most promising one due to its facile synthesis, bio-compatibility and possibilities to modification of hydroxyl groups of each cyclodextrin by variety of functional groups. The CD molecules of polyrotaxane can slide along with PEG axle at a correlation time of the order of $0.1\text{-}1\text{ ms}^{-1}$ and the sliding of α -CD can be observed even in the cross-linked polyrotaxane gel.¹¹ Gels of this kind can be regarded as



Scheme 3.1. Schematic representation of the preparation of hydrophobic and hydrophilic polyrotaxane cross-linkers and their applications for the preparation of RN gels in DMSO.

intermediates between physical and chemical gels. The gel network is formed by strong covalent interactions of polymer chains like chemical gels and can reorient its cross-linking points under deformation like physical gels. Sliding gels can be prepared simply by cross-linking among macro-cycles of different polyrotaxane units, which yields a gel having improved mechanical strength. However, introduction of this novel sliding phenomenon into the gel network for different polymer systems, which in most cases are not suitable to form complicated polyrotaxane like architecture to obtain sliding gels, is rather difficult and progress in this area, is still in the rudimentary stage.

Recently, we have reported¹² the synthesis of poly(NIPA) gels using small amount of hydrophobic vinyl modified polyrotaxane as a cross-linker. The gels show very distinctive features to typical poly(NIPA) gel (TN gel); the gels are very soft and flexible in nature, mechanically stable and undergo homothetic deformation after a temperature jump etc. The gels imply significant improvements to the conventional poly(NIPA) gel; but owing to the hydrophobicity of the cross-linker used, the gels have been reported to be heterogeneous in aqueous medium in nature.

Research to-date include numerous attempts to obtain fast shrinking poly(NIPA) gels. The various means used to enhance shrinking rate of poly(NIPA) gels are the preparation of hydrogels with a heterogeneous structure¹³ or with a macro porous network based on the porosigen technique,¹⁴ introduction of small amount of hydrophilic moieties to the gel network,¹⁵ and introduction of freely mobile dangling chains onto the gel network.¹⁶ It is highly desirable to obtain hydrogels capable of faster shrinking and swelling as well as homogeneous deformation; however it still remains an elusive goal and a new route is yet to be opened up.

In this study, we develop a water soluble polyrotaxane cross-linker and prepared hydrogels using the cross-linker. The novel shrinking and swelling behaviors of the gels have been compared with TN gels and hydrogels prepared with hydrophobic polyrotaxane as a cross-linker. The phenomenon of sliding has been explained for the novel hydrogels prepared using hydrophilic movable cross-linker. Finally, we propose a mechanism to correlate the swelling/shrinking behavior and mechanical properties with change in the nature of the cross-linker.

3.2. Experimental

3.2.1. Materials

Polyrotaxanes, PR and HPR, were purchased from Advanced Soft materials Inc., Tokyo, Japan and used without further purification. *N*-isopropylacrylamide (NIPA) from Kohjin Co., Tokyo, Japan was purified by recrystallization from toluene/n-hexane. *N,N'*-methylene-bis-acrylamide (BIS) from Acros Organics, Geel, Belgium, α,α' -azoisobutyronitrile (AIBN) from (Kanto Chemical Co., Japan), dibutylene-tetrakis(4-methylbenzoate) (DBTDL) and butyl hydroxyl toluene (Tokyo Kasei Kogyo Co., Japan) were reagent-grade materials and were used as received unless otherwise noted. 2-Acryloyloxyethyl isocyanate was purchased from Showa Denko K.K, Japan. Milli-Q ultra pure water was used throughout the experiments.

3.2.2. Preparation of MPR and MHPR

PR and HPR (500 mg), DBTDL as the catalyst (1 drop), and butylhydroxy toluene (inhibitor, 0.78 mg) were dissolved in 30 ml of anhydrous DMSO. A solution of 2-acryloyloxyethyl isocyanate (78 mg) was dissolved in 10 ml of DMSO and added drop wise to the mixtures with vigorous stirring in the dark. The mixtures were then continuously stirred overnight at 40 °C to ensure that the reactions are complete. MPR and MHPR were reprecipitated from the reaction mixtures using excess methanol and

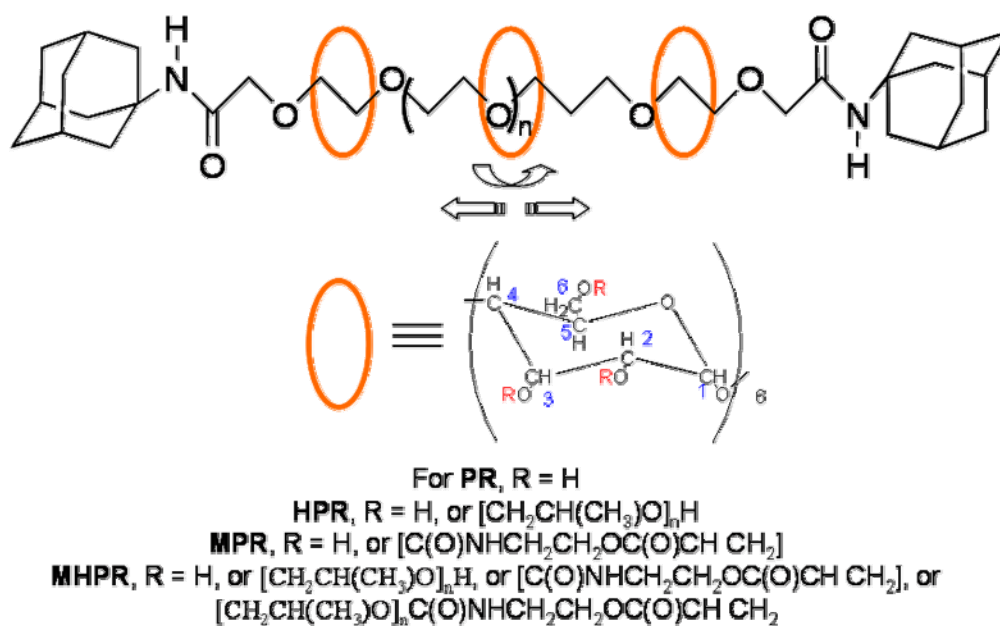


Figure 3.1. Supramolecular structures of water insoluble polyrotaxane, PR; water soluble polyrotaxane, HPR; water insoluble polyrotaxane cross-linker, MPR; and water soluble polyrotaxane cross-linker, MHPR.

Table 3.1. Sample codes of RNx and TNx gels (DMSO as a solvent)

Sample codes (RN gel)	NIPA Monomer (M)	MPR (wt%)	MHPR (wt%)	BIS (mM)	AIBN (mM)
R _{wi} N(1)	1	2.27	×	×	8.13
R _{ws} N(1)	1	×	2.27	×	8.13
R _{wi} N(2)	2	2.27	×	×	8.13
R _{ws} N(2)	2	×	2.27	×	8.13
TN(1)	1	×	×	16.7	8.13
TN(1)0.05	1	×	×	50	8.13
TN(2)	2	×	×	33.4	8.13

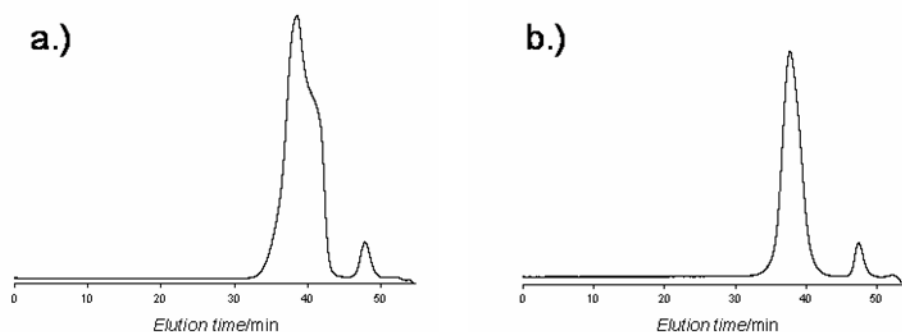


Figure 3.2. GPC profiles of polyrotaxane based a.) hydrophobic cross-linker, MPR and b.) hydrophilic cross-linker, MHPR. In each case the feeding ratio, F.R. was 2.

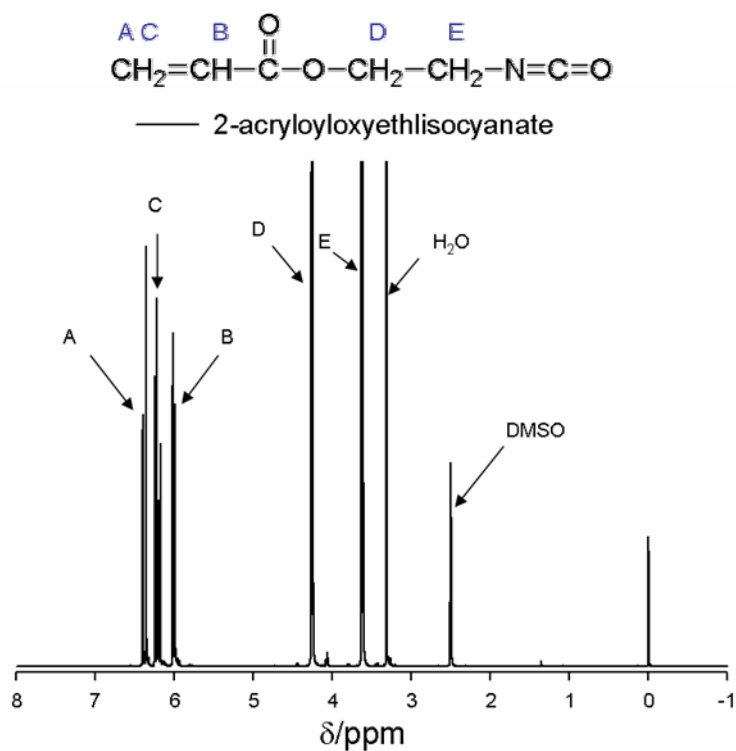


Figure 3.3. ^1H -NMR spectrum of 2-acryloyloxyethyl isocyanate in DMSO- d_6 with TMS as an internal standard.

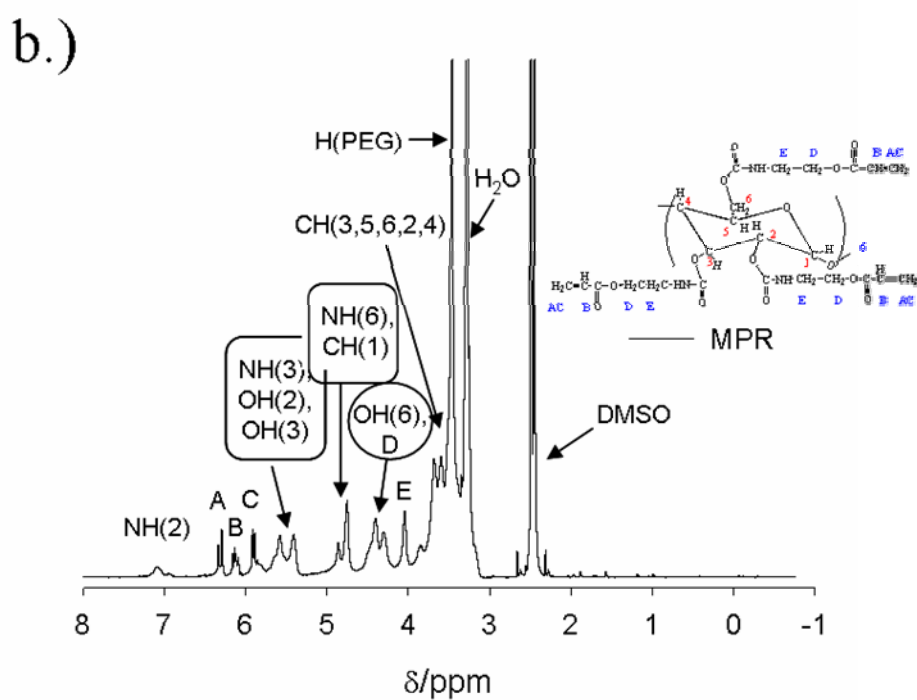
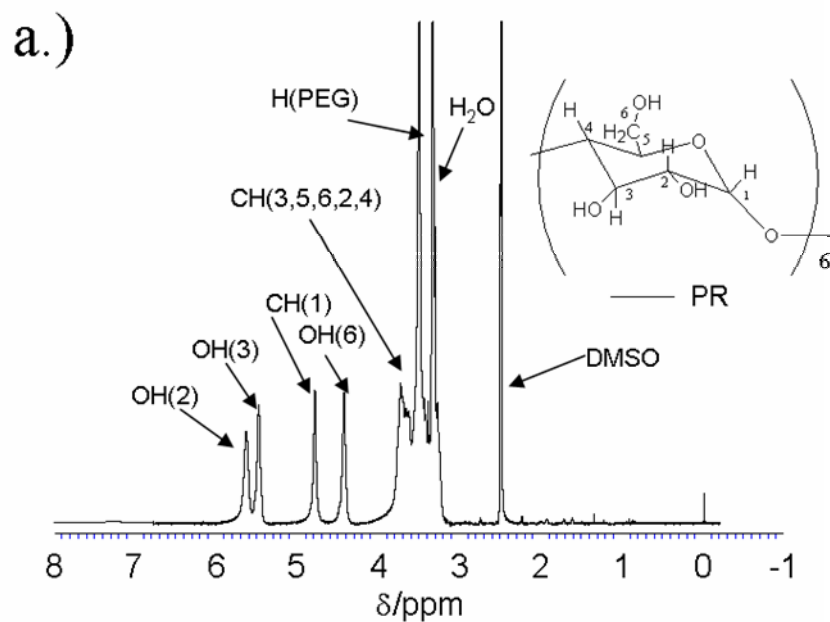
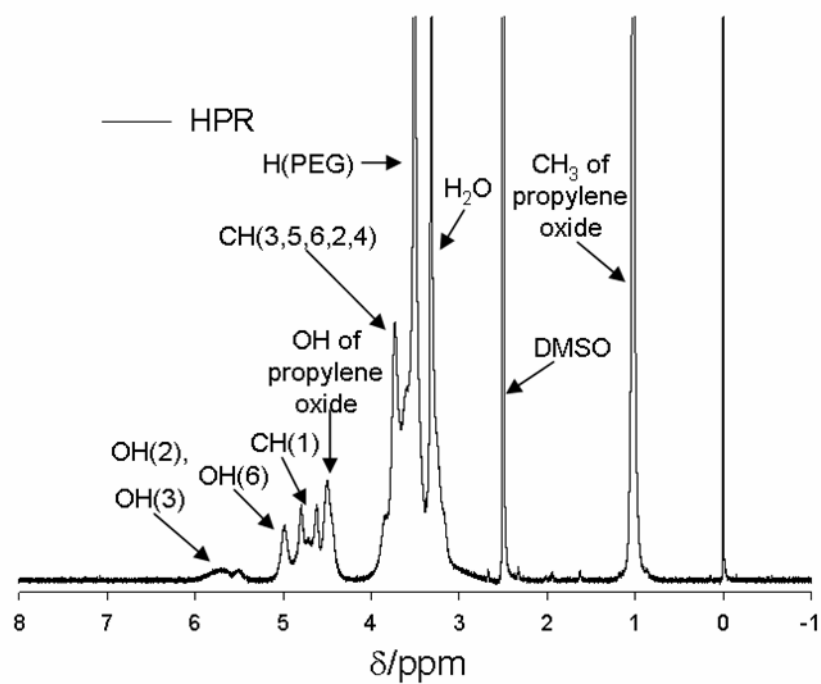


Figure 3.4. ^1H -NMR spectra of a.) PR and b.) MPR in DMSO- d_6 with TMS as an internal standard.

a.)



b.)

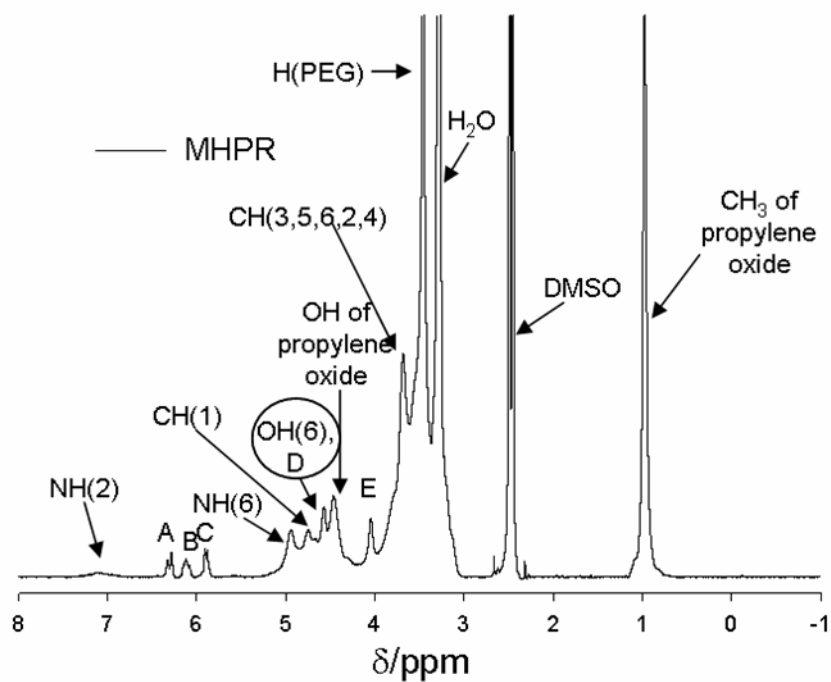


Figure 3.5. ^1H -NMR spectra of a.) HPR and b.) MHPR in DMSO- d_6 with TMS as an internal standard.

acetone followed by keeping at refrigerator. The products were washed several times with methanol and acetone and then freeze dried.

3.2.3. Preparation of Rotaxane-NIPA, RN gel

RN gels were prepared by conventional free radical polymerization where the concentrations of NIPA monomer was varied from 1 to 2 M; but the amount of cross-linkers was kept constant (2.27 wt % with respect to the solvent) (Table 3.1.). Varying amount of NIPA, 2.27 wt% MPR and MHPR respectively, and 8.125 mM AIBN (initiator) were dissolved in anhydrous DMSO. N₂ bubbling was passed through the pre-gel solutions for 30 m followed by sonication to remove excess nitrogen from the solution. The pre gel solution was infused to glass slides separated by Teflon spacers for the preparation of slab gels. Cylindrical gels were prepared using micro-capillary with an inner diameter of 270 μ m. The gelations were carried out at 60 °C for 24 h. The gels were thoroughly washed with DMSO followed by water for two weeks to take away the unreacted monomer and reaction residues.

3.2.4. Preparation of typical poly(NIPA), TN gel

TN gels were prepared following the method described earlier for the preparation of RN gels. Varying amount of bi-functional BIS was used as a cross-linker for gelation. For all cases, NIPA was polymerized with almost 100% conversions, since after gelations no more residue of pregel solutions were observed.

3.2.5. ¹H-NMR spectra

¹H-NMR spectra were carried out with 400MHz NMR A-400 (JEOL) spectrometer. Tetramethylsilane (TMS) was used as an internal standard for the analysis of chemical shifts.

3.2.6. Setup for shrinking and swelling kinetics

The cylindrical gels were poured into a desired solvent in a controlled glass cell. Two circulators fixed at two different target temperatures were connected to the glass cell. By changing the path of the solvent, temperature inside the cell can quickly be switched from one temperature to another and the temperature inside the cell was stable to ± 0.2 °C over few hours. The switching time to reach the temperature at target temperature was about 2 minutes. The volume change of the cylindrical gels was monitored under an inverse microscope equipped with color measuring unit. The video of the morphological change of gels were recorded using BUFFALO PCast TV capture software in a computer and then pictures were captured at different time intervals. To measure the kinetics of shrinking and swelling behaviors of gels, first the gel was equilibrated at initial temperature and then suddenly move out the gel sample to another cell where the cell was fixed at final desired temperature. The switching time was ± 5 sec. The change in diameter of the cylindrical gel was measured by a digital microscope (Keyence, VHX-500).

3.2.7. Transmittance spectra of gels

The transmission spectra were obtained by using an Ocean optics inc. QE65000 optical-fiber spectrometer in which deuterium-halogen (Mikropack) lamp was used as a light source. The diameter of the slab gel samples were *ca.* 2 mm.

3.2.8. Thermo Gravimetric / Differential Thermal Analysis, TG/DTA

TG/DTA data were measured by TG/DTA6300 of Seiko Instruments Inc., Japan. For each measurement 5 mg dried powdered sample was taken in a platinum sample pan and analyzed in the range of 20 °C - 450 °C at a heating rate of 10 °C per minute.

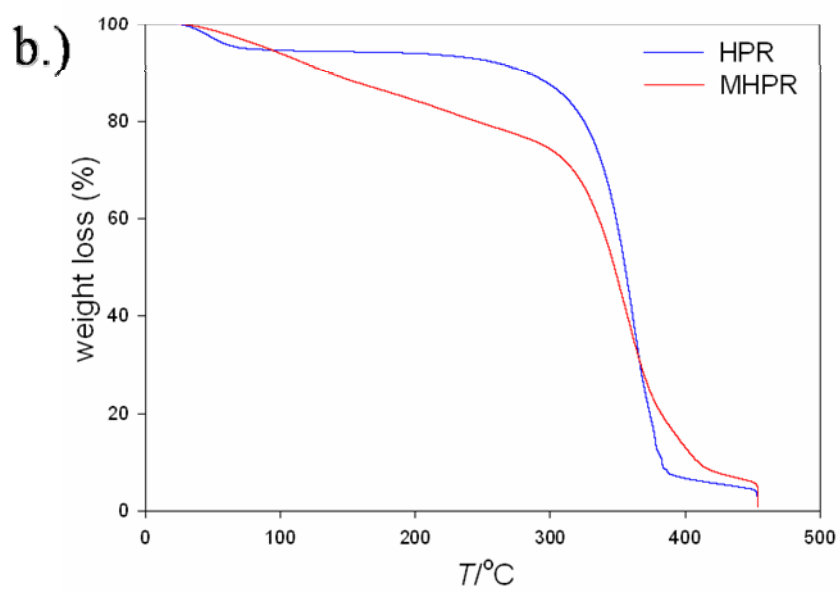
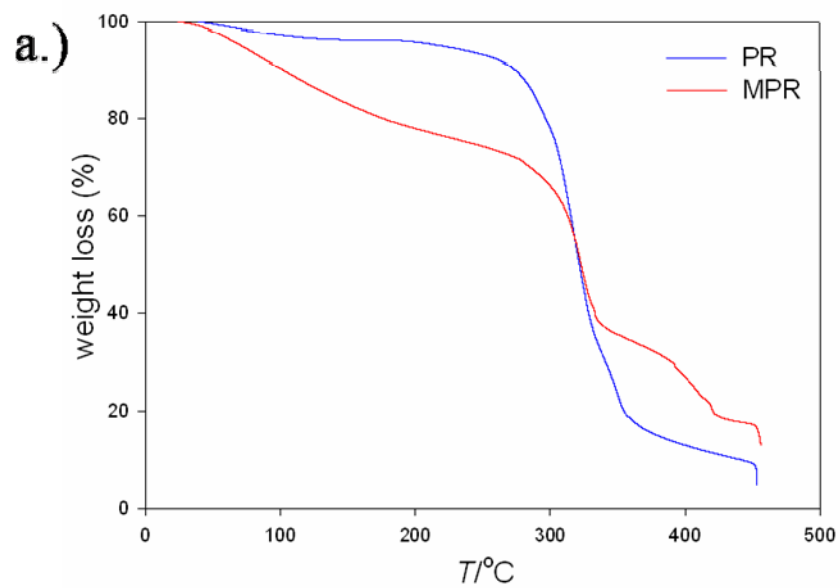


Figure 3.6. Thermo-gravimetric plots of a.) PR and MPR b.) HPR and MHPR at a heating rate of 10 °C per minute.

3.2.9. Scanning Electron Microscope, SEM

The equilibrium swollen hydrogel samples in water at 4 °C were quickly frozen in liquid nitrogen and then fractured carefully there. Samples were then freeze dried under vacuum at -52 °C for 3 days. The internal morphology of the samples was studied by a scanning electron microscope (SEM, JEOL JSM-5600). Samples were coated with Au prior to the SEM observations.

3.2.10. Rheometric Solids Analyzer, RSA

The mechanical properties of gels were measured with a Rheometric Solid Analyzer, RSA III of Rheometric Scientific, Inc. The detailed of the instrumentation and measurement process have been given to the previous chapter. Two types of gel samples were used for the measurements, as prepared gel and gel swollen in different solvents at room temperature. As prepared slab gels (thickness = 4 mm) were cut into square shapes (10 mm \times 10 mm) prior to each measurement. On the other hand after reaching equilibrium swelling states of the as prepared gels, the swollen gels were cut into square shapes (10 mm \times 10 mm). The deswelling of gels was avoided throughout the measurements by immersing the gel samples in the desired solvent. To ensure the samples are always in contact with the instrument, a constant pre-strain of 5 % was applied to the samples from the transducer prior to each measurement. The moduli of the samples were measured at a frequency range of 0.01 to 100 Hz. Frequency controlled dynamic strain sweeps were run on all of the samples to confirm that the viscoelastic measurements were consistently collected in the linear viscoelastic regime. The storage and loss moduli as a function of strain amplitude ranging from 0.01 to 20% at room temperature was carried out at a fixed frequency, $\omega = 1 \text{ rad sec}^{-1}$ for this purpose. The strain controlled dynamic frequency sweep test was performed in the linear viscoelastic region (3%) for every sample.

3.3. Results and Discussion

3.3.1. Preparations and characterizations of polyrotaxane cross-linkers and their gels

Polyrotaxanes used in this study belong to two distinct categories: unmodified polyrotaxane, PR and hydroxypropylated polyrotaxane, HPR (see Figure 3.1.). These have been used as starting materials for the preparation of hydrophobic and hydrophilic polyrotaxane cross-linkers respectively. The detail of syntheses of PR and HPR are reported in the literatures.¹⁷

PR consists of α - cyclodextrin (inclusion ratio 26%), poly(ethylene glycol) carboxylic acid (MW = 35000) and adamantanamine (terminal bulky moieties). The weight average molecular weight of PR, MW= 97040 and polydispersity index, $M_w/M_n = 1.55$. On the other hand, HPR, was originated from the hydroxypropylation of α -CD of PR. Inclusion ratio of the hydroxypropylated α -CD into the HPR is 29%. Molecular substitution (MS) i.e. average mole number of the introduced propylene oxide groups per α -CD unit is 9.18. ($M_w = 125824$ and $M_w/M_n = 1.4$).

PR is insoluble in the most of the solvents particularly in water due to the presence of strong inter- and intra-molecular hydrogen bonds among the hydroxyl groups of α -CDs. In contrast, introduction of propylene oxide to PR reduces the hydrophilicity of hydroxyl groups which suppresses the tendency to form hydrogen bonds. Eventually HPR becomes soluble in water.

PR and HPR were modified by a 2-acryloyloxyethyl isocyanate having both isocyanate and vinyl groups in its parent structure. The isocyanate group forms a stable carbamate bond with the hydroxyl groups to yield cross-linkers, which we refer to as MPR and MHPR, respectively. Degrees of substitution (DS) ($0 \leq DS \leq 18$), i.e., the average number of substituted hydroxyl groups per α -CD unit of the MPR and

MHPR, calculated using ^1H NMR spectra (see Figure 3.3.- 3.5.) were found to be 2.25 and 1.13.

Poly(NIPA) gels were prepared by conventional free radical polymerization in presence of MPR and MHPR cross-linkers in di-methylsulfoxide (DMSO) medium. The gels are very soft and transparent soon after preparation. For the sake of comparison, typical NIPA, TN gels were also prepared using bi-functional *N,N'*-methylene-*bis*-acrylamide (BIS) as a cross-linker. The gel samples used in this study are denoted as TN_x for typical NIPA, TN gels and $\text{R}_{\text{wi}}\text{N}_x$, $\text{R}_{\text{ws}}\text{N}_x$ for hydrophobic and hydrophilic rotaxane-NIPA, RN gels respectively, where *N* stands for NIPA, R_{wi} is water insoluble polyrotaxane cross-linker, R_{ws} is water soluble polyrotaxane cross-linker and *x* is the amount of NIPA (in molarity). For RN gel the total weight percent of cross-linker MPR and MHPR with respect to the solvent and were maintained constant, at 2.27 wt%. In the subsequent sections, we will ignore mentioning this value to avoid insignificant repetitions.

PNIPA chains in TN gel are randomly cross-linked by large number of bi-functional cross-linker BIS in which the cross-links fix the polymer chains to different segments having different lengths. Under deformation all of the stress is, thereby, localized on the shortest poly(NIPA) chains and soon the cross-linked polymer networks start to respond elastically. This gives rise to stiffness of the gels, although they are mechanically fragile in nature. In contrast, RN gels are inherently soft and flexible in nature since covalently cross-linked PNIPA chains, under deformation, have the ability to slide and rotate through the movable cross-linkers.

3.3.2. Transparency tests of RN gels

Figure 3.7 and 3.8 represent the transmission spectra of $\text{R}_{\text{wi}}\text{N}_x$ and $\text{R}_{\text{ws}}\text{N}_x$ gels in water and DMSO at room temperature. RN gels are highly transparent in DMSO in

the region of visible wavelength (Figure 3.7.), which is indicative of the formation of homogeneous gel networks. When these gels are immersed and equilibrated in water (Figure 3.17.), the transparency of $R_{wi}N$ gel decreases markedly. However, $R_{ws}N$ gels still remain transparent. In $R_{wi}N$ gel, unreacted hydroxyl groups of α -CD of MPR can form intra- and inter-molecular hydrogen bonds with the neighboring MPR; this additional physical interaction as well as the water insolubility of the cross-linker MPR, ease the aggregation of cross-linked polymer networks to form clusters in the highly cross-linked region. The clusters, being larger in size than the wavelength of the visible light, can not transmit visible light. Hydrophobic rotaxane-NIPA, $R_{wi}N$ gels are, therefore, remarkably opaque in water.

On the other hand, presence of hydrophobic propylene oxide in the MHPR reduces the possibilities of formation of hydrogen bond and increases the solubility in water. Hence, aggregation of cross-linked polymer chains becomes unlikely and hydrophilic rotaxane-NIPA, $R_{ws}N$ gels are transparent in both solvents.

When light travels in a medium where the existed clusters are much smaller than the wavelength of visible light, Rayleigh scattering occurs and it is inversely proportional to the fourth power of the wavelength.¹⁸ That is, shorter wavelength will scatter more than the longer wavelength. Plotting $\ln(-\ln T)$ vs $\ln \lambda$ for $R_{wi}N(1)$ and $R_{ws}N(1)$ gels (Figure 3.8.) give a straight lines with slopes -2.39 and -2.84 respectively, indicating that the scattering of these samples deviates from Rayleigh scattering. The sizes of the aggregated clusters are close to or greater than the wavelengths of visible light, Mie scattering occurs for both gels. Although in both RN gels exhibit Mie scattering but the sizes of the clusters are relatively smaller in case of $R_{ws}N(1)$ gel.

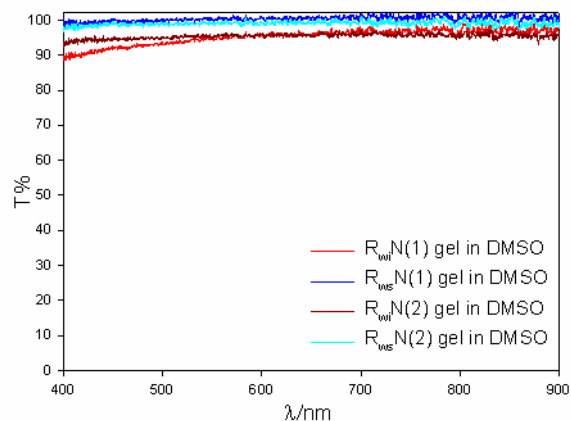


Figure 3.7. The change in transmission spectra of $R_{wi}N(1)$, $R_{ws}N(1)$, $R_{wi}N(2)$ and $R_{ws}N(2)$ gels in the visible light wavelength range in DMSO at room temperature (25 °C).

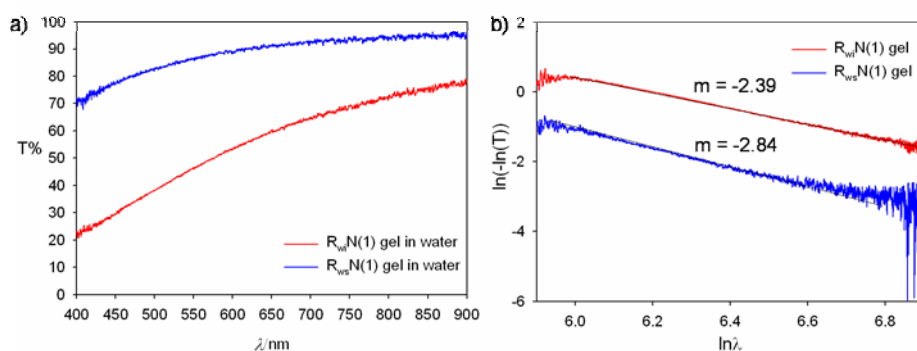


Figure 3.8. a.) The change in transmission spectra of $R_{wi}N(1)$ (red line), $R_{ws}N(1)$ (blue line) gels in the visible light wavelength range in water at room temperature (25 °C) b) $\ln(-\ln T)$ vs $\ln \lambda$ plot.

3.3.3. Swelling behaviors of RN gels

In Figure 3.9.a., the static equilibrium swelling ratio, d/d_0 , of $R_{wi}N(1)$ and $R_{ws}N(1)$ gels, where d and d_0 are the diameter of the equilibrated gels under a certain condition and the diameter of cylindrical gel at a preparative state, respectively, were plotted as a function of temperature. In analogous to TN gels, RN gels also have a sharp volume phase transition in water around 32.0 °C for the existence of LCST of poly(NIPA) chains at that particular temperature.

It has been reported that the sub-chains in the polymer networks under the preparation conditions behave like Gaussian chains.¹⁹ Hence the quantitative estimation of the static conditions of the sub chains in the equilibrium state of the gels can be measured from the lengths of gels i.e the linear expansion factor of the polymer chains will be equivalent to d/d_0 ($\alpha = d/d_0$). In the swollen state of gels α can be expressed by $\alpha \approx (Bn_0N)^{1/5}$ where B is the second virial coefficient, $B = \nu_m(\frac{1}{2} - \chi)$, ν_m is the molar volume of the monomer, N is the length of the sub chains and n_0 is the average monomer concentration in the gel network at reference state. At a glance, it can be assumed from the above equations that $R_{ws}N$ and $R_{wi}N$ gels will exhibits identical degree of swelling behavior below the LCST of NIPA, as the molar volume of the monomer and cross-linkers were maintained same. Experimentally it has been found that $R_{ws}N$ gel has higher degree of swelling behavior than $R_{wi}N$ gel at the lower temperatures. At temperatures above the LCST, $\alpha^{-3} \cong -\frac{B}{2Cn_0}$ where C is the third virial coefficient.²⁰ The swelling degree in the collapsed network depends on the initial monomer concentration, and the length of a subchain does not affect the swelling degree. But in case of $R_{ws}N$ gel the

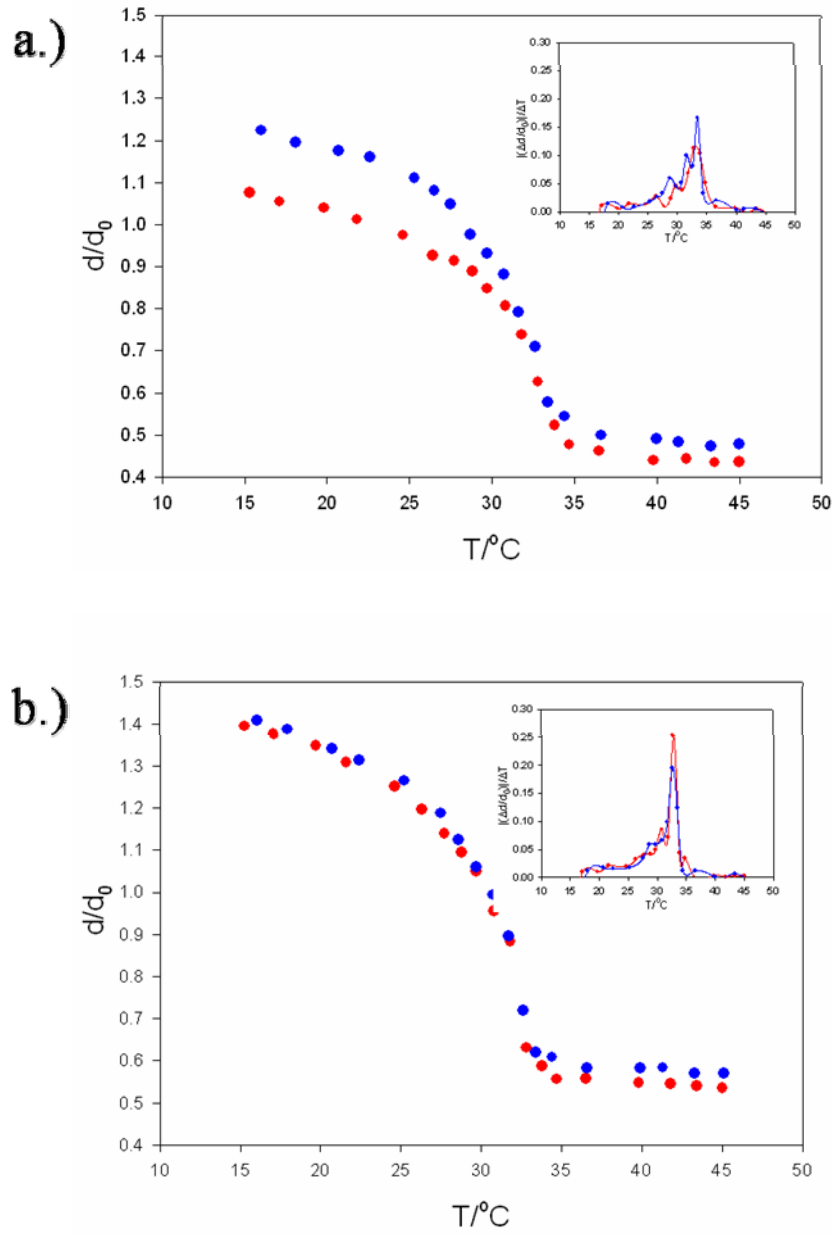


Figure 3.9. Equilibrium swelling ratio of cylindrical a.) $R_{wi}N(1)$ (red closed circle) and $R_{ws}N(1)$ (blue closed circle) b.) $R_{wi}N(2)$ (red closed circle) and $R_{ws}N(2)$ (blue closed circle) hydrogels in water as a function of temperatures. The inset of the plot represents $|(\Delta d/d_0)/\Delta T|$ vs T plots to determine volume phase transition temperatures of these hydrogels.

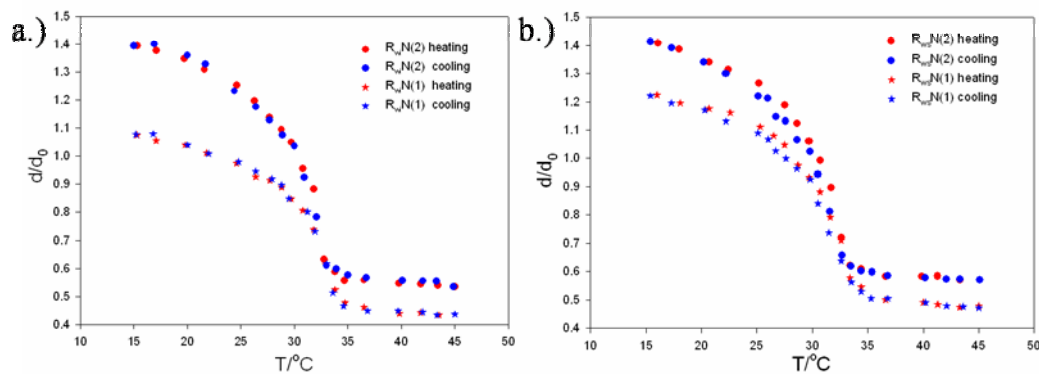


Figure 3.10. Static equilibrium swelling ratio of cylindrical a.) $R_{wi}N_x$ b.) $R_{ws}N_x$ hydrogels in water as a function of temperatures where, the red and blue symbols indicate equilibrium swelling ratio under heating and cooling respectively.

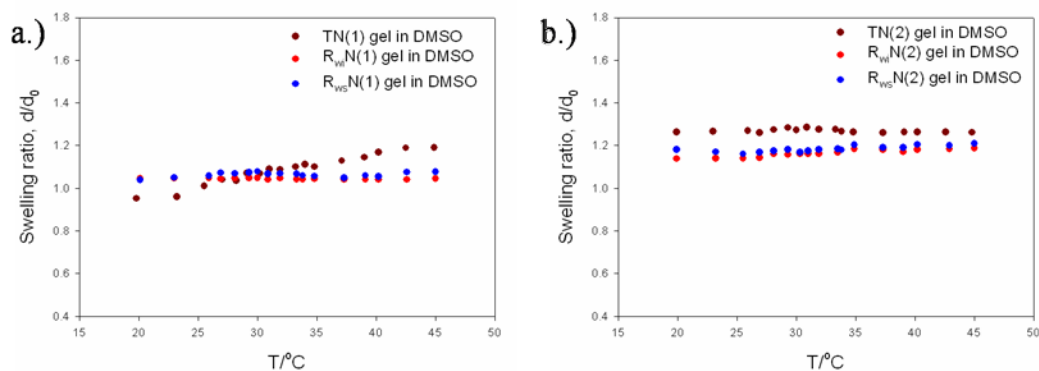


Figure 3.11. Equilibrium swelling ratio of cylindrical a.) $TN(1)$, $R_{wi}N(1)$ and $R_{ws}N(1)$ b.) $TN(2)$, $R_{wi}N(2)$ and $R_{ws}N(2)$ hydrogels in DMSO as a function of temperatures.

hydrophilicity of the MHPR allows to keep sufficient water molecules surrounding the polymer network at all temperatures to restrain the collapse of the gels. As the temperature is raised water molecules may come out from the $R_{wi}N$ gel networks, but additional strongly bound water molecules in the hydrophilic moieties of the $R_{ws}N$ gels network can not come outside easily to give rise to higher degree of swelling at high temperatures.

Interestingly both gels have the same volume phase transition temperature. When a hydrophilic moieties like acrylic acid or sodium acrylate monomers²¹ or hydrophilic surfactants²² etc, are incorporated into the poly(NIPA) gel which leads to an increase in the volume phase transition temperature. The phenomenon of swelling and deswelling of poly(NIPA) gel is governed by the balance between attractive hydration and repulsive dehydration force. When hydrophilic groups are attached to the polymer networks, water up-take by the gel network increases. To expel out these extra physically bound water molecules from the gel networks, additional energy is required and an increase in the volume phase transition temperature of the gel is apparent. However, the imbalance due to the introduction of hydrophilic MHPR can be counter-balanced by the movement of cross-linked polymer networks necessitating no additional energy for the volume phase transition of the gel and thereby, the transition temperature remains same for both gels.

The LCST of the PNIPA chains in aqueous media, in usual cases, is regulated by the net force evolved after the balances between hydrophilic repulsive and hydrophobic attractive forces. But since a relatively much lower cross-linker density is used in $R_{wi}N(2)$ and $R_{ws}N(2)$ gels (figure 3.9.b.), the effect of cross-linker on the swelling ratio are shindered by poly(NIPA) chains. Hence irrespective of the nature of the cross-linker, both gels show similar degree of swelling behaviors below the LCST.

However, above the LCST, the hydrophilicity of the MHPR inside the $R_{ws}N(2)$ gel network opposes to collapse like $R_{wi}N(2)$ gel.

In DMSO, no abrupt volume change for the gels is apparent. Although DMSO is a better solvent than BIS for the cross-linkers of our interest, it is not a good solvent for PNIPA chains compared to water. Hence in all cases, the main constituents PNIPA chains decide their equilibrium swelling state under certain conditions (Figure 3.11.).

Figure 3.10. represents the degree of swelling behavior of identical gels under static cooling. The degree of swelling behavior of $R_{wi}N_x$ and $R_{ws}N_x$ gels were almost identical under both static heating and cooling investigations. The movable cross-links inside the gel can memorize their shape memory at certain conditions, since no destruction of gel networks occurs.

3.3.4. Morphological changes of hydrogels after a temperature jump

Figure 3.12. and 3.13. represent morphological changes of TN and RN hydrogels after a temperature jump from 20 °C to 40 °C. TN(2) hydrogel changes its volume through the bubble formation. Bubbles start to form immediately after exceeding volume phase transition temperature. TN gels inherently have spatial inhomogeneities. After a temperature jump, the shrinking of the gel start at the interface by the formation of phase separated structure. This phase separated impermeable layer on the surface entraps the water molecule of the bulk gel. When the hydrostatic pressure is stronger enough, the solvent water molecules inside the bulk gel can expel out by disruption of impermeable layer which creates bubble on the surface of the gels. The $R_{wi}N(2)$ gel changes its volume without any bubble formation. The strong and quick hydrophobic aggregation of the cross-linked polymer chains can expel out water molecules quickly prior to the formation of any phase separated impermeable layer on the surface of gel.

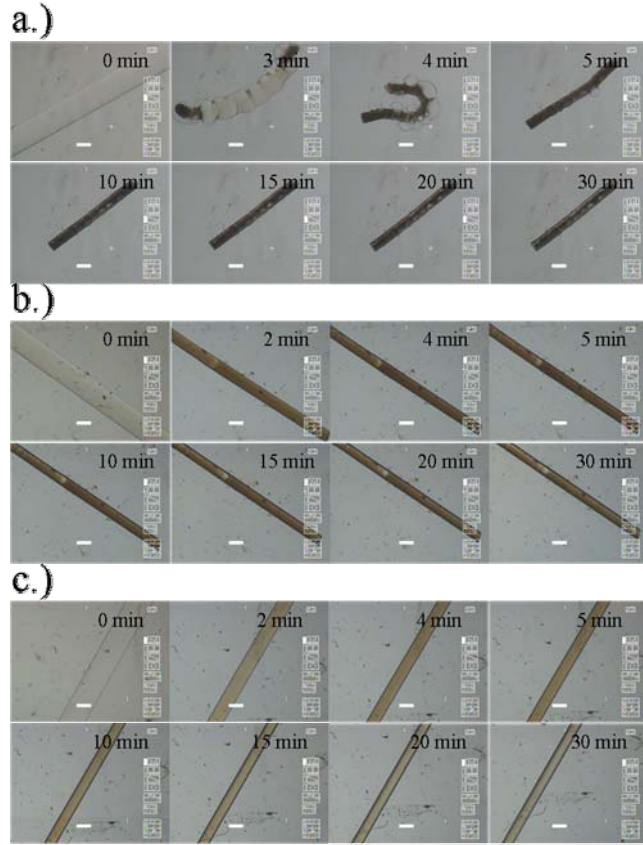


Figure 3.12. Optical micrographs of morphological changes during shrinking of sub-micrometer sized cylindrical a.) TN(1) b.) R_wN(1) and c.) R_{ws}N(1) hydrogels after a temperature jump from 20 °C to 40 °C



Figure 3.13. Optical micrographs of morphological changes during shrinking of sub-micrometer sized cylindrical a.) TN(2) b.) R_wN(2) and c.) R_{ws}N(2) hydrogels after a temperature jump from 20 °C to 40 °C

The $R_{ws}N(2)$ gel also changes its volume through the bubble formation. However, bubbles are not formed as fast as $TN(2)$. The hydrophilicity of the cross-linker MHPR is responsible for initial collapse of the gel network without bubble formation. In case of $R_{ws}N(2)$ gel, the PNIPA chains play dominant role for the characteristic behaviors of the gels. Since cross-linker density is small enough to emphasize their effect over PNIPA chains, either 2M gels show large hysteresis after a temperature jump.

The $TN(1)$ and $TN(1)0.05$ hydrogels change their volume through bubble formation. Bubbles start to form immediately after a temperature jump. The gels having lower cross-linker amount have been found to show large hysteresis. $R_{wi}N(1)$ and $R_{ws}N(1)$ gels exhibit homothetic deformation during shrinking. When the temperature of gels increases above the volume phase transition, both of the gels shrink isotropically without any bubble formation and the deformation rate becomes very fast. The $R_{wi}N(1)$ gels, after a temperature jump, reaches very close to an equilibrium shrunken state but it retains its opacity for long time aging indicating the heterogeneity of gel; while the $R_{ws}N(1)$ gel reaches to an equilibrium transparent shrunken state very rapidly.

In this study, we observed faster shrinking kinetics for homogeneous gels only by using a novel cross-linker. This contrasts to the generalized behavior that homogeneous gel shrinking kinetics is slower than that for an inhomogeneous gel.²³ The time to reach equilibrium shrinking state of the gels is proportional to the square of a characteristic length of the gel due to the collective diffusion process of the gel network.²⁴ The kinetics for shrinking and swelling of the gel is strongly dependent upon the gel size and shape (Figure 3.14. and Figure 3.15.). Bubble formation is the indication of spatial inhomogeneities in the gel. Therefore, by using movable cross-

linker, the gel network can adjust its volume fraction in space and spatial inhomogeneities can be completely removed.

3.3.5. Shrinking kinetics of RN gels

Figure 3.14. represents the shrinking kinetics of $R_{wi}N(1)$ and $R_{ws}N(1)$ gels after a temperature jump from 20 °C to 40 °C. When the temperature of gels increases above the LCST of NIPA, both of the gels shrink isotropically without any bubble formation on the surfaces. Both gels are found to exhibit two stages relaxation during shrinking process but abrupt volume changes in the gels are occurred in the first stages. The $R_{wi}N(1)$ gel, after a temperature jump, reaches very close to an equilibrium shrunken state after which further volume change is very slow but it retains its opacity for long time aging indicating the heterogeneity of gel; while the $R_{ws}N(1)$ gel reaches to an equilibrium transparent shrunken state very rapidly. This indicates that in the shrunken state $R_{ws}N(1)$ gel is homogeneous and the gel must not in glassy state at that temperature.

The first stage relaxation times, τ_1 for $R_{wi}N(1)$ and $R_{ws}N(1)$ gels are calculated from the slope of Figure 3.14. as 1.264×10^2 sec and 2.11×10^2 sec while last stage relaxation time, τ_2 are 1.27×10^4 sec and 6.1×10^3 sec respectively. To estimate the shrinking speed, the $d(t)$ vs t curves were fitted to a single exponential function. As significant amount of volume changes were observed in the first stage, only first relaxation time was considered to fit the curves. The function of gel diameter, $d(t)$ is expressed as follows

$$d(t) = A \exp(-t/\tau_1) + d(\infty)$$

where A is a constant, τ_1 is the characteristic shrinking relaxation time of the first stage, and $d(\infty)$ is the diameter of the gel in the equilibrium collapsed state.

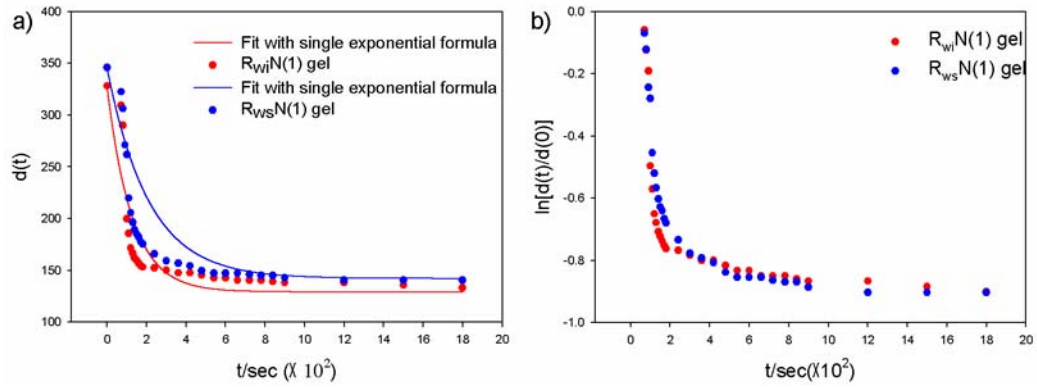


Figure 3.14. a.) Fast shrinking kinetics of cylindrical $R_{wi}N(1)$ and $R_{ws}N(1)$ hydrogels after a temperature jump from 20 °C to 40 °C. $R_{ws}N(1)$ gel reaches to an equilibrium shrunken state very quickly while $R_{wi}N(1)$ gel is far from the equilibrium collapsed state. b.) two stages shrinking are observed for both gels.

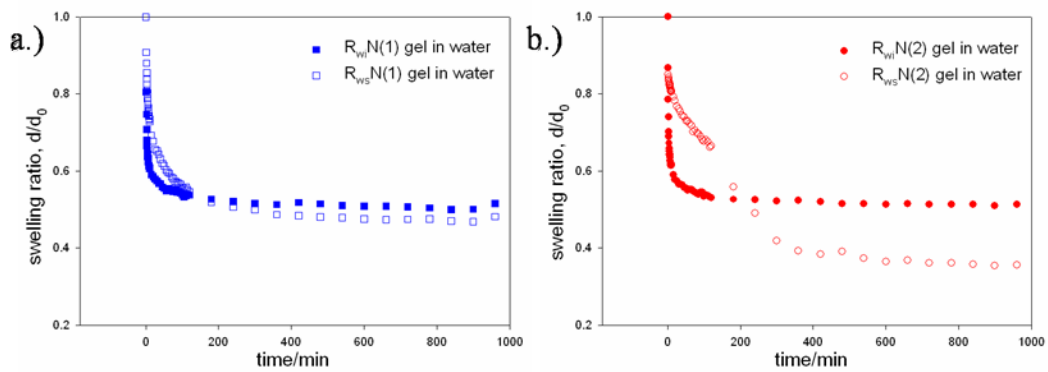


Figure 3.15. Shrinking kinetics of sub-millimeter size disk shaped a.) $R_{wi}N(1)$ and $R_{ws}N(1)$ b.) $R_{wi}N(2)$ and $R_{ws}N(2)$ hydrogels after a temperature jump from 20 °C to 40 °C.

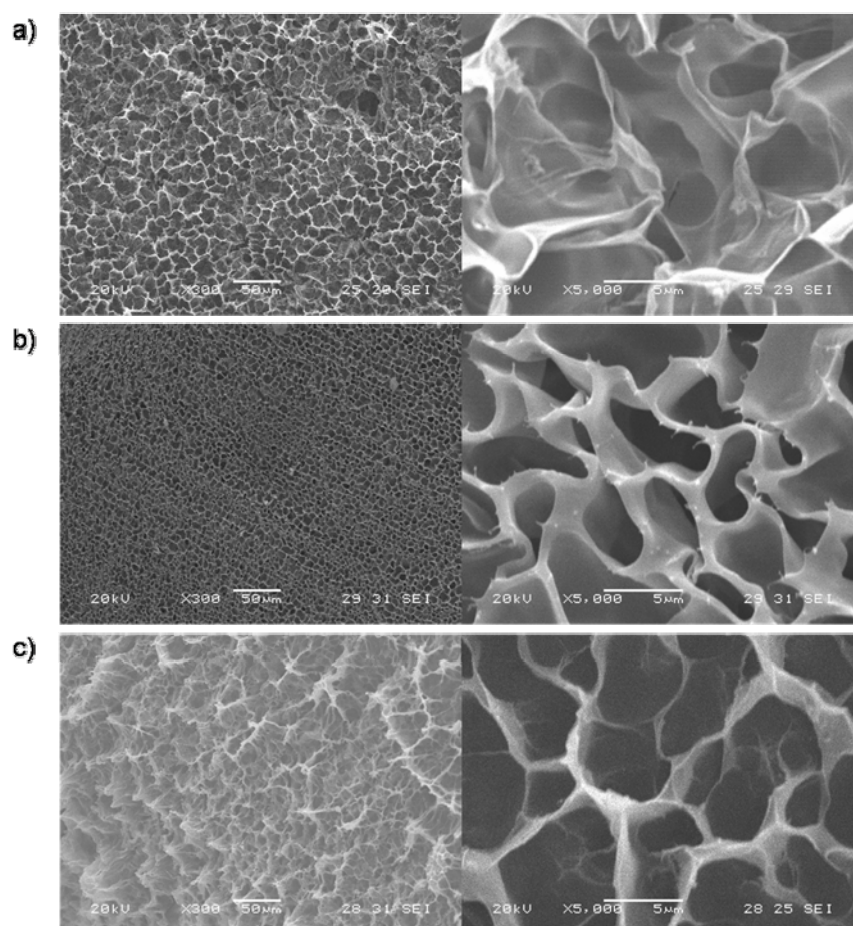


Figure 3.16. SEM images of the a) TN(1) b) $R_{wi}N(1)$ and c) $R_{ws}N(1)$ gels after reaching to equilibrium swollen states in water

In either case, the experimental values deviate from the fitted values to the left, which indicates that much fast shrinking occurs for both gels after a temperature jump. When multi-functional cross-linker MPR or MHPR are used for gelation, they not only form a cross-linked polymer network, but also huge dangling free poly (NIPA) chains are attached on the active sides of α -CD of polyrotaxane cross-linkers. These dangling one end free PNIPA chains have less mechanical constraints. Even cross-linked PNIPA chains in the $R_{wi}N(1)$ and $R_{ws}N(1)$ gels may exhibit higher degree of freedom due to the presence of movable cross-links. After a temperature jump above the LCST of NIPA, these dangling PNIPA chains as well as cross-linked PNIPA chains can quickly collapse to form shrunken phase.

Hydrophobic aggregation among shrunken phases then commences to form larger nuclei. At the same time water rich regions combine with each other to form a water channel through which water can be expelled out from the gel networks quickly.

Transmission spectra show that $R_{wi}N(1)$ and $R_{wi}N(2)$ gels are opaque in the region of visible wavelength. That is volume fraction of the cross-linked polymer chains are widely distributed in space and bring heterogeneity to the gel network. After a temperature jump, a hydrophobic nuclei or shrunken phase are formed and randomly oriented in space. Thus nuclei or shrunken phase becomes large with time by moving out water molecules from the gel networks. As a result a clear water rich region and a water deficient shrunken phase region are grown up. At high temperatures these shrunken phases generate some internal forces to the gel network by the movement through the movable cross-linker. The ability to move the shrunken phase develops sufficient squeezing forces to expel out water molecules from the $R_{wi}N(1)$ gel and the gel reaches to a shrunken state very close to the equilibrium shrunken state. The hydrophobic cross-linker MPR used for the synthesis of $R_{wi}N(1)$

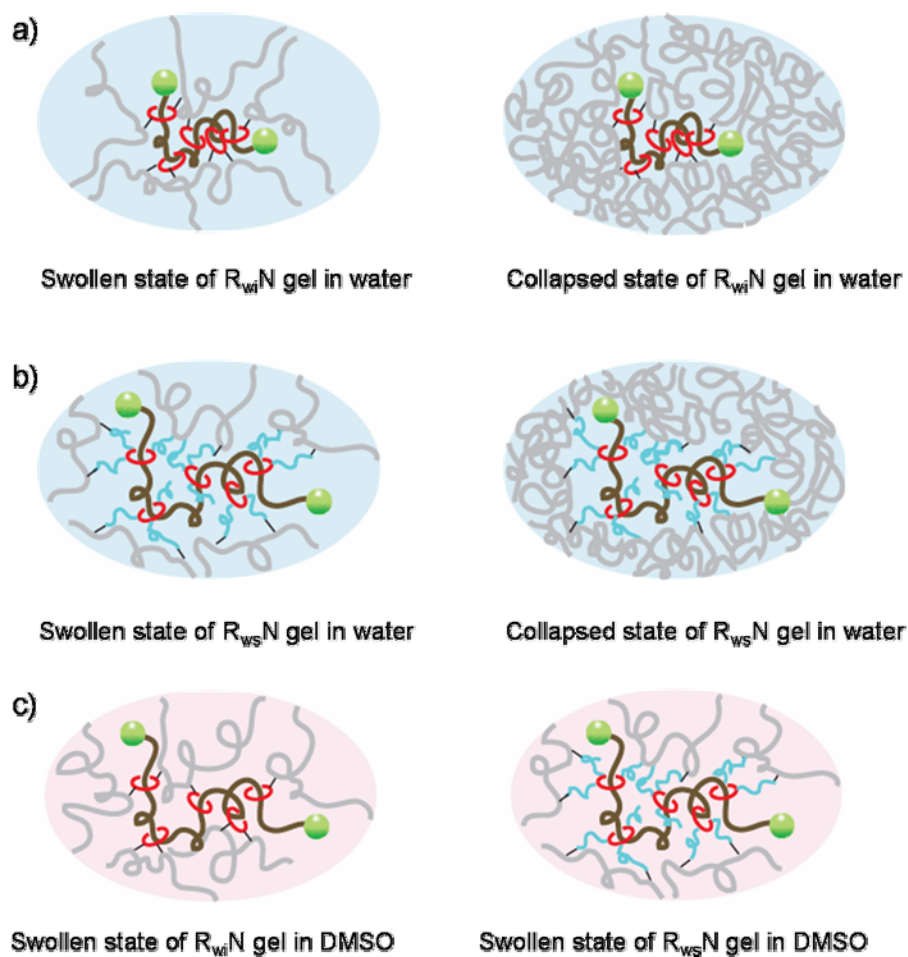


Figure 3.17. Pictorial representations of swollen and collapsed states of a) $R_{wi}N$ gel, and b) $R_{ws}N$ gel in water at below and above the LCST.

gel exists as an aggregated state in water. Hence the persistent length for sliding of the macro cycles along with attached polymer chains decreases to some extent at higher temperature. This results the formation of pinned network structure in the $R_{wi}N(1)$ gel after the first stage and decrease the shrinking speed markedly in the second stage.

In contrast, the movability of the polymer chains is not altered in the $R_{ws}N(1)$ gel by the aggregation of the cross-linker MHPR. After a temperature jump, the shrinking force developed from the dehydration of poly(NIPA) chains, helps to aggregate shrunken phase quickly owing to the superior movability of the cross-links. The aggregation inside the bulk gel creates huge hydrostatic pressure and water molecules can come out quickly before forming any phase separated pinned network. The shrinking proceeds via the growth of nucleation but do not enter to the unstable spinodal region. The second relaxation stage may be originated due to the final rearrangement of the aggregated nuclei to give a transparent and equilibrium shrunken state. The $R_{ws}N(1)$ gel, thereby, immediately turns to an equilibrium shrunken state without any deformation on the gel surfaces.

In case of the TN(1) gel, when the amount of cross-linker is increased shrinking rate is also enhanced. TN(1) gel shows very slow shrinking after a temperature jump than the TN(1)0.05 gel. This is in agreement with literature for the critical slow volume change of conventional poly(NIPA) gels.²⁵ The gel is reported to collapse by micro-phase separation because of the spinodal decomposition. TN gel has lightly and highly cross-linked region. These different types of region give spatial inhomogeneities²⁶ to the hydrogel. When the gel is heated slowly, the highly cross-link rich regions can adjust their position to reach an equilibrium shrunken state.²⁷ On the other hand after a temperature jump the TN gel can not adjust their cross-link region by moving their domains close to each other within a short period of time. This

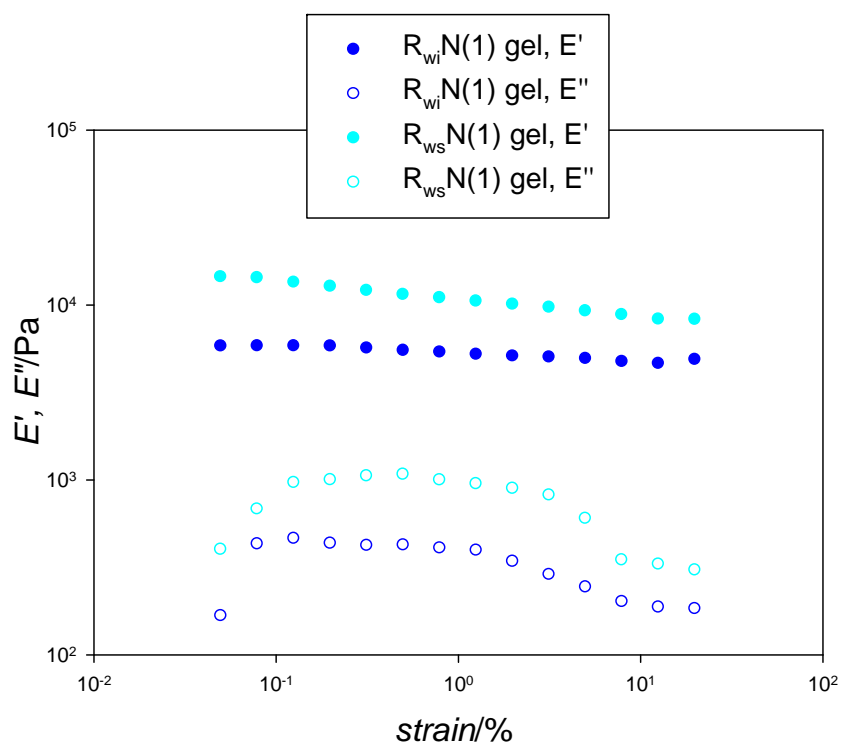


Figure 3.18. Frequency controlled (1 radsec^{-1}) dynamic strain sweep test for $R_{wi}N(1)$ and $R_{ws}N(1)$ gels in air (as prepared state).

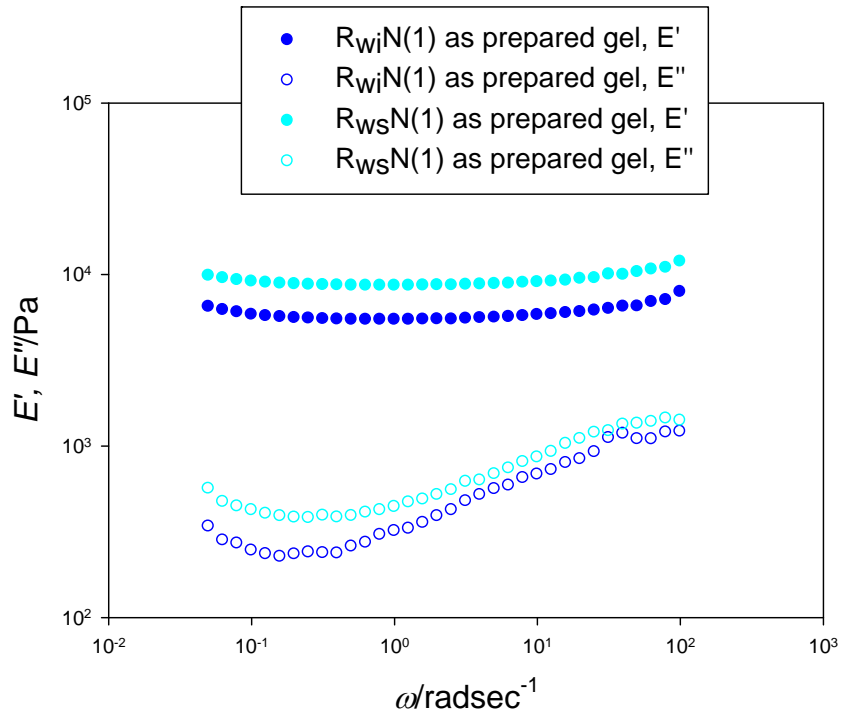


Figure 3.19. Strain-controlled dynamic frequency sweep test of storage moduli, E' and loss moduli, E'' for $R_{wi}N(1)$ and $R_{ws}N(1)$ gels in air (as prepared state).

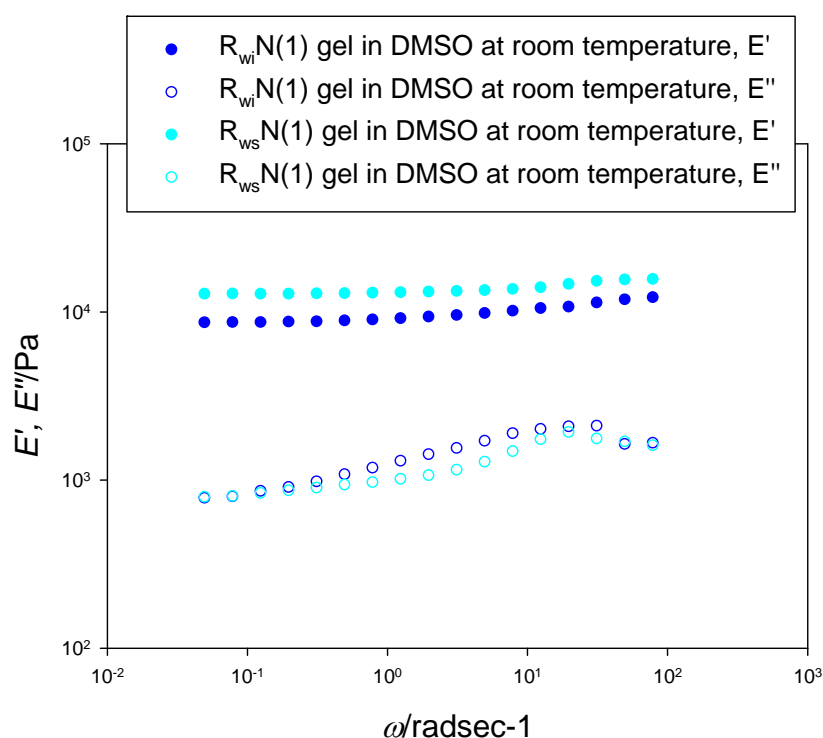


Figure 3.20. Strain-controlled dynamic frequency sweep test of storage moduli, E' and loss moduli, E'' for $R_{wi}N(1)$ and $R_{ws}N(1)$ gels in DMSO at room temperature.

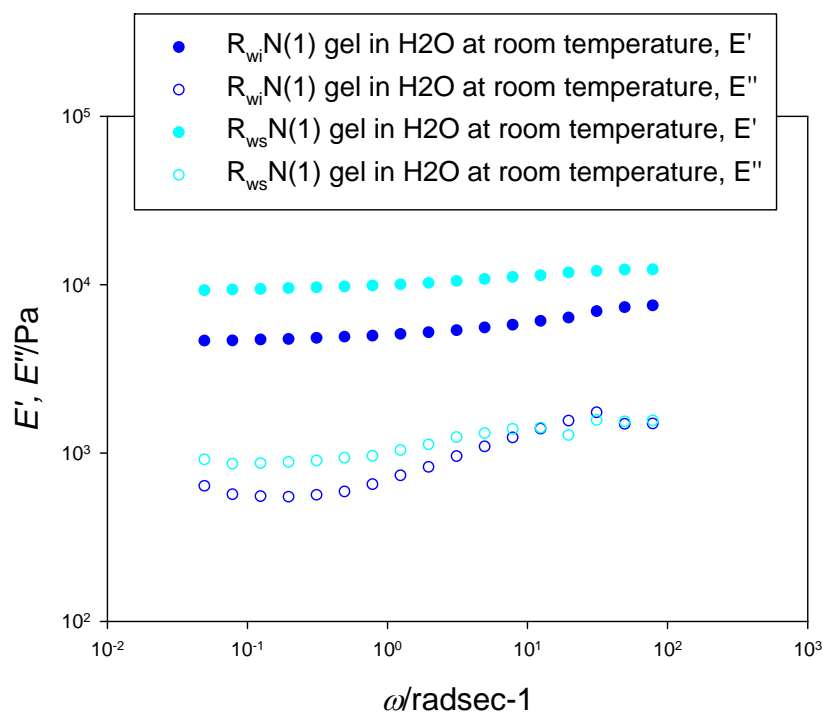


Figure 3.21. Strain-controlled dynamic frequency sweep test of storage moduli, E' and loss moduli, E'' for $R_{wi}N(1)$ and $R_{ws}N(1)$ gels in water at room temperature.

gives rise to slow shrinking rate for TN gels.

The polymer chains in a gel are covalently bonded to each other and all segments in the gel network move collectively. The diffusion coefficient of individual segment in a gel is, therefore, the collective diffusion of all segments. In case of the TN gel, the fixed cross-linking network lowers the diffusivity of the polymer network. In contrast, the RN gel having the cross-linking network in which polymer chains can slide or rotate through the cross-linker and the diffusion rate is enhanced. This assists collapse of the gel at high temperatures.

3.3.6. Mechanical properties

Figure 3.18. represents frequency controlled (1 radsec^{-1}) dynamic strain sweep test for $R_{wi}N(1)$ and $R_{ws}N(1)$ as prepared gels in air at room temperatures. Strain was dynamically applied to the samples ranging from 0.01% to 20%. Either gels were mechanically very stable in the entire course of measurements. No rupture or deformation was experienced by any samples. With increasing strain % the storage moduli for $R_{wi}N(1)$ and $R_{ws}N(1)$ gels decreases gradually. But the decrease rate is relatively higher for $R_{ws}N(1)$ gels. From the strain sweep test, a 3% strain which is in the linear viscoelastic regime for either sample was selected for the frequency sweep measurements. In the linear viscoelastic region the storage moduli for both samples are independent of the experienced strain.

Figure 3.19 shows strain-controlled dynamic frequency sweep test of storage moduli, E' and loss moduli, E'' for $R_{wi}N(1)$ and $R_{ws}N(1)$ gels in air for freshly prepared gel samples. $R_{wi}N(1)$ gel has lower E' and E'' values in the entire frequency regions than $R_{ws}N(1)$ gel. At low frequencies RN gels have low loss moduli. It is believed that at low frequencies the movability of the polymer chains along with macro cycles can occur easily which brings low E'' values in the viscoelastic curve.

But at high frequencies polymer chains do not have enough time to respond or rearrange the polymer networks through the movement of polymer chains as fast as frequency change. As a result higher loss moduli are observed at higher frequencies.

In DMSO $R_{wi}N(1)$ and $R_{ws}N(1)$ gels have almost same moduli value although $R_{ws}N(1)$ gel has slightly higher E' and E'' value (Figure 3.20). On the other hand, in water $R_{ws}N(1)$ gel has higher storage and loss moduli value which indicates that $R_{ws}N(1)$ gel forms much stiffer gel networks (Figure 3.21.). It is found that $R_{ws}N(1)$ gel at low temperatures has higher degree of swelling behavior than $R_{wi}N(1)$ gel i.e. in the same cross-sectional area of the gels networks, $R_{ws}N(1)$ gel has much amount of water. The hydrophilicity of the polyrotaxane cross-linker in the $R_{ws}N(1)$ gel is responsible to uptake additional hydrophilically bound water molecules in the gel networks which increases the stiffness of the $R_{ws}N(1)$ gel. As a result in the entire frequency range the $R_{ws}N(1)$ gel in water exhibits higher E' and E'' values.

3.3.7. Kinetics of swelling

Figure 3.24. represents the swelling kinetics of RN and TN gels after a temperature jump from 40 °C to 20 °C. The diameter of the gel increases in proportion to the square root of time for both cases, since the diffusion of the polymer network is responsible for gel swelling. The kinetic of gel swelling RN gels are very fast and after a temperature jump no critical slow kinetics of the gels are observed. The gel swelling only depends on the diffusion of incoming flux of water into the gel and co-operative diffusion of network chains. Since for the RN gel, cross-linked polymer chains experience more freedom through the movable cross-linker, the gel of this kind exhibits higher swelling kinetics than the TN gel. The diffusion of the polymer network plays the main role for the fast gel swelling.

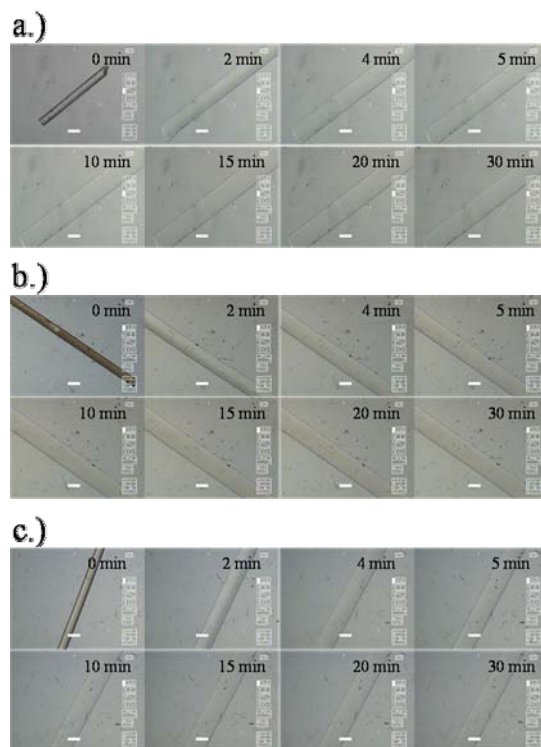


Figure 3.22. Optical micrographs of morphological changes during swelling of sub-micrometer sized cylindrical a.) TN(1) b.) $R_{wi}N(1)$ and c.) $R_{ws}N(1)$ hydrogels after a temperature jump from 40 °C to 20 °C

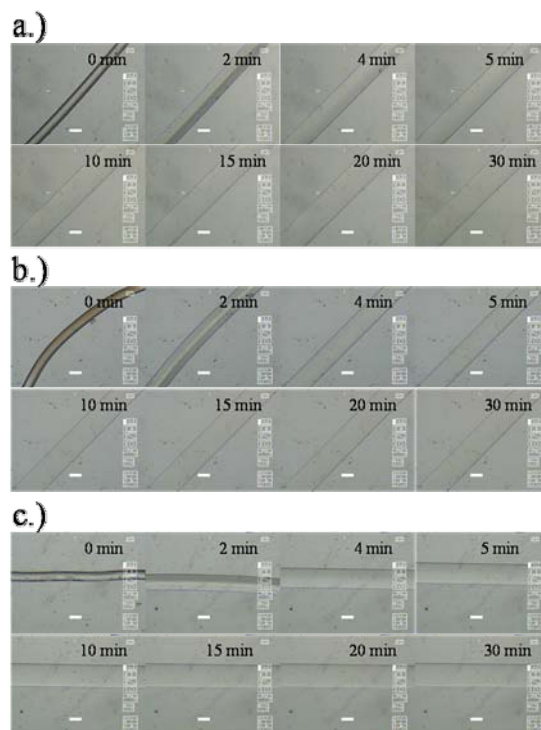


Figure 3.23. Optical micrographs of morphological changes during swelling of sub-micrometer sized cylindrical a.) TN(2) b.) $R_{wi}N(2)$ and c.) $R_{ws}N(2)$ hydrogels after a temperature jump from 40 °C to 20 °C

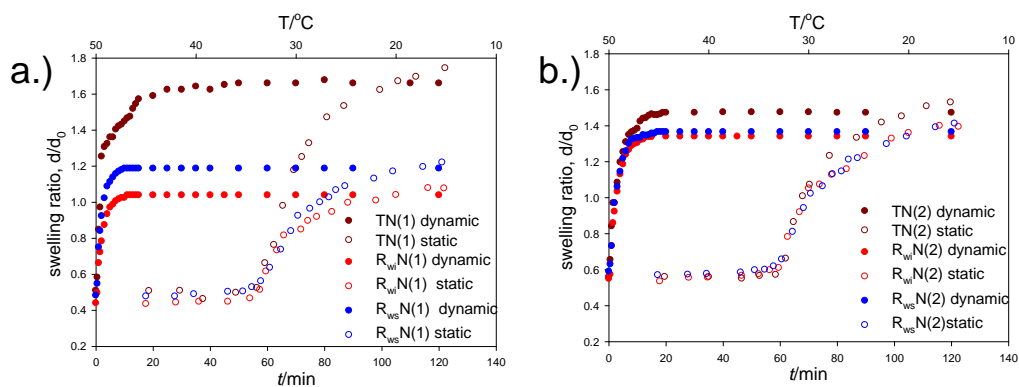


Figure 3.24. Swelling kinetics of abrupt volume changes of different types of sub-micrometer sized cylindrical hydrogels after a temperature jump from 40 °C to 20 °C (closed circles) and their static swelling behaviors are also plotted as a function of temperature (open circles)

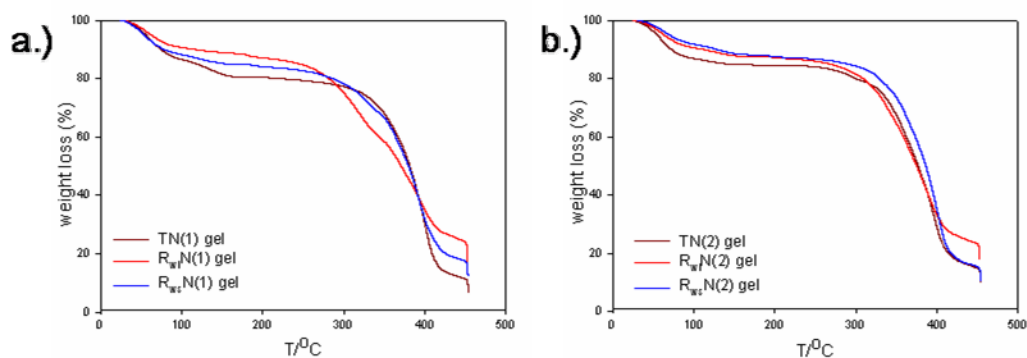


Figure 3.25. Thermo-gravimetric plots of a.) TN(1), $R_{wi}N(1)$ and $R_{ws}N(1)$ b.) TN(2), $R_{wi}N(2)$ and $R_{ws}N(2)$ hydrogels at a heating rate of 10 °C per minute.

3.3.8. Thermo Gravimetric / Differential Thermal Analysis (TG /DTA)

An increase in BIS fraction results in increased crystallinity of the gel network as well as the decomposition temperature for TN gels. PR and HPR both are highly crystalline materials, but after modification with isocyanate monomer, MPR and MHPR, become flexible and get rubbery compliance (Figure 3.6.). The decomposition temperature of the yielded product remains same, but the decomposition of samples becomes low after 60% weight loss. These behaviors of cross-linkers also retain in the gels (see Figure 3.25). Gels prepared using MPR as a cross-linker lose its weight with temperature, but after exceeding a certain temperature weight loss becomes low. The decomposition temperature of the gels has been found to increase with increase in the amount of the monomer. In contrast, when MHPR is used for gelation, huge initial weight loss of sample is observed for $R_{ws}N(1)$. It should be noted that different forms of water exist inside the gels, such as, non-freezable water which exhibits strong interaction with the network, bound water that freezes at -10 -20 °C and free water. The initial weight loss corresponds to the loss of strongly bound water molecules from the $R_{ws}N(1)$ gel network.

3.4. Conclusion

We report the synthesis of hydrophilic polyrotaxane based cross-linker, MHPR and employed it for the synthesis of RN gels. The swelling behavior and the volume phase transition of $R_{ws}N(1)$ gels have been carried out and compared and contrasted with those for $R_{wi}N(1)$ and TN gels. In water, TN and RN gels exhibit sharp volume phase transition around the lower critical solution temperature (LCST) of NIPA. For RN gels, the volume phase transitions of gels have been found not to depend on the nature of cross-linker. Although at low temperatures the $R_{ws}N(1)$ gel shows higher degree of swelling than the $R_{wi}N(1)$ gel but the volume phase transition temperature

does not change. After a temperature jump, RN gel shrinks isotropically without any bubble formation, and the rate of deformation is very fast. The TN gels always exhibit strong hysteresis during shrinking, while the use of the MPR and MHPR as cross-linkers, completely eliminates the hysteresis of conventional poly(NIPA) gels. The soft and mechanically stable nature of the RN gel can be used potentially as biomaterials since the softness of the gel will reduce the mechanical and frictional irritation to surrounding tissue. It also can potentially be used for the protein release or drug delivery system.

References:

1. Okano, T.; Bae, Y. H.; Jacobs, H.; Kim, S. W. *J Controlled Release*. **1990**, 11, 255.
2. Kanekiyo, Y.; Sano, M.; Iguchi, R. *J Polym Sci Part A: Polym Chem*. **2000**, 38, 1302.
3. Bae, Y.H.; Okano, T; Hsu, R; Kim, S.W. *Makromol. Chem. Rapid Commun*. **1987**, 8, 481.
4. Osada, Y; Okuzaki, H; Hori, H. *Nature*. **1992**, 355, 242.
5. Bhattacharya, S.; Moss, R. A.; Ringsdorf, H.; Simon, J. *Langmuir*. **1997**, 13, 1869.
6. Liu, F; Tao, G.L; Zhuo, R.X. *Polym. J*. **1993**, 25, 561.
7. de Gennes, P.G. *Physica A*. **1999**, 271, 231.
8. Okumura, Y.; Ito, K. *Adv. Mater*. **2001**, 13, 485.
9. Frisch, H. L.; Wasserman, E. *J. Am. Chem. Soc*. **1961**, 83, 3789.
10. Harrison, T.; Harrison, S. *J. Am. Chem. Soc*. **1967**, 89, 5723.
11. Zhao, C.; Domon, Y.; Okumura, Y.; Okabe, S.; Shibayama, M.; Ito, K. *J. Phys. Condens. Matter*. **2005**, 17, S2841.
12. Imran, A.B.; Takeoka, Y.; Seki, T.; Kataoka, T.; Kidowaki, M.; Ito, K. *Chem. Commun*. **2008**, 41, 5227-5229.
13. Okajima, T.; Harada, I.; Nishio, K.; Hirotsu, S. *J. Chem. Phys*. **2002**, 116, 9068.
14. a. Cheng, S.X.; Zhang, J.T.; Zhuo, R.X. *J. Biomed. Mater. Res*. **2003**, 67A, 96. b. Zhang, J.T.; Cheng, S.X.; Zhuo, R.X. *J. Polym. Sci., Part A: Polym. Chem*. **2003**, 41, 2390. c. Oxley, H.R.; Corkhill, P.H.; Fitton, J.H.; Tighe, B.J. *Biomaterials*. **1993**, 14, 1064. d. Zhang, X.Z.; Chu, C.C.; Zhuo, R.X. *J. Polym. Sci., Part A: Polym. Chem*. **2005**, 43, 5490. e. Zhang, X.Z.; Zhuo, R.X. *Eur. Polym. J*. **2000**, 36, 2301. f. Kaneko, T.; Asoh, T.; Akashi, M. *Macromol. Chem. Phys*. **2005**, 206, 566.

15. a. Ebara, M.; Aoyagi, T.; Sakai, K.; Okano, T. *J. Polym. Sci., Part A: Polym. Chem.* **2001**, 39, 335. b. Gutowska, A.; Bae, Y.H.; Feijen, J.; Kim, S.W. *J. Controlled Release*. **1992**, 22, 95.
16. a. Ju, H.K.; Kim, S.Y.; Lee, Y.M.; *Polymer*. **2001**, 42, 6851. b. Kaneko, Y.; Nakamura, S.; Sakai, K.; Aoyagi, T.; Kikuchi, A.; Sakurai, Y.; Okano, T. *Macromolecules*. **1998**, 31, 6099. c. Kobuta, N.; Matsubara, T.; Eguchi, Y. *J. Appl. Polym. Sci.* **1998**, 70, 1027. d. Sakai, K.; Kikuchi, A.; Sakurai, Y.; Okano, T. *Nature*. **1995**, 374, 240.
17. a. Araki, J.; Zhao, C.; Ito, K. *Macromolecules*. **2005**, 38, 7524. b. Araki, J.; Ito, K. *J. Polym. Sci. Part A: Polym. Chem.* **2006**, 44, 6312.
18. Van Tent, A.; Nijenhuis, K. Te. *J. Colloid Interface Sci.* **1992**, 150, 97.
19. a) Hirokawa, Y.; Tanaka, T. *J. Chem. Phys.* **1984**, 81, 6379-6380. b) Khokhlov, A. R. *Polymer* **1980**, 21, 376-380. c) Baker, J. P.; Blanch, H. W.; Prausnitz, J. M. *Polymer* **1995**, 36, 1061-1069. d) Marchetti, M.; Prager, S.; Cussler, E. L. *Macromolecules* **1990**, 23, 1760-1765.
20. Grosberg, A. Y.; Khokhlov, A. R. *Statistical Physics of Macromolecules*; AIP Press: **1994**.
21. a. Kokufuta, E.; Wang, B.; Yoshida, R.; Khokhlov, A.; Hirata, M. *Macromolecules*. **1998**, 31 6878. b. Ogawa, K.; Ogawa, Y.; Kokufuta, E. *Colloids and surfaces A: Physicochem. Eng. Aspect.* **2002**, 209, 267. c. Liu W, Zhang B, Lu WW, Li X, Dunwan Z, Yao KD, Wang Q, Zhao C, Wang C *Biomaterials* 2004 25:3005 d. Eeckman F, Moe's AJ, Amighi K *Int J Pharm* **2002**, 241, 113
22. a. Miyagishi, S.; Takagi, M.; Kadono, S.; Ohta, A.; Asakawa, T. *J. Colloid Interface Sci.* **2003**, 261, 191. b. kokufuta, E.; Zhang, Y.; Tanaka, T.; Mamada, A. *Macromolecules*. **1993**, 26, 1053.

23. Okajima, T.; Harada, I.; Nishio, K.; Hirotsu, S. *J. Chem. Phys.* **2002**, 116, 9068.
24. Tanaka, T.; Fillmore, J. D. *J. Chem. Phys.* **1979**, 70, 1214.
25. a. Hirotsu, S. *Jpn. J. Appl. Phys., Part 2*, **1998**, 37, 284. b. Bansil, R.; Liao, G.; Falus, P. *Physica A*. **1996**, 231, 346. c. Li, Y.; Wang, G.; Hu, Z. *Macromolecules*. **1995**, 28, 4194. d. Sekimoto, K.; Suematsu, N.; Kawasaki, K. *Phys. Rev. A*. **1989**, 39, 4912. e. Onuki, A.; Puri, S. *Phys. Rev. E*. **1999**, 59, R1331.
26. a. Shibayama, M. *Macromol. Chem. Phys.* **1998**, 199, 1. b. Mendes, E.; Oeser, R.; Hayes, C.; Boue, F.; Bastide, J. *Macromolecules*. **1996**, 29, 5574.
27. Hirose, H.; Shibayama, M. *Macromolecules*. **1998**, 31, 5336.

CHAPTER

4

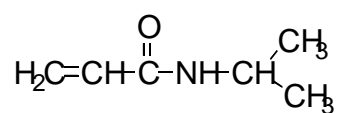
Synthesis of super absorbent and highly elastic novel polyelectrolyte gel using polyrotaxane based cross-linker.

Abstract

Ionic hydrogels using hydrophilic polyrotaxane as a movable cross-linker have been reported here. Propylene oxide modified α -Cyclodextrins which are threaded into the long polyethylene glycol ($MW = 35000\text{g mol}^{-1}$) and capped by bulky 1-adamantanamine molecules of the polyrotaxane (HPR) was used to increase the solubility of polyrotaxane in water. HPR was modified by small amount 2-acryloyloxyethylisocyanate monomer through the formation of stable carbamate bond to obtain polyrotaxane-based multifunctional cross-linker, MHPR. Ionic gels were synthesized by free radical co-polymerization of thermo-sensitive monomer *N*-isopropylacrylamide (NIPA) and pH sensitive weakly dissociate-able monomer Sodium acrylate (SA) with the varying amounts of the cross-linker MHPR. A transparent, homogeneous and highly elastic gel was formed. The gel shows high mechanical stability under repeated deformation. It has very high elongation at break ca. 900% strain. The gel exhibits super absorbent characteristic. It can uptake more than 60,000% water of its dried state. This is so far reported highest water absorbed by any polymeric materials. After a temperature jump, the gel changes its volume isotropically. No deformation on the surfaces of the gels was observed in any state during shrinking. Introduction of ionic groups to the rotaxane-NIPA gel network may increases the electrostatic repulsion among the polymer chains and restricts the aggregation of gel networks. Hence, the movability of the cross-linker is highly effective in the gel networks and the gel shows very high mechanical and super absorbent behaviors. The polyrotaxane based ionic gel was compared and contrasted with the ionic gel prepared by using bi-functional *N,N'*-methylene-bis-acrylamide, BIS as a cross-linker.

4.1. Introduction

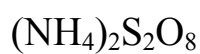
A polymer gel is an elastically cross-linked polymer network that absorbs a significant fraction of solvent molecules within its structure but insoluble in any solvents.¹ Polymeric hydrogels are very similar to living organisms and often exhibit good biocompatibility thereby brings about significant attention to polymer scientists. *N*-isopropylacrylamide, NIPA has LCST temperature around 32 °C. Below the LCST it exists as soluble coil form but above the LCST it turns to insoluble aggregated globular form. The fascinating characteristics of NIPA have been employed for the synthesis of varieties types of intriguing polmeric hydrogel. Chemically cross-linked poly(NIPA) gels and its copolymer gels in water undergo a phase transition in response to infinitesimal temperature changes.² A volume phase transition of chemical gels was first theoretically proposed by Dusek et. al³ and experimentally realized by Tanaka et. al.⁴ Poly(*N*-isopropylacrylamide-*co*-sodium acrylate) gel has been widely studied in various fields, such as materials science, physics, chemistry, biology, and pharmacology.⁵ Although the unique features of ionic stimuli sensitive gels have attracted considerable attention in fundamental and practical science field but the poor mechanical strengths and shrinking kinetics restricts their widespread uses for practical applications. Recently a new type of polymer gel is reported by our group⁶ based on the mechanism of sliding gel, in which the cross-linking points can slide or rotate in the gel networks. This brings potential improvements in the polymer gel in the sense of mechanical strength. As the cyclic molecules of polyrotaxane can rotate and slide along with the polymer chains, the polymer chains attached to the cyclic molecules will have much degree of freedom.⁷



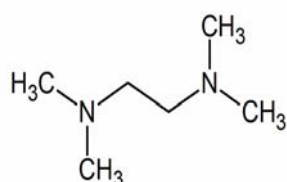
N-isopropylacrylamide,
NIPA



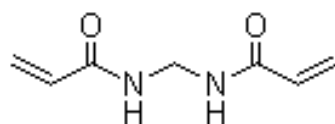
Sodium
acrylate, SA



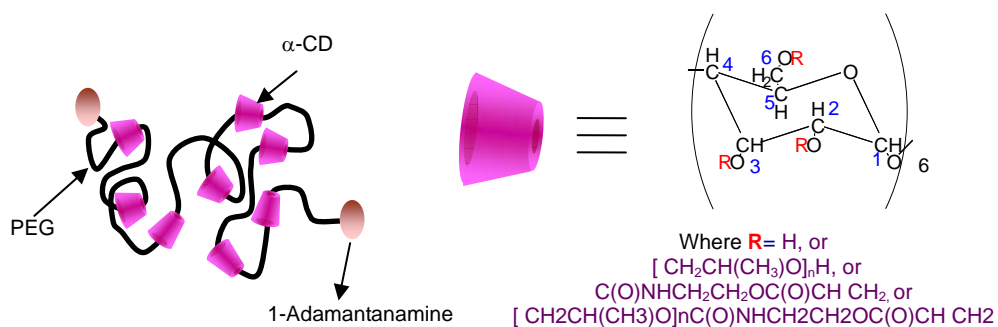
APS



TEMED



N,N'-Methylenebis(acrylamide),
BIS



MHPR (MR = 1.98)

Figure 4.1. Chemical structures of common reagents used in this study

Although the gels prepared by hydrophobic⁸ and hydrophilic polyrotaxane⁹ as cross-linkers bring significant improvements in mechanical stability but the gels do not show appreciable tensile strength under deformation. It can be assumed that this is due to the decrease of the mobility of cross-links by the aggregation of the polymer chains in the gel networks.

In this work we aim at synthesizing ionic rotaxane- NIPA gels by introducing slow dissociate able anionic co-monomer in the gel network. The electrostatic interactions in the networks of the rotaxane-NIPA gels have been increased by introducing a tiny amount of ionic groups (Sodium acrylate). In the gel networks the ionic interactions in the polymer chains must increase the degree of freedom of the polymer chains which are attached to α -CD and restrict any possible aggregation of the polymer chains in the gel networks which is the vital criteria to have mechanically improved polymer gels.

4.2. Experimental.

4.2.1. Materials

Hydroxypropylated polyrotaxane, HPR, was purchased from Advanced Soft materials Inc., Tokyo, Japan and used without further purification. *N*-isopropylacrylamide (NIPA) from Kohjin Co., Tokyo, Japan was purified by recrystallization from toluene/n-hexane. Sodium acrylate (SA) from (Sigma-Aldrich, MO, USA), BIS from (Acros Organics, Geel, Belgium), Ammonium persulfate and *N,N,N',N'*-tetramethylethylenediamine (TEMED) from (Wako Pure Chemical Industries, Ltd., Japan), dibutyltetrahydroxydiphosphate (DBTDL) and butyl hydroxyl toluene (Tokyo Kasei Kogyo Co., Japan) were reagent-grade materials and were used as received unless otherwise noted. 2-Acryloyloxyethyl isocyanate was purchased from

Showa Denko K.K, Japan. Milli-Q ultra pure water was used throughout the experiments.

4.2.2. Preparation of Rotaxane-NIPA-Sodium acrylate, $R_{ws}N$ -S gels

A series of $R_{ws}N$ -S gels were prepared by a free radical copolymerization of monomers in water. *N*-isopropylacrylamide (thermosensitive, principal monomer), Sodium acrylate (pH sensitive monomer), Tetramethylethylenediamine, TEMED (20 μ l), accelerator and hydrophilic polyrotaxane cross-linker, MHPR were dissolved in 5ml Milli-Q water. The concentrations of NIPA and SA monomer were maintained constant, as 1.9 M and 0.1 M respectively but the amounts of MHPR were varied from 0-5 wt% (Table 3.3.). N_2 -bubbling was passed through the pre-gel solutions to remove any dissolved oxygen from the solutions. 6mg Ammonium persulfate, APS was added to the solutions as an initiator and then quickly transferred to a test tube which contained micro-capillary tubes of 270 μ m and 375 μ m inner diameters. Gelations were carried out at 10 $^{\circ}$ C for 24 hours. The gels were repeatedly washed by water to remove any unreacted chemicals for two weeks. During repeated washing, it can be considered that all of the sodium cations originating from the sodium acrylate groups are replaced by the protons of water.

4.2.3. Preparation of BIS- NIPA-Sodium acrylate, TN-S gels

TN-S gels were prepared by free radical copolymerization of NIPA and SA. NIPA(2-1.6 M), SA (0-0.6 M), *N,N'*-methylenebis(acrylamide) (5- 50 mM), and 20 μ L of *N,N,N',N'*-tetramethylethylenediamine (TEMED) were dissolved in 5ml of distilled deionized water. The sum of the concentrations of NIPA and SA monomers were maintained as 2 M (Table 3.1. and 3.2.). N_2 gas was bubbled through the solution for 20 minutes to remove the dissolved oxygen. The gelation was initiated by adding APS (6 mg) into the pregel solution. To make uniform cylindrical shape gels, some

micro-capillary tubes of 270 μm and 375 μm inner diameters were previously inserted in the test tube. The gelation reaction was carried out at ca. 10 $^{\circ}\text{C}$ for 24 h. The gels were repeatedly washed by water for two weeks.

4.2.4. Preparation of polyelectrolyte buffer solutions

To prepare a polyelectrolyte buffer solution, partially neutralized 5 mM poly(Acrylic acid) buffer solution was used. Poly(Acrylic acid) [MW 1×10^6] was purchased from Wako Chemicals Co. Ltd. The pH of poly(Acrylic acid) aqueous solution is varied from 3 to 11 by neutralizing with a small amount of 1N NaOH. The pH of the buffer solutions may change to the pH to 7 in case of higher pH after prolong period absorption of CO_2 from the atmosphere. To avoid this effect, the solutions were kept on blanket with N_2 gas, which is preferably passed through water for getting saturated vapor of water. It is well known that presence of salt in the solution significantly effect the change of the gel volume. Hence the salt effect was ignored by using polyelectrolyte buffer solution instead of the buffer of low molecular weight electrolytes. In addition, poly(Acrylic acid) pH buffer was found to have appreciable stability with temperature as reported previously.¹⁰

4.2.5. Measurements of swelling ratio

A special type of closed-system cell was used to measure the equilibrium degree of swelling behaviors of gels (Figure 4.4.). It contains two long quartz capillary tubes where the cylindrical gels are kept at specific pH buffer solutions and sealed two ends of the capillary by using rubber stopper. The quartz capillary was encapsulated in a transparent square glass cell. The temperature inside the square glass cell can be regulated by circulating temperature-controlled water around the quartz capillary and thereby the temperature of the gel samples can precisely be controlled. A temperature sensor is associated in the inner portion of square glass cell

to measure the temperature inside the cell. The diameter of the gel inside the cell was measured with an inverted optical microscope which is equipped with a color measure unit. The swelling ratio, d/d_0 , where d is the diameter of the gel and d_0 is the diameter of the capillary, were measured as a function of temperatures. The video of the morphological change of gels were recorded using BUFFALO PCast TV capture software in a computer and then pictures were taken at different time intervals. The kinetics of shrinking and swelling behaviors of gels were quantitatively analyzed from these pictures.

4.2.6. Gel Permeation Chromatography, GPC

GPC measurements was carried out on a Tosoh HLC-8220GPC high-performance liquid chromatography system (Tokyo, Japan) using a refractive-index detector equipped with three columns in series: a TSK Super AW-H guard column and two TSK Super AWM-H gel columns (6.0 mm in diameter and 150 mm in length; pore size = 9 μm). DMSO/0.1 M LiBr was used as the eluent (temperature = 50 $^{\circ}\text{C}$, and flow rate = 0.5 mL/min). The molecular weight and dispersity index were calculated using poly(ethylene oxide) standards.

4.2.7. Thermo Gravimetric / Differential Thermal Analysis, TG/DTA

TG/DTA data were measured by TG/DTA6300 of Seiko Instruments Inc., Japan. For each measurement 50 mg swollen gel sample was taken in a platinum sample pan and analyzed in the range of 20 $^{\circ}\text{C}$ - 450 $^{\circ}\text{C}$ at a heating rate of 10 $^{\circ}\text{C}$ per minute.

4.2.8. Scanning Electron Microscope (SEM)

The SEM images of the gel samples were performed by a scanning electron microscope (SEM, JEOL JSM-5600). The equilibrium swollen hydrogel samples in water at room temperature were quickly immersed in liquid nitrogen. Samples were

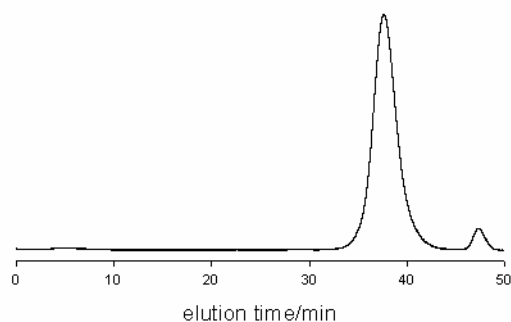


Figure 4.2. GPC profile for water soluble polyrotaxane cross-linker, MHPR (DS = 1.98)

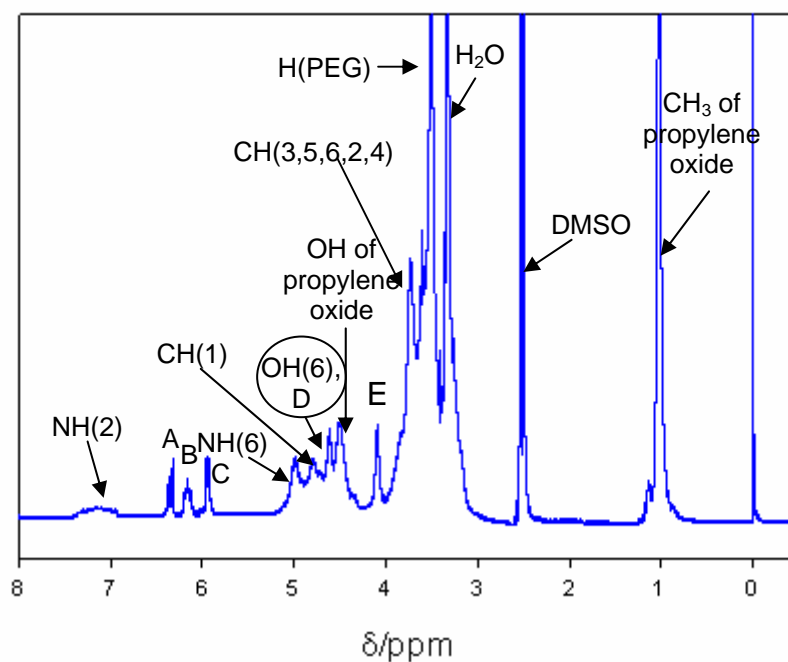


Figure 4.3. ^1H -NMR spectrum of water soluble polyrotaxane cross-linker, MHPR (DS = 1.98) in DMSO-d_6 .

then freeze dried under vacuum at -52 °C for 3 days. Freeze dried samples were coated properly with gold prior to the SEM observations.

4.2.9. Mechanical Strength tests

The viscoelastic properties and stress-strain curves of the gels were measured with a Rheometric Solid Analyzer, RSA III of Rheometric Scientific, Inc. The rheometer consists of one normal force transducer (1kFRT) that can detect normal forces within up to 35 N (3500 g) and a motor having frequency range between 6.28×10^{-6} to 502 rad sec⁻¹, amplitude range ± 1.5 mm, response time <5 msec to 90% of final value, and strain resolution of 0.00005 mm. For the viscoelastic measurements, 4 mm thick slab gel samples were prepared and cut into rectangular shapes (10 mm \times 10 mm). The gel samples were under compression with a constant pre-strain of 5 % during measurements to ensure the gel samples was always under compression. The strain controlled dynamic frequency sweep test was used as a test setup and the selected 3% strain was in the region of the linear viscoelastic region of the sample. The change of E' and E'' were observed in the frequency range 0.01 to 100 rad sec⁻¹.

For the stress-strain curves, 0.5 mm thick gel samples were prepared and cut into rectangular shapes of 5 mm width and 7-10 mm length. Place the samples between the two fixtures and tighten the screws of sample loading bolts of either end. It was insured that sample is aligned in the fixtures and neither wrinkles nor kinks are experienced by gel samples prior to the measurements. Transient strain controlled multiple extension mode was used as test set up. In the whole time zone, extension value was selected at a rate of 0.1 mm/sec. The measurements were carried out in air at room temperature. The reproducibility of the stress-strain curves was checked under successive measurements.

Table 4.1. Preparation of TN-S gels by varying the amounts of ionic monomer

Samples code	NIPA (M)	BIS (mM)	TEMED	APS	SA (M)	Solvent, water
TN-S1	2	33	20 μ l	6 mg	0	5 ml
TN-S2	1.975	33	20 μ l	6 mg	0.025	5 ml
TN-S3	1.9	33	20 μ l	6 mg	0.1	5 ml
TN-S4	1.85	33	20 μ l	6 mg	0.15	5 ml
TN-S5	1.6	33	20 μ l	6 mg	0.4	5 ml

Table 4.2. Preparation of TN-S gels by varying the amounts of cross-linker

Samples code	NIPA (M)	BIS (mM)	TEMED	APS	SA (M)	Solvent, water
TN-S50	1.9	50	40 μ l	12 mg	0.1	10 ml
TN-S33	1.9	33	40 μ l	12 mg	0.1	10 ml
TN-S20	1.9	20	40 μ l	12 mg	0.1	10 ml
TN-S13.3	1.9	13.3	40 μ l	12 mg	0.1	10 ml
TN-S10	1.9	10	40 μ l	12 mg	0.1	10 ml
TN-S8	1.9	8	40 μ l	12 mg	0.1	10 ml
TN-S6.6	1.9	6.6	40 μ l	12 mg	0.1	10 ml
TN-S5.0	1.9	5.0	40 μ l	12 mg	0.1	10 ml

Table 4.3. Preparation of R_{ws}N-S gels by varying the amounts of cross-linker

Samples code	NIPA (M)	MHPR (wt%)	TEMED	APS	SA (M)	Solvent, water
R _{ws} N-S0.5	1.9	0.5	20 µl	6mg	0.1	5 ml
R _{ws} N-S0.8	1.9	0.8	20 µl	6mg	0.1	5 ml
R _{ws} N-S1	1.9	1	20 µl	6mg	0.1	5 ml
R _{ws} N-S2	1.9	2	20 µl	6mg	0.1	5 ml
R _{ws} N-S5	1.9	5	20 µl	6mg	0.1	5 ml

4.3. Results and Discussion

4.3.1. Preparation of water soluble polyrotaxane cross-linker, MHPR

HPR was used as starting materials for the preparation of hydrophilic polyrotaxane cross-linkers. The detail of syntheses of MHPR is reported in the chapter 3. HPR was modified by a 2-acryloyloxyethyl isocyanate as the same way mentioned in the chapter 3. The isocyanate group forms a stable carbamate bond with the hydroxyl groups of polyrotaxane to yield cross-linker, which we refer to as MHPR. Here the feeding ratio, F.R, of 2-acryloyloxyethyl isocyanate monomer with respect to the number of the OH groups present in each α -CD was 5. But the degree of substitution (DS) ($0 \leq DS \leq 18$), i.e., the average number of substituted hydroxyl groups per α -CD unit of the MHPR, calculated using ^1H NMR spectra was found to be 1.98 (Figure 4.3.). The structure of the cross-linker is further evidenced from the FT-IR spectrum. The number average molecular weight, $M_n = 121402$, the weight average molecular weight, $M_w = 172891$ and dispersity index, $M_w/M_n = 1.424$ were calculated from the GPC of MHPR.

4.3.2. Effect of salt on the swelling behaviors of ionic gels

Salt has significant effect on the volume phase transition temperatures of TN-S and $R_{ws}N$ -S gels.¹¹ In this study instead of the buffer solutions of low molecular weight electrolytes, salt-free polyelectrolyte buffer solution was used to prevent the salt effect of ionic gels. It is well known that the addition of inorganic salt in the swelling solvent lowered the transition temperature of the ionic gel.¹² The swelling behavior of the gel solely depend on the anionic species but independent of cationic species. H-bond may form with the anionic species of the salt. Hence, reduces the amount of hydrophobic hydration in the networks and increases the hydrophobic interaction. As a result volume phase transition occurs at low temperature. The gel

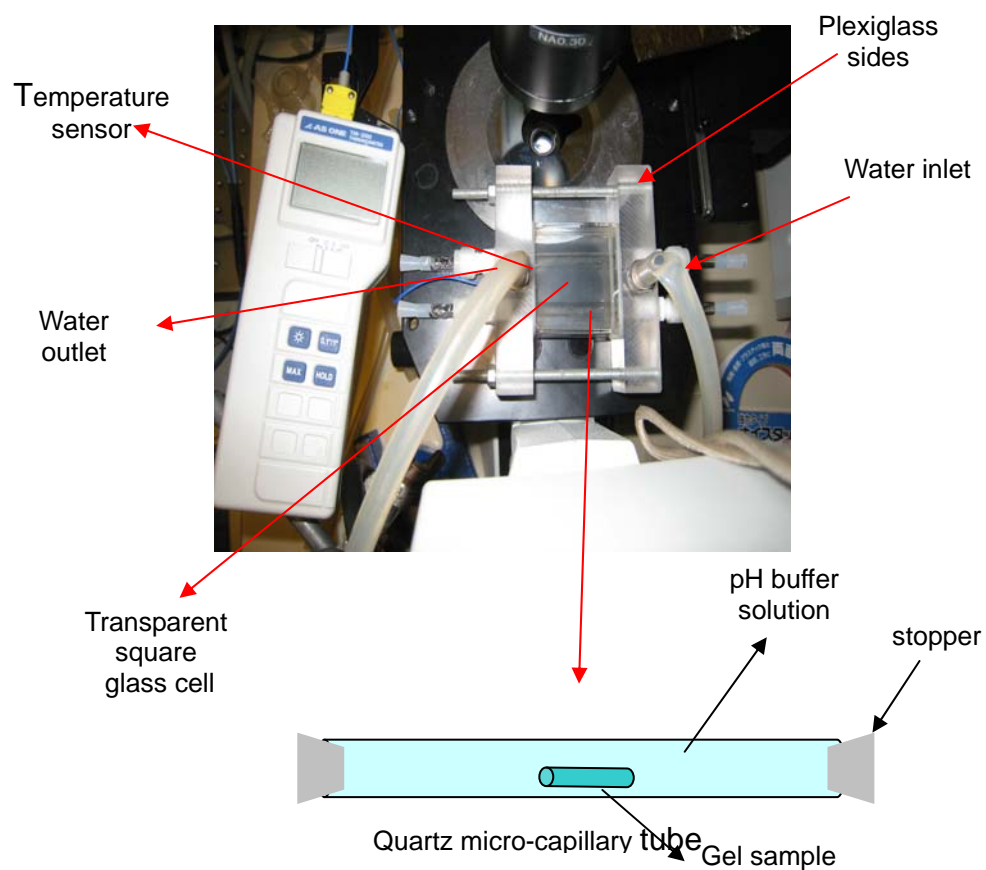


Figure 4.4. A special type of closed- system cell for the measurement of swelling ratio and kinetic of shrinking and swelling of the gels.

volume gradually decreases with increasing salt concentration in the solution and changes abruptly after a certain level of concentration. The continuous volume changes of TN-S and R_{ws}N-S gels in the salt free solution turn to a discontinuous one in the salt solution.

The phenomena can also be explained in term of chemical potential, μ . Chemical potential of water molecules decreases with increase in temperature or concentrations of additives due to the contribution of entropy. The water molecules come out from the gel networks to the bulk when the μ of water is lower than that of the water molecule associated in the gel networks. The presence of salts reduce the chemical potential of water, which causes the desorption of water molecules from the gel networks. At a given temperature, the chemical potential of water in the salt solution decreases with increasing the salt concentration due to the free energy mixing. Therefore, increase in salt concentration and increase in temperature has the same effect of decreasing the chemical potential of water. The chemical potential of water in solution containing an additive (species i) at concentration of C_i is expressed as.¹³

$$\mu_{H_2O}(T, C_i) = \mu^0_{H_2O}(T) + RT \ln a_w(C_i)$$

where $\mu_{H_2O}(T)$ is the chemical potential of water at temperature T , $a_w(C_i)$ is the activity of water in the presence of an additive C_i . Hence, the decreases of the chemical potential of water caused by the addition of inorganic salts is given by

$$\Delta\mu_{H_2O}(T, C_i) = -RT \ln a_w(C_i)$$

When the value of $\Delta\mu_{H_2O}$ is positive, water molecules preferably bind to the polymer chains and hydrated state is highly stable. The higher the difference more water molecules will bind to the polymer chains.

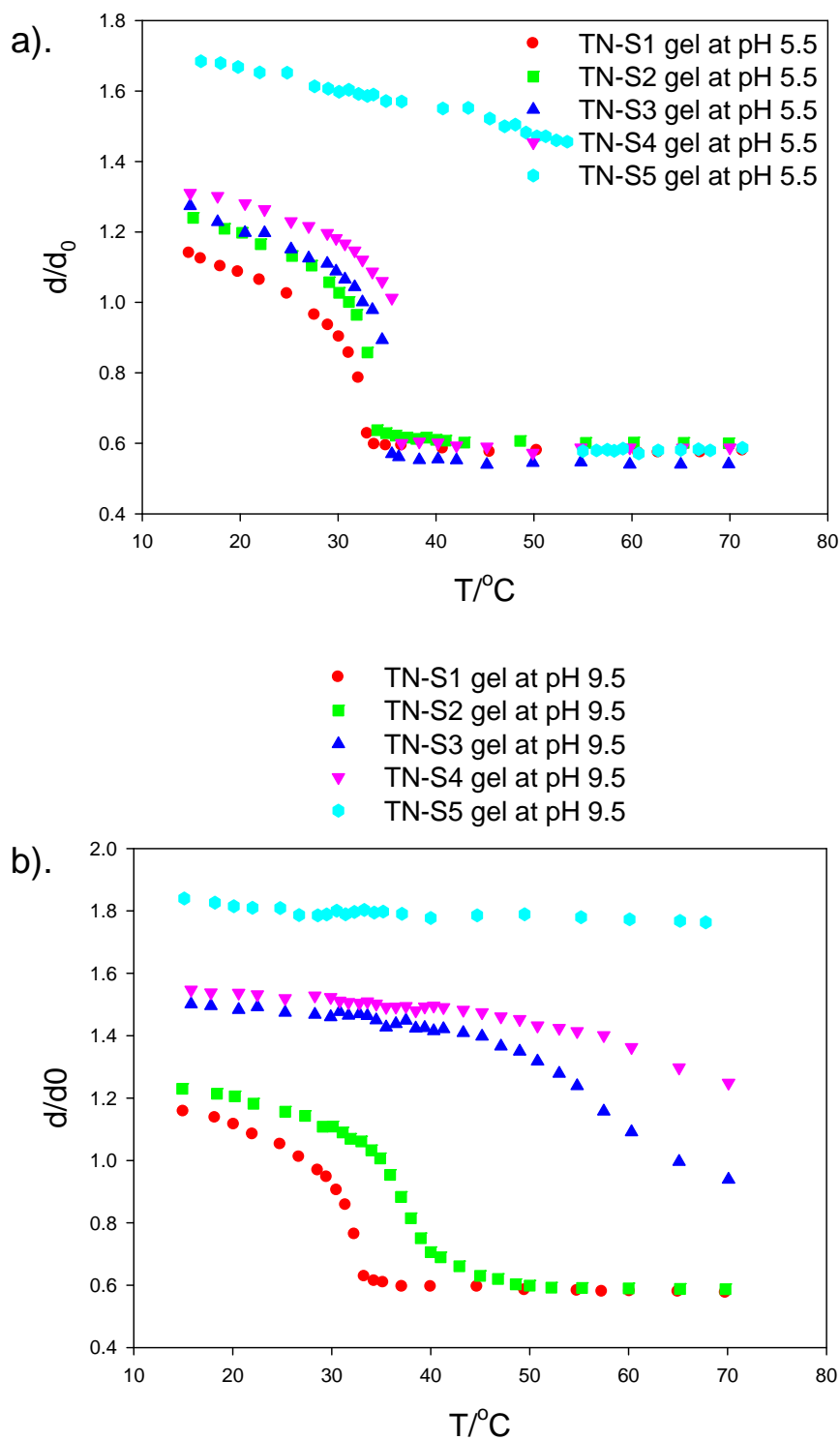


Figure 4.5. Degree of swelling behavior of different types of TN-S gels (where the gels were prepared by varying the amount of ionic monomer, SA) as a function of temperatures at a) pH = 5.5 and b) pH = 9.5

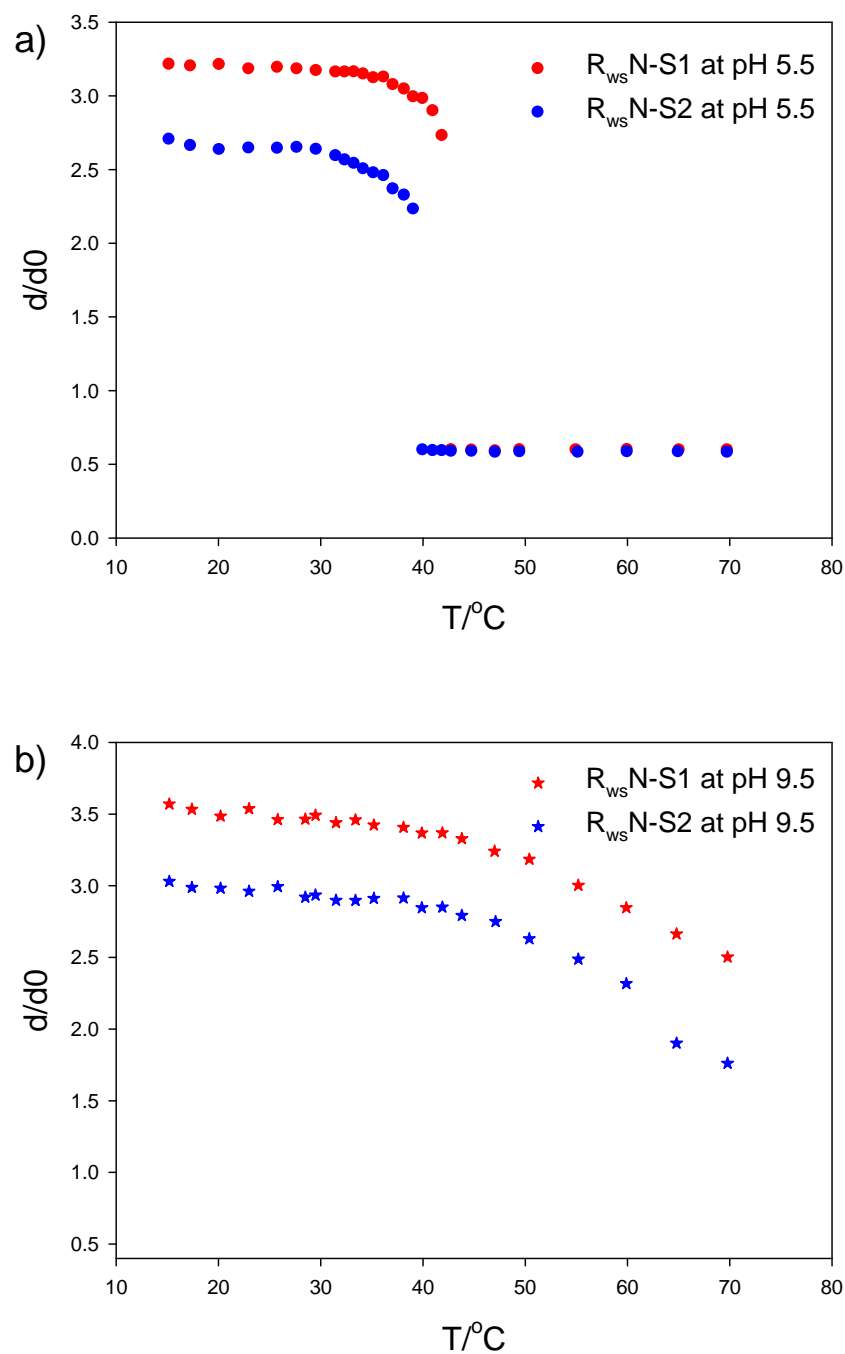


Figure 4.6. Degree of swelling behavior of $R_{ws}N-S1$ and $R_{ws}N-S2$ gels as a function of temperatures a) at pH = 5.5 and b) at pH = 9.5

4.3.3. Swelling behavior at pH 5.5

Figure 4.5.a. shows the degree of swelling behavior of different types of TN-S gels as a function of temperatures at pH = 5.5. In all cases the amount of cross-linker BIS was maintained constant as 33 mM but the amounts of ionic groups were varied from 0-0.4 M. TN-S1 gel i.e neutral NIPA gel changes its volume almost continuously as a function of temperatures. But when ionic groups are introduced in the TN gel, the gel volume changes discontinuously at high temperatures. The transition temperature shifts to the higher temperature with increase in the amounts of ionic groups. For every cases, the equilibrium collapsed states fall in the single straight line. Since the total amount of monomers were maintained constant for TN-S gels.

Figure 4.6.a. represents the degree of swelling behavior of $R_{ws}N-S1$ and $R_{ws}N-S2$ gels as a function of temperatures at pH = 5.5. In both cases, discontinuous volume phase transitions are observed. The increase in cross-linker, MHPR into the gel networks favors the shift of volume transition at low temperatures. $R_{ws}N-S1$ gel has higher swelling ratio than $R_{ws}N-S2$ gel at low temperatures but at high temperature both gels have same collapsed state. During the cooling process a huge hysteresis in the swelling curves is observed for the $R_{ws}N-S$ gels (Figure 4.7.a.). The volume phase transition in the cooling process occurs at lower temperatures than the heating process. Figure 4.8. demonstrates the change in volume phase transition temperatures, T_c of TN-S3 and TN-S4 gel during heating and cooling process at pH = 5.5 buffer solutions. During the heating process TN-S4 gel which contains much amount of ionic groups has higher T_c (36.5 °C) than TN-S3 gel (35.5 °C). But in the cooling process both gels have T_c at the same temperature. In the heating process of $R_{ws}N-S$ gel, when the amount of cross-linker is increased, T_c decreases accordingly (Figure 4.9.). $R_{ws}N-S1$

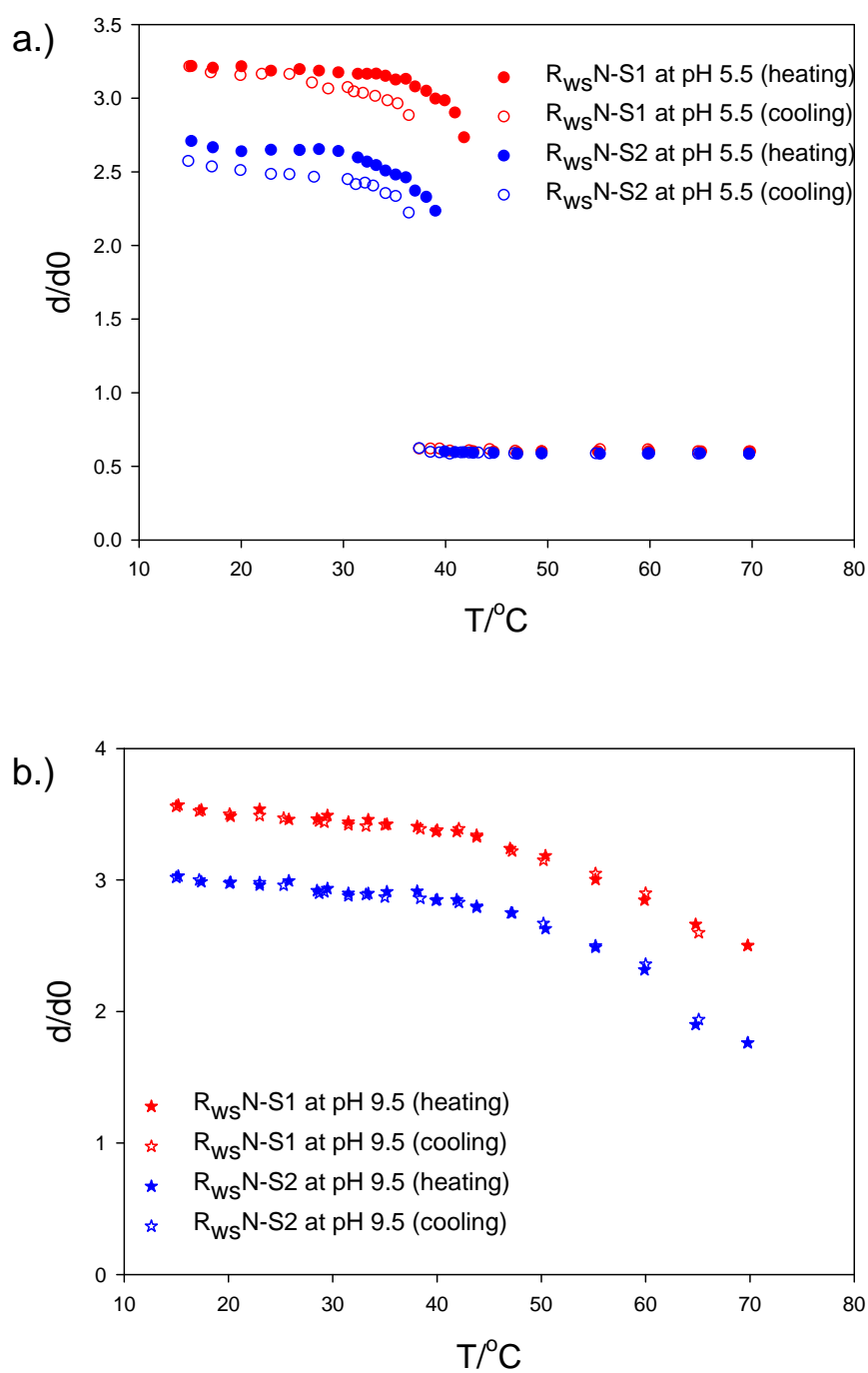


Figure 4.7. Static equilibrium degree of swelling behaviors of $R_{ws}N-S1$ and $R_{ws}N-S2$ gels during heating and cooling processes a.) at pH = 5.5 and b.) at pH = 9.5 polyelectrolyte buffer solutions.

gel has T_c at 42.8 °C while $R_{ws}N$ -S2 gel has T_c at 40 °C. But in the cooling process either gel has same T_c at 36.5 °C.

Figure 4.10.a. shows the comparison of degree of swelling behavior of neutral poly(NIPA), TN gel, ionic poly(NIPA), TN-S5.0 gel and neutral rotaxane-poly(NIPA), $R_{ws}N$ gel and ionic rotaxane-poly(NIPA), $R_{ws}N$ -S1 gel as a function of temperatures at pH = 5.5. Swelling behavior of TN gel and $R_{ws}N$ gels are independent of the pH of swelling media. At low temperatures they have very small degree of swelling than the ionic gels. TN and $R_{ws}N$ gels change their volume continuously while discontinuous volume transitions are observed for TN-S5.0 and $R_{ws}N$ -S1 gels.

At low temperatures TN-S5.0 and $R_{ws}N$ -S1 gels exhibit higher degree of swelling but $R_{ws}N$ -S1 gel has significantly higher swelling ratio. Due to the hydrophilic nature of the cross-linker, MHPR, the volume phase transition of the $R_{ws}N$ -S1 gel occurs at relatively high temperatures.

Figure 4.11. demonstrates the effect of swelling media on the degree of swelling behaviors for $R_{ws}N$ -S1 gel as a function of temperatures. $R_{ws}N$ -S1 gels in water have almost similar swelling behavior in pH = 5.5 of polyelectrolyte buffer solution. It should be noted that the water might have the pH around 6 i.e. acidic in nature. Hence in water and at pH = 5.5, gels volume change discontinuously as a function of temperatures.

In the $R_{ws}N$ -S and TN-S gels the carboxyl groups are fully dissociated to COO^- and Na^+ in the as prepared state. But after a repeated wash with water, the Na^+ could be exchanged by the proton of water molecules. Hence, the $-COOH$ groups of the gel networks becomes sufficiently neutral. Rest of the dissociated COO^- and H^+ contributes to the internal osmotic pressure (swelling force).

Introduction of ionic monomer into the poly(NIPA) gel has two effects: positive osmotic pressure due to ionization in one case and negative osmotic pressure due to the attractive force of the hydrogen bonding in the other.¹⁴ At pH <6.3, the degree of ionization, α , decreases as a function of temperature.¹⁵ That is, the dissociation constant of carboxyl groups in ionic gel decreases with increasing temperature. A steep decrease of α is observed above 34 °C. But a large fraction of un-ionized carboxyl groups is still found at high temperatures. This indicates that a significant fraction of the carboxyl group in the shrunken gel was unionized. The sharp decrease in α with increasing temperatures is directly correlated with the discontinuous volume phase transition observed in TN-S and R_{ws}N-S gels. It has been found that nonionic R_{ws}N gels underwent a sharp and continuous volume change as a function of water. When a tiny amount of ionizable groups are incorporated into the gel networks, the volume changes drive toward a discontinuous one. Here the osmotic pressure of the ionic groups makes the transition to a discontinuous one and shifts the volume transition to high temperature. As the total concentrations of the monomers were kept constant, the collapsed states of the gels have similar degree of swelling behavior.

In general, the volume phase transition is a result of the competing forces of repulsive electrostatic interaction among the ions and the hydrophobic interaction the isopropyl groups present in the co-polymers of the gel networks. The electrostatic repulsion preferably occurs at low temperatures in the R_{ws}N-S gel, the gel becomes swollen state. On the other hand, the hydrophobic interaction dominates at higher temperatures and the gel turns to collapsed state. Although the hydrophobic interaction for R_{ws}N-S gel is not as active as in non-ionic poly(NIPA) gel at pH = 5.5 but the decrease of ionization leads to the decrease in donnan osmotic pressure of

counter ions. And the unionized COOH groups of gel network may form strong hydrogen bond with CONH groups. All of these three effect i.e reduced donnan osmotic pressure, ability to form H-bond between COOH and CONH groups and the weak hydrophobic interactions are the responsible factors for the discontinuous volume change of the gels at $\text{pH} = 5.5$. When the contents of Sodium acrylate are increased, the ionization of the gel is also increases. Hence the volume phase transition temperature shifts to the higher temperatures.

4.3.4. Swelling behavior at $\text{pH} 9.5$

Figure 4.5. b shows the degree of swelling behavior of different types of TN-S gels (where the gels were prepared by varying the amount of ionic monomer, SA) as a function of temperatures at $\text{pH} = 9.5$. At $\text{pH} 9.5$, all gels change their volume continuously with the temperatures. It has been found that, when the amount of ionic monomer, SA is more than 0.1 M, TN-S gels can not reach to an equilibrium collapsed state. TN-S5 gel ($\text{SA} = 0.4 \text{ M}$) almost loses its thermo-sensitivity.

Figure 4.6.b. represents the degree of swelling behavior of $\text{R}_{\text{ws}}\text{N-S1}$ and $\text{R}_{\text{ws}}\text{N-S2}$ gels at $\text{pH} = 9.5$ buffer solution. $\text{R}_{\text{ws}}\text{N-S}$ gels exhibit continuous volume change at $\text{pH} 9.5$ but none of the gel can reach to equilibrium collapsed state like TN-S gels. Decrease in cross-linker amount in the $\text{R}_{\text{ws}}\text{N-S}$ gels decrease the thermal sensitivity of the gel. During the cooling process, $\text{R}_{\text{ws}}\text{N-S}$ gels can completely memorized its volume. No hysteresis loop is observed in the swelling curves(Figure 4.7.b.).

In the figure 4.10.b. ionic poly(NIPA), TN-S5.0 gel and ionic rotaxane-poly(NIPA), $\text{R}_{\text{ws}}\text{N-S1}$ gel have continuous volume changes with the change in temperature. Introduction of ionic groups suppresses the hydrophobic interaction of the polymer chains in the gel networks. Hence the gels volumes change continuously as a function of temperatures.

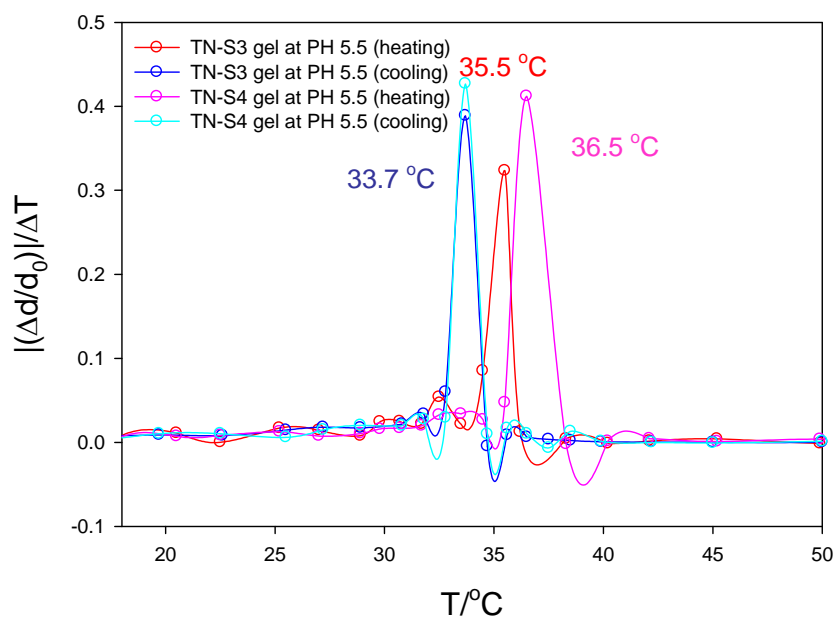


Figure 4.8. Change in volume phase transition temperatures, T_c of TN-S3 and TN-S4 gel during heating and cooling process at pH = 5.5 polyelectrolyte buffer solutions.

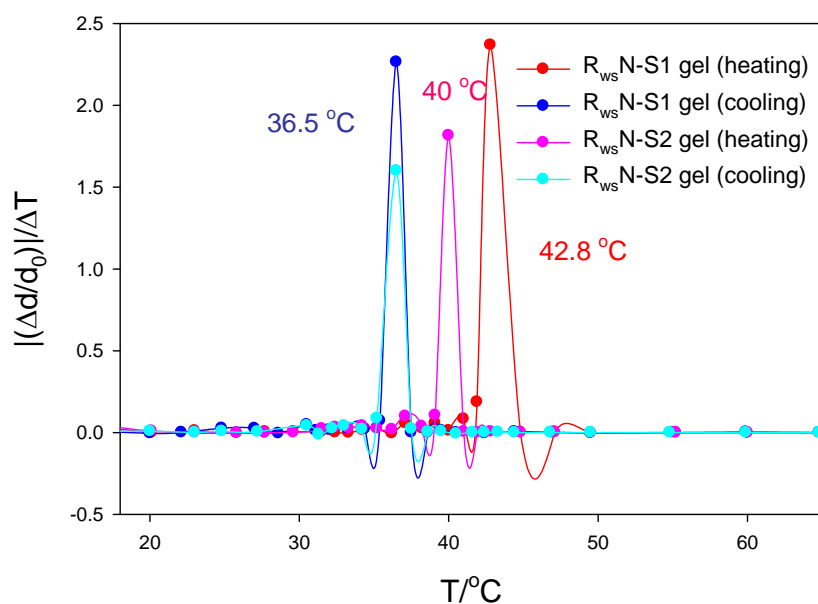


Figure 4.9. Change in volume phase transition temperatures, T_c of $R_{ws}N$ -S1 and $R_{ws}N$ -S2 gel during heating and cooling process at pH = 5.5 polyelectrolyte buffer solutions.

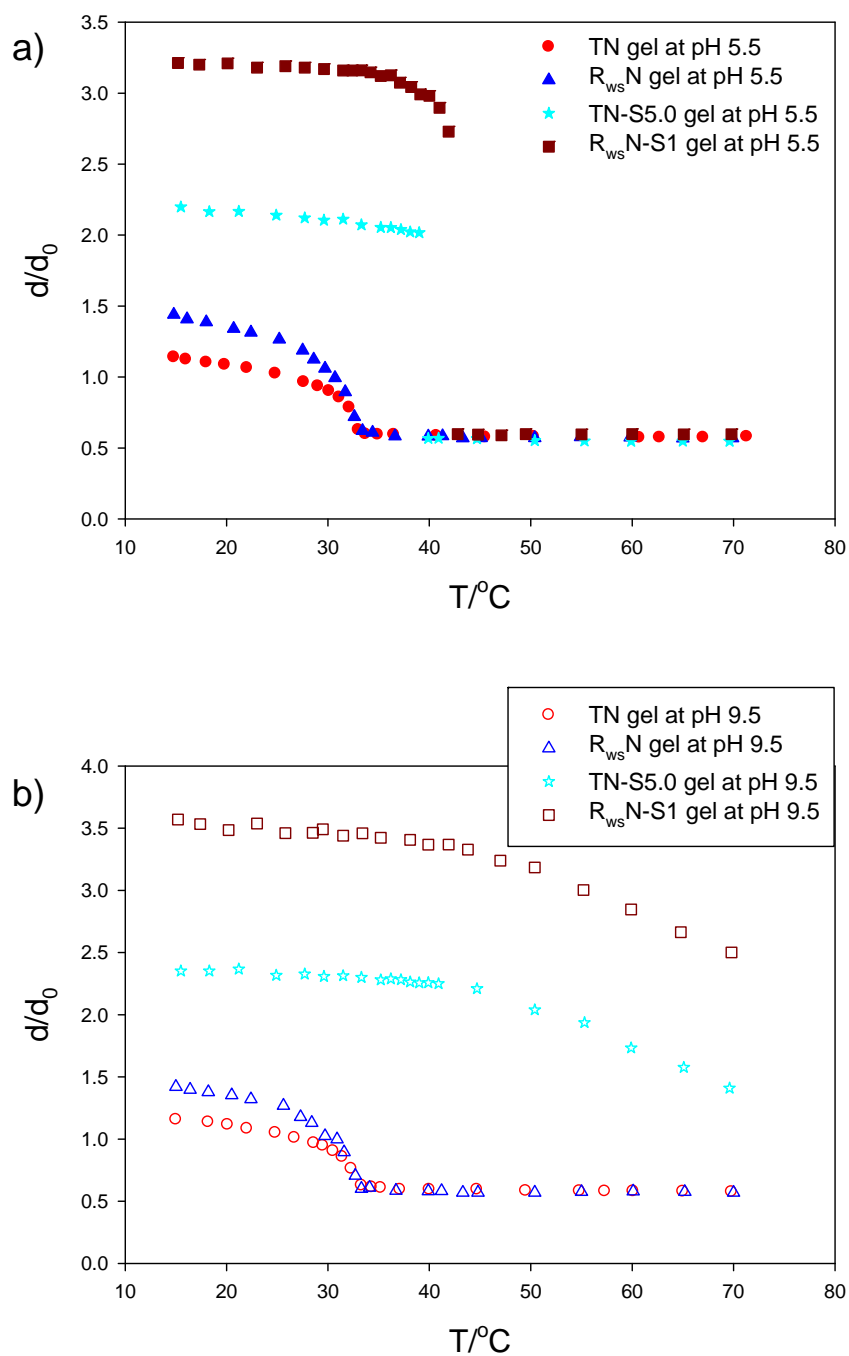


Figure 4.10. Degree of swelling behavior of neutral poly(NIPA), TN gel, ionic poly(NIPA), TN-S5.0 gel and neutral rotaxane-poly(NIPA), R_{ws} N gel and ionic rotaxane-poly(NIPA), R_{ws} N-S1 gel as a function of temperatures at a) pH = 5.5 and b) pH = 9.5

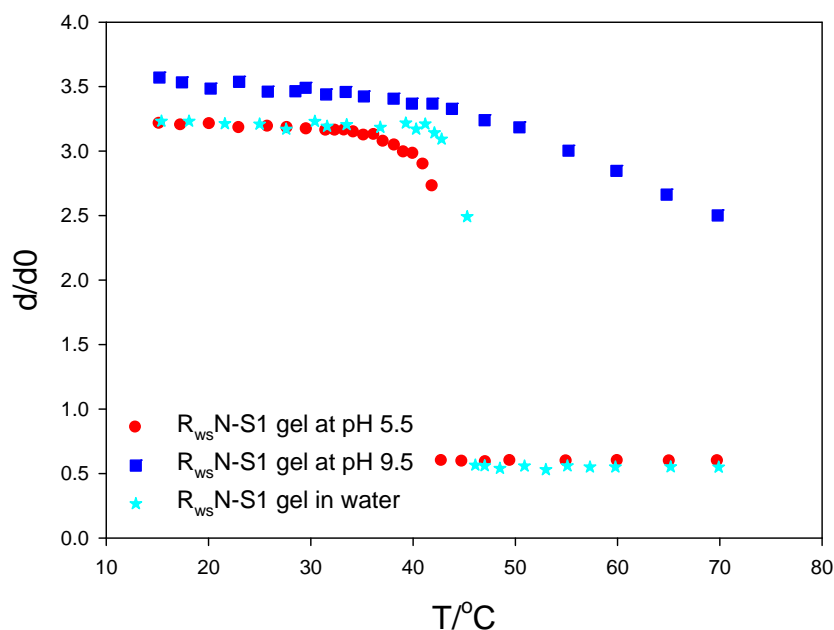


Figure 4.11. Effect of swelling media on the degree of swelling behaviors for $R_{ws}N$ -S1 gel as a function of temperatures.

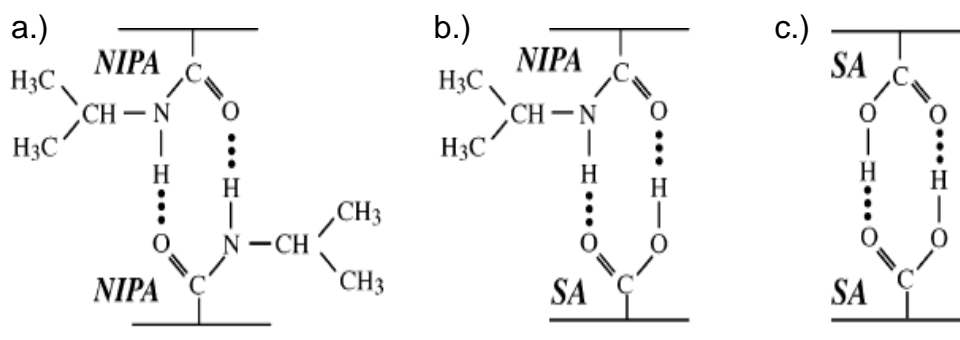


Figure 4.12. Formation of possible types of hydrogen bonds between carboxyl group of SA and the amide group of NIPAA in $R_{ws}N$ -S gel networks a) hydrogen bond between NIPAA and NIPAA, b) hydrogen bond between NIPAA and SA, and c) hydrogen bond between SA and SA.

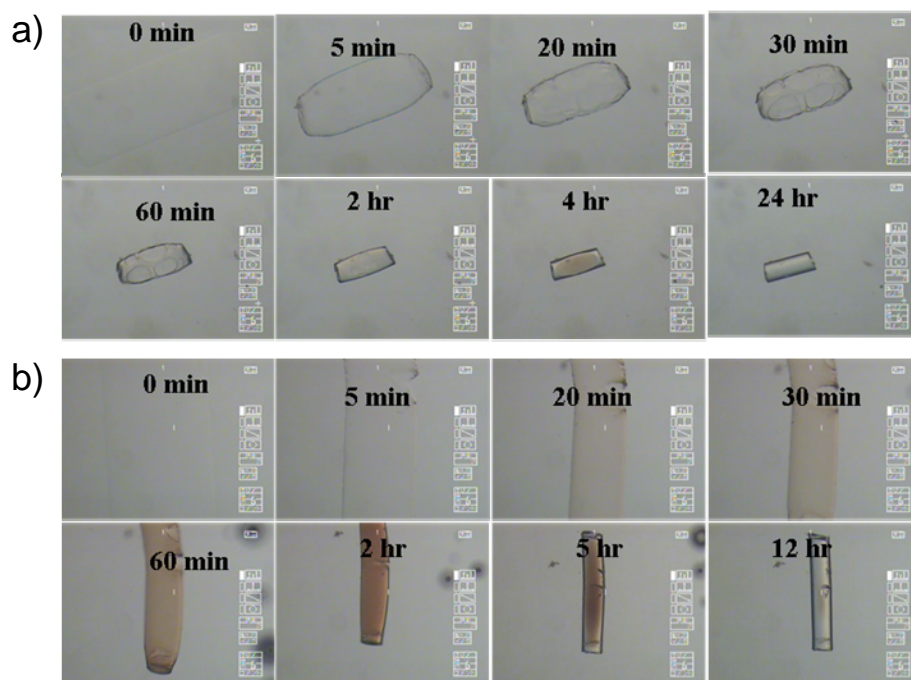


Figure 4.13. Optical micrographs for the shrinking patterns of a.)TN-S5.0 and b.) R_{ws} N-S1 gels after a temperature jump from 20 °C to 50 °C at pH 5.5

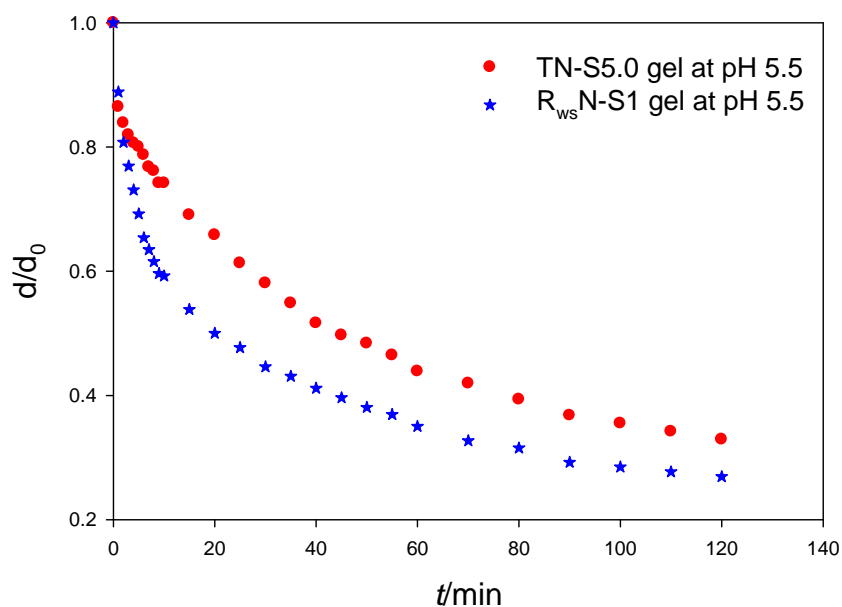


Figure 4.14. Shrinking kinetics of TN-S5.0 and R_{ws} N-S1 gels after a temperature jump from 20 °C to 50 °C.

At pH = 9.5, α is independent of temperature. That is, the most of the carboxyl groups exist as carboxylate ions. Thereby, increase the donnan osmotic pressure of the gels, which alter the inherent discontinuity of the TN-S and $R_{ws}N$ -S gels to the continuous one. Here, the hydrophobic interaction of NIPA chains is not adequate enough, even at high temperatures, to overcome the increased donnan osmotic pressure owing to the repulsion among ionic groups. As a result volume changes continuously at pH = 9.5 with increasing temperatures.

4.3.5. Shrinking Kinetics of TN-S and $R_{ws}N$ -S gel at pH 5.5

Figure 4.13. shows the optical micrographs for the shrinking patterns of TN-S5.0 and $R_{ws}N$ -S1 gels after a temperature jump from 20 °C to 50 °C at pH 5.5. The time to reach equilibrium shrunken states for either gels are slow but $R_{ws}N$ -S1 gel shrinks relatively much faster rate. During the shrinking process bubble formation was observed on the surface of the TN-S gel. In contrast, $R_{ws}N$ -S1 gel shrinks isotropically and no bubble formation or deformation of the gel surface was observed in any stages during shrinking. $R_{ws}N$ -S1 gel gradually becomes opaque after a sudden temperature jump and it again reaches to an equilibrium transparent shrunken state after long time aging at high temperature.

Figure 4.14. represents the kinetics plots of shrinking for TN-S5.0 and $R_{ws}N$ -S1 gels after a temperature jump from 20 °C to 50 °C. The plot clearly indicates that $R_{ws}N$ -S1 gel has much faster shrinking kinetic than the TN-S5.0 gel. The shrinking and swelling of gels are usually governed by the co-operative diffusion of the polymer gel networks and solvent molecules. In the TN-S gel, the gel networks are formed by the fixed covalent bonds. Hence, the diffusion co-efficient of the gel networks is small. This plays a decisive role for the very slow shrinking rate of TN-S gels.



Figure 4.15. Volume change of $R_{ws}N-S0.8$ gel in water. Left: the dried gel (129 mg) and right: the water-swollen gel (80g) The $R_{ws}N-S0.8$ gel absorbs water up to ca. 62,000 wt% to its dried state.

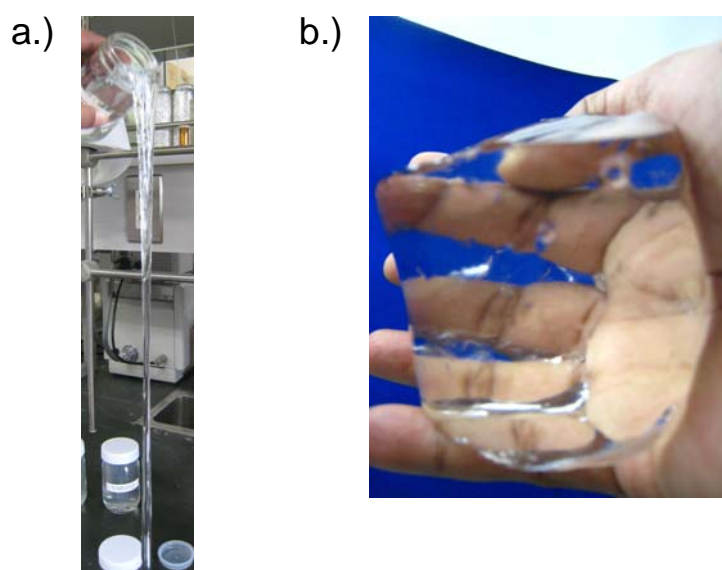


Figure 4.16. Stability of a.) $R_{ws}N-S0.5$ gel, b.) $R_{ws}N-S0.8$ gel after equilibrated in water. When the cross-linker amount is $0.5 \text{ wt}\% \leq$, infinite dilution occurs but still the gel exhibits rubber-like elasticity. But when the cross-linker amount is $0.8 \text{ wt}\% \geq$, the highly swollen gel maintains its size and shape, and can tolerate appreciable amount of external strain in the swollen state.

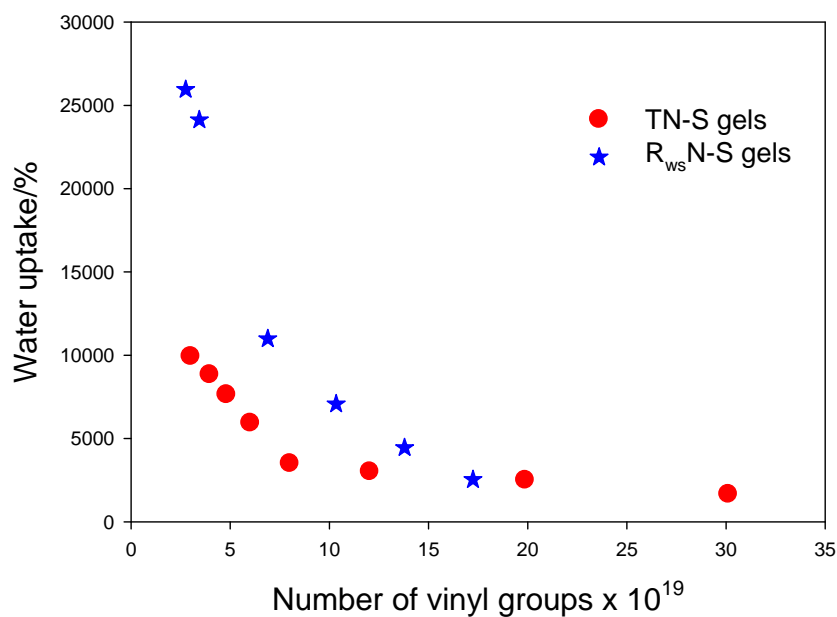


Figure 4.17. Water uptake percentage of TN-S and R_{ws}N-S gels as function of the number of active vinyl groups of the cross-linkers BIS and MHPR used for the preparations of TN-S and R_{ws}N-S gels respectively in the initial pre-gel solutions.

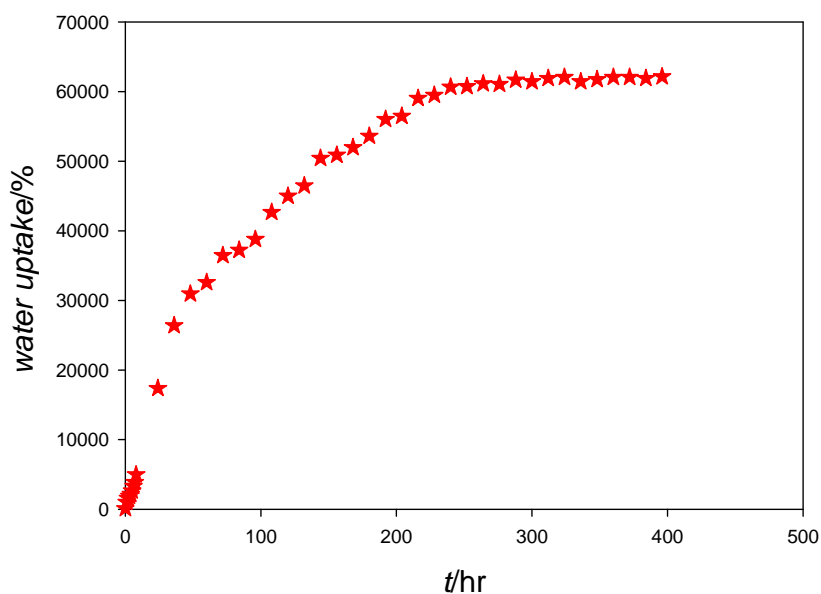


Figure 4.18. Slow swelling dynamic of dried rectangular sized R_{ws}N-S0.8 gel samples (129 mg) at 4 °C. The gel can absorb ca. 62000 wt% of water of its dried state.

On the other hand, the fast shrinking kinetics of rotaxane –NIPA gels have been described in the chapter 2 and chapter 3. The presence of movable cross-links helps to coalesce the locally shrunken phases close to each other. Ultimately the gel quickly reaches to a shrunken state. But introduction of ionic co-monomer into the gel networks decrease the shrinking rate of $R_{ws}N$ -S1 gel to some extent. Electrostatic repulsions among the ionic groups hindered the hydrophobic interactions of the isopropyl groups of poly(NIPA) chains. As a result relatively slow shrinking rate was observed for $R_{ws}N$ -S1 gel than the neutral $R_{ws}N$ gel.

4.3.6. Super absorbency of $R_{ws}N$ -S gels

$R_{ws}N$ -S gels can absorb huge amount of water in its network structure. The $R_{ws}N$ -S0.8 gel absorbs water up to ca. 62,000 wt% to its dried state. When the amount of cross-linker is 0.5% or less than to it, infinite dilution occurs in the gel (Figure 3.16.). $R_{ws}N$ -S0.5 gel loses its size and shape and acts like a highly viscous liquid. Interestingly, the gel shows appreciable elasticity even in the infinite dilution state. But when the cross-linker amount is 0.8 wt% or more than to it, the gel gigantically absorbs water to the networks. $R_{ws}N$ -S0.8 gel after extreme swelling in water has distinct size and shapes and it can tolerate appreciable amounts of external strain or deformation in that state.

Figure 4.17. represents the water uptake percentage of TN-S and $R_{ws}N$ -S gels as function of the number of active vinyl groups of the cross-linkers BIS and MHPR used for the preparations of gels. The bi-functional BIS has two vinyl groups in each molecule, on the other hand the total number of vinyl groups in the multifunctional cross-linker, MHPR have been estimated from the 1H -NMR spectrum and found as ca. 200 per MHPR. From the figure it can be concluded that, at high cross-link density, the water uptake percentage increases linearly with the number of the vinyl groups.

But for the lightly cross-linked $R_{ws}N-S$ gel, the water uptake percent drastically increases. Water uptake percentages of the gels were measured after keeping the gel in water at 4 °C for 2 days. TN-S gels were found not to have notable volume change after two days. But $R_{ws}N-S$ gels have been found to have a slow swelling dynamic in water. The $R_{ws}N-S$ 0.8 gel takes long time to reach equilibrium swollen state. Rectangular sized (129 mg) dried $R_{ws}N-S$ 0.8 gel reaches to equilibrium swollen state (80 g) after ca. 12 days. The extreme swelling characteristic of the $R_{ws}N-S$ gels results from the electrostatic repulsion between the charges on the polymer chains, and the osmotic pressure of the counter ions present in the gel networks. The electrostatic interactions increases distance of hydrated polymer chains and expands the gel networks through the movements of cross-links in water at low temperatures. Hence, the gel can uptake huge amount of water.

4.3.7. *TG/DTA analysis of $R_{ws}N-S$ gel*

In the $R_{ws}N-S$ gel, huge initial weight loss of sample is observed around 100 °C(Figure 4.19.). After the initial weight loss of the gel, the total weight of the sample approaches to zero. In contrast, in the TN-S gels after the initial weight loss, an appreciable amount of gel networks remain. The initial weight loss of the samples must come from the loss of water molecules from the gel networks. This also suggests the super absorbent capacities of $R_{ws}N-S$ gels in water.

4.3.8. *SEM*

Figure 4.20. represents the SEM images of TN-S5.0 and TN-S50 gels after freeze drying the equilibrated water-swollen gels. In the TN-S50 gel, interior morphology is not seen due to high cross-link density, while small and randomly oriented pores are observed for TN-S5.0 gel. The average pore sizes of TN-S5.0 gels are found as 12 ± 4 μm . In contrast, much bigger pores are found in $R_{ws}N-S5$ and

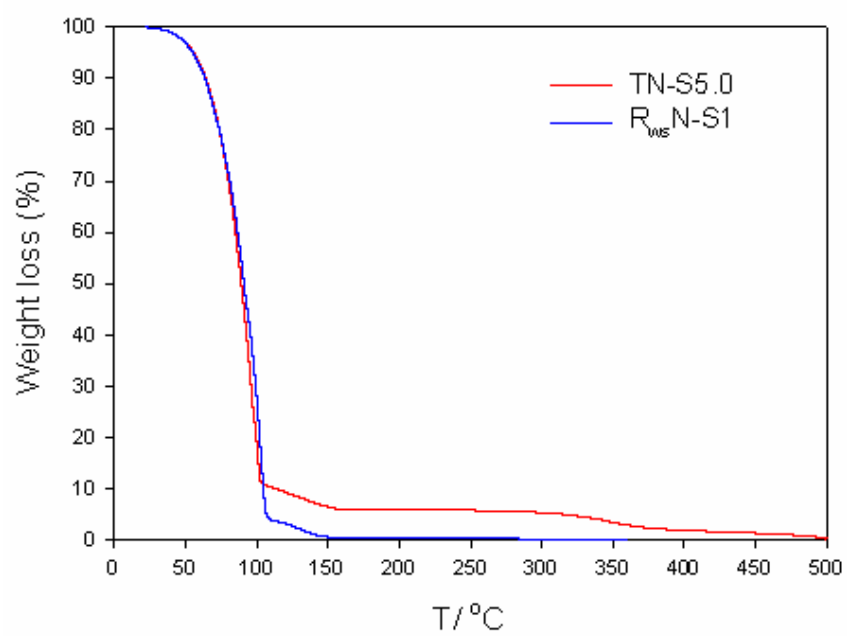


Figure 4.19. Thermo gravimetric analysis of TN-S5.0 and R_{ws}N-S1 gels swollen in water.

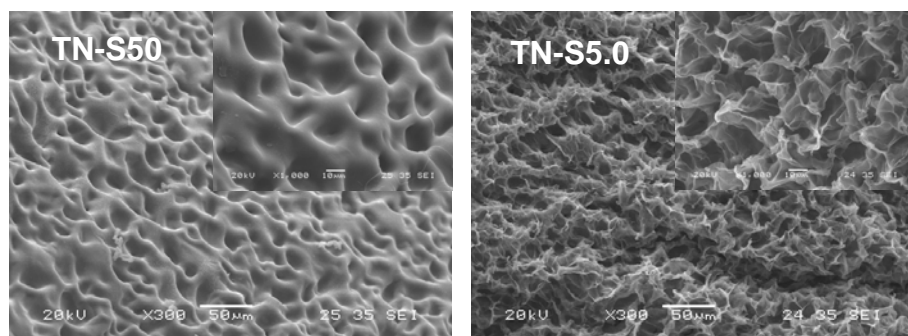


Figure 4.20. SEM images of TN-S50 and TN-S5.0 gels after freeze drying the equilibrated water-swollen gels. ($\times 300$)

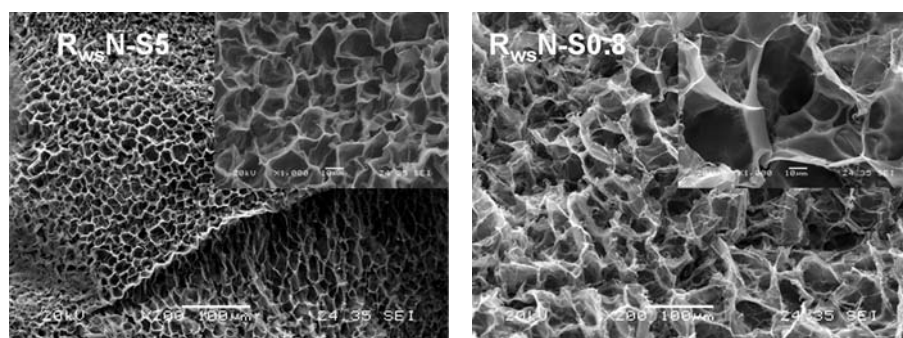


Figure 4.21. SEM images of $R_{ws}N-S5$ and $R_{ws}N-S0.8$ gels after freeze drying the equilibrated water-swollen gel. ($\times 200$)

$R_{ws}N-S0.8$ gels (figure 4.21.). In the $R_{ws}N-S5$ gel the pore sizes are small ($15\pm4\ \mu m$) but well oriented in space. But in case of lightly cross-linked gel, $R_{ws}N-S0.8$ the pore sizes are very big ($50\pm5\ \mu m$). In the swollen states these pore are filled with water. So it may be concluded that in $R_{ws}N-S$ gel, small networks density can uptake huge amount of solvent molecules.

4.3.9. Mechanical properties of polyelectrolyte gels

Irrespective to the cross-linker amount, TN-S gels have very poor tensile strength. They are brittle and fragile in nature. The gel can be ruptured easily by applying compression on it (Figure 4.22). In contrast, $R_{ws}N-S$ gels have very high mechanical strength. Figure 4.23. exhibits the physical observations of the mechanical strength of $R_{ws}N-S0.8$ gel. $R_{ws}N-S$ gels have very strong dependence of cross-linker amount on their mechanical strength. When a higher amount of MHPR is used for gelation, the gel becomes very hard and opaque and loses its tensile strength. On the other hand lightly cross-linked, $R_{ws}N-S0.8$ gels have very high tensile strength, high tolerance of compression and surprisingly have high resistance during cut by usual cutter (Figure 4.23.).

Figure 4.24. demonstrates strain controlled dynamic strain sweep test for freshly prepared TN-S5.0 and $R_{ws}N-S0.8$ gel in air. Both gels show appreciable tolerance of strain in the whole strain% region. To measure the strain controlled dynamic frequency sweep test for the gel samples, 3% strain was selected from the linear viscoelastic region of this curve and fixed as test set up during the measurements. Figure 4.25. represents strain controlled dynamic frequency sweep test for as prepared TN-S5.0 and $R_{ws}N-S0.8$ gel in air at room temperature. When frequencies are applied to the gels, the gel samples deform and the intercross-linking distance of the gel networks change; thereby, resulting in an increased inter polymeric

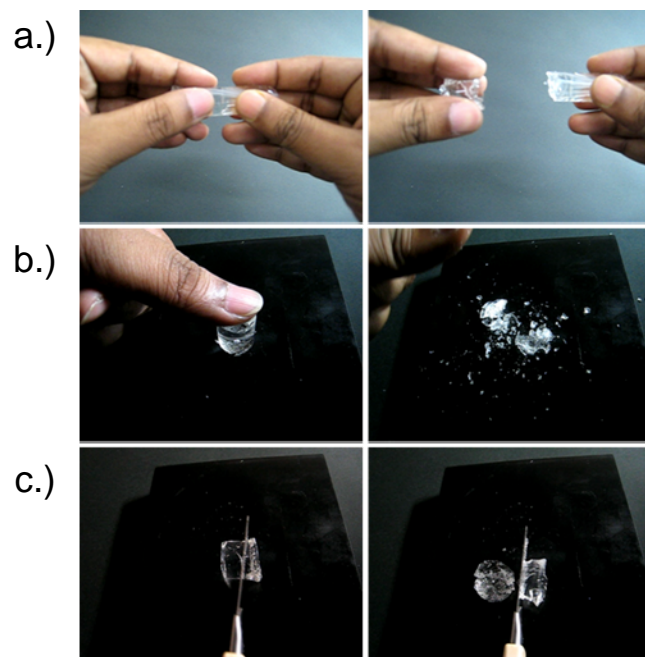


Figure 4.22. Physical observations of the mechanical strength test of TN-S33 gel a.) poor tensile deformation b.) very brittle in nature c.) easily cut able by usual cutter.

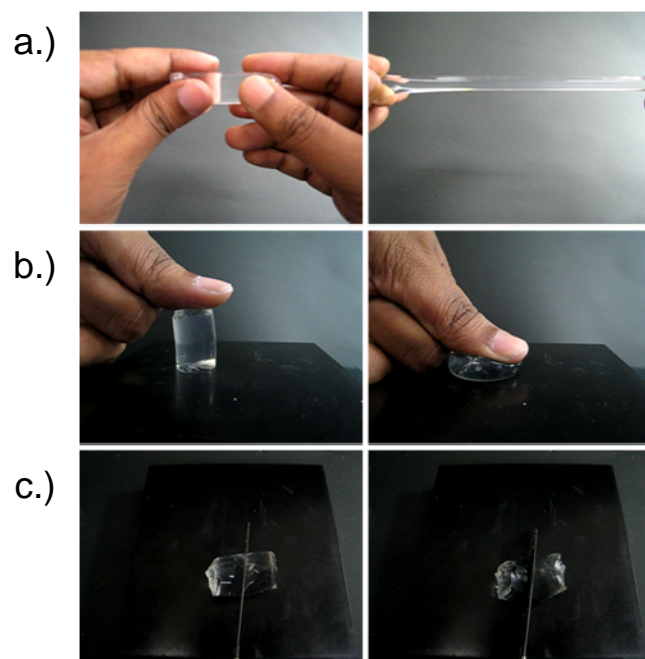


Figure 4.23. Physical observations of the mechanical strength test of $R_{ws}N-S0.8$ gel a.) high tensile strength b.) does not rupture under repeated compression c.) can not be cut by usual cutter.

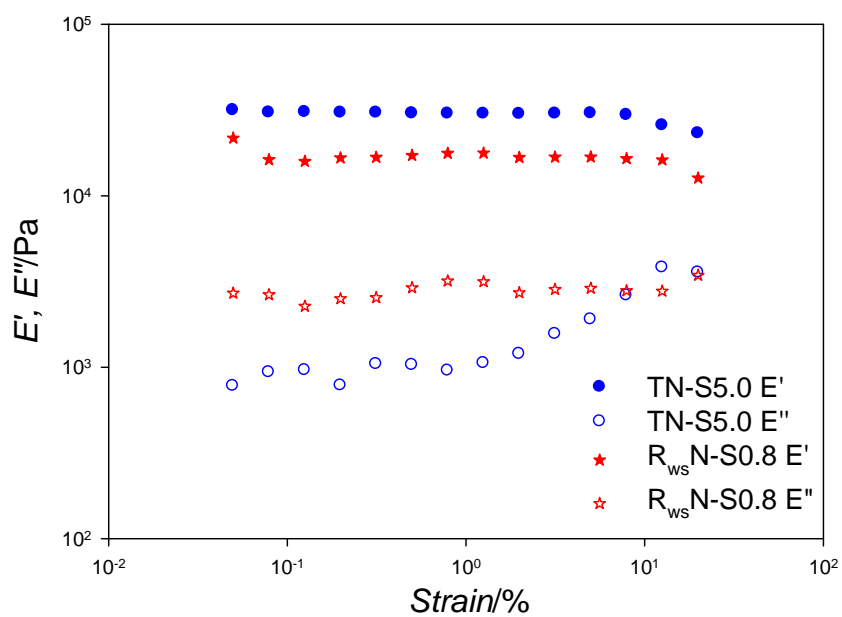


Figure 4.24. Strain controlled dynamic strain sweep test for as prepared TN-S5.0 and R_{ws} -N-S0.8 gel in air at room temperature.

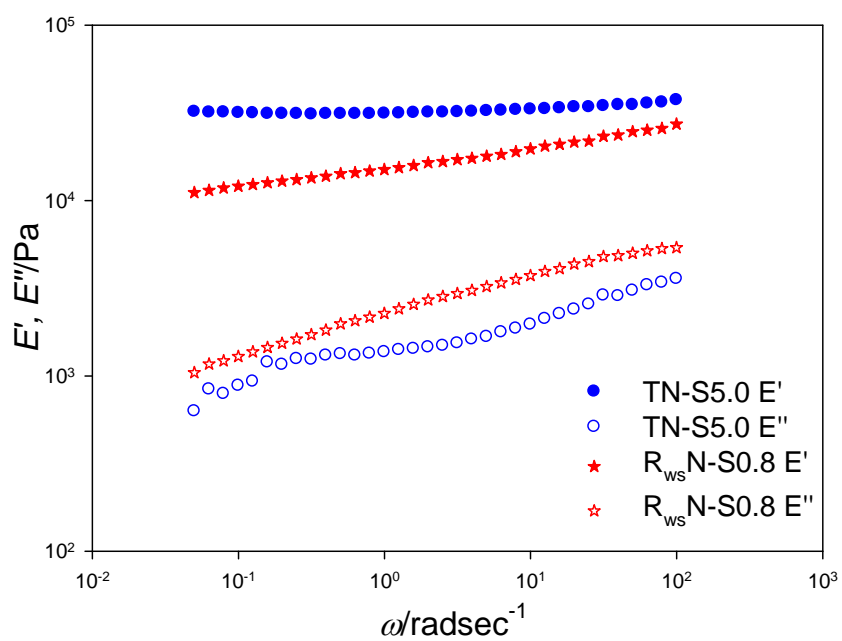


Figure 4.25. Strain controlled dynamic frequency sweep test for as prepared TN-S5.0 and R_{ws} -N-S0.8 gel in air at room temperature.

potential energy. The most of the energy gained from the frequency transforms for elastic deformation. But due to the presence of movable cross-links in the $R_{ws}N-S0.8$ gel, the gel networks try to equalize the experienced tension via the movements of the polymer chains. It is imagined that the sliding and rotating ability of the cross-links in the $R_{ws}N-S$ gels occur easily at low frequencies. At high frequencies, the polymer chains can not reorient or rearrange their networks through the movements of cross-links and as a result starts to respond elastically. Hence, $R_{ws}N-S0.8$ gel has low storage moduli, E' as well as loss moduli, E'' at low frequencies but with the increase in frequencies both moduli increases markedly. The frequency dependencies of E' and E'' for $R_{ws}N-S0.8$ gel is reproducible with replicate measurements implying that the viscoelastic damping at low frequencies does not correspond to the damage of the gel networks. In contrast, storage moduli for TN-S gels are independent of frequencies. In the TN-S gels, the fixed storage moduli originate from the elastic response of the fixed cross-linked polymer gel networks.

Physical gel exhibits J-shaped stress–strain curves with large hysteresis which is originated from the rearrangement of the irreversible and non-covalent cross-links of the gel networks under deformation. In contrast, chemical gel exhibits s-shaped stress-strain curves without any hysteresis. The fixed covalently bonded gel networks can not rearrange the cross-links under deformation and thereby no hysteresis is found in the stress-strain curve. It has been reported that slide-ring gel shows a J-shaped stress-strain curve without any hysteresis loop.¹⁶ The results were qualitatively explained with free junction model where no elastic instability was observed.

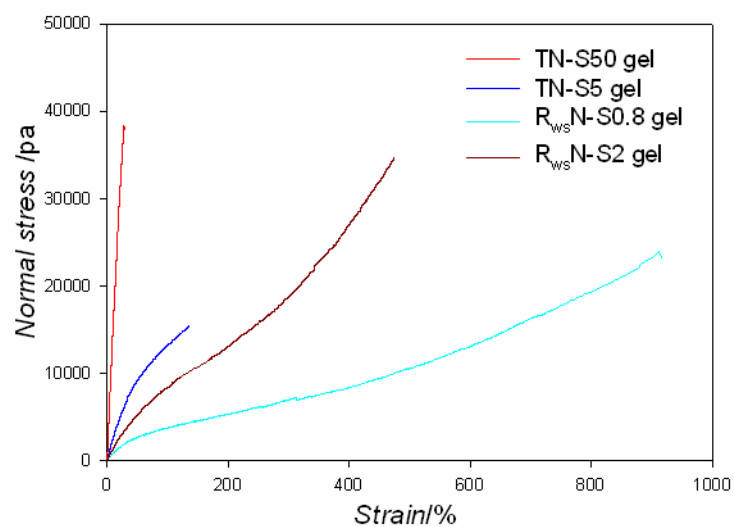


Figure 4.26 Stress-strain curve of the TN-S and R_{ws}N-S gels.

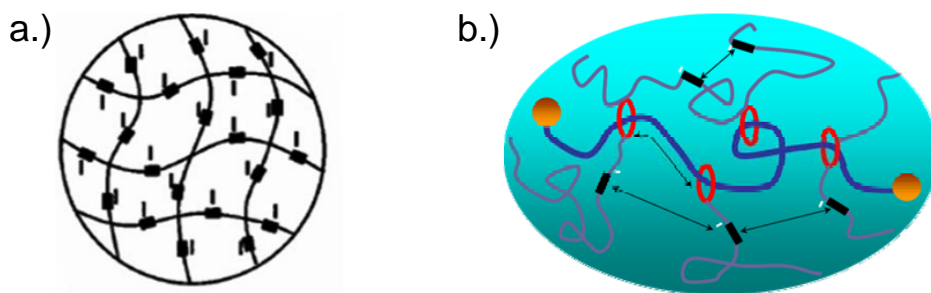


Figure 4.27. Proposed mechanism for the electrostatic repulsion of the ionic groups inside the a.) TN-S gel and b.) R_{ws}N-S gel. Ionic interaction is limited for TN-S gels while ionic interactions in the R_{ws}N-S gel networks must increase the dispersity of the macrocycles along with polymer chains and thereby exhibits super absorbency and higher mechanical strength.

Figure 4.26. shows the stress-strain curve of the TN-S and $R_{ws}N-S$ gels prepared by varying amounts of cross-linker. TN-S gel shows s-shaped stress-strain curves as reported earlier for the conventional chemical gel. In the micro-level, TN-S gel networks are formed by the fixed covalent bond between cross-linkers and polymer chains. Under deformation the fixed cross-links can not avoid the localization of the experienced stress and soon loses its mechanical integrity. This micro level behavior is also reflected in the stress-strain curve of macroscopic TN-S gel. Irrespective to the cross-linker amount, TN-S gel exhibits very low tensile strength and maximum elongation at break ca. 130% strain was found for TN-S5.0 gel.

But in the $R_{ws}N-S0.8$ gel a quite different stress-strain curve was observed than the conventional physical gel and chemical gel.¹⁷ Initially $R_{ws}N-S0.8$ gel responds like a chemical gel then it responds like physical gel. We believe that the presence of movable cross-links in the micro structure of $R_{ws}N-S$ gel is responsible for this type of anomalous stress-strain curve. $R_{ws}N-S0.8$ gel has a tensile strength of nearly 24 kPa and elongation at break is approximately 900%. The average elongations at break of the $R_{ws}N-S0.8$ gel were varied from ca. 700 to 1200% strain. But with increasing cross-linker amounts the tensile strength of the $R_{ws}N-S$ gel decrease accordingly. Interestingly the tensile strength of the gel is higher than the slide-ring gel¹⁷ and almost similar to the nanocomposite gel.¹⁸

4.4. Scopes and future prospects of $R_{ws}N-S$ gel

It has been reported that the conventional ionic co-polymer gels of NIPA-MAPTAC(methacrylamide propyl trimethylammonium chloride) and NIPA-SS (styrene sodium sulfonate) show no volume phase transition.¹⁹ Introduction of strongly dissociated styrene sodium sulfonate into the poly(NIPA) gel transforms the discontinuous volume change into a continuous one. So, polyrotaxane based ionic

gels using MAPTAC and SS will be synthesized and characterized to have some interesting properties.

2-Acrylamido-2-methylpropane sulfonic acid, AMPS has thermal and hydrolytic stability. It contains a spacer which allows the charged group to have high mobility in the cross-linked polymer chains of gel networks. The sulfonic acid part of the AMPS group is strongly acidic in nature. It can dissociate its proton easily. NIPA-AMPS copolymer gel will be fabricated using hydrophilic polyrotaxane as a cross-linker.

Instead of acidic and basic media, swelling and shrinking behaviors of $R_{ws}N-S$ or above mentioned gels will be observed in the ionic surfactants like sodium dodecyl sulphate, SDS and in inorganic salt solutions. It has been reported that non-ionic poly(NIPA) gels exhibit super absorbent property in SDS even in the presence of salt by the formation of micelles structures.²⁰ At low concentration, SDS acts like a simple salt. That is, it has an ability to break hydrophobic hydration around the NIPA chains of the poly(NIPA) gel, thus leading to a decrease in the transition temperature. On the other hand, in the case of higher SDS concentrations, DS^- ions are bound to the polymer chains, thereby increasing ionic interactions and increasing the osmotic pressure of the gel due to counter ions. And a rise in the transition temperature of the gel has been reported.²¹ In NaCl solution; the donnan osmotic pressure of the gel networks decreases and enhances the shrinkage of the gel by increasing the dehydration of the NIPA chains. The effect of SDS or NaCl salt in the $R_{ws}N-S$ gel may bring intriguing informations to the swelling and volume phase transition temperature. Hence, their effect on polyrotaxane based ionic gel will be investigated in details.

4.5. Conclusion

Polyrotaxane based ionic gels could be used as an alternate of bio-materials like tissues, muscle, blood vessel, skin etc. The super absorbent characteristic of the gel has potential for the application of consumer products for example cosmetics, diaper, sanitary napkin etc.

References

1. Gels Handbook, *vol. 1* (Eds.: Y. Osada, K. Kajiwara), Academic press, San Diego, USA, **2000**.
2. Hirokawa, Y.; Tanaka, T. *J. Chem. Phys.* **1984**, *81*, 6379.
3. Dusek, K.; Patterson, D. *J. Polym. Sci., Polym. Phys. Ed.* **1963**, *6*, 1209.
4. Tanaka, T.; Fillmore, D. J.; Sun, S. T.; Nishio, I.; Swislow, G.; Shah, A. *Phys. Rev. Lett.* **1980**, *45*, 1636.
5. a. Hirotsu, S.; Hirokawa, Y.; Tanaka, T. *J. Chem. Phys.* **1987**, *87*, 1392. b. Hirotsu, S. *Ferroelectrics* **1997**, *203*, 375. c. Kawasaki, H.; Sasaki, S.; Maeda, H. *J. Phys. Chem. B* **1997**, *101*, 4184. d. Hirotsu, S. *Macromolecules* **1992**, *25*, 4445. e. Bai, G.; Suzuki, A. *J. Chem. Phys.* **1999**, *111*, 10338. f. Kawasaki, H.; Sasaki, S.; Maeda, H. *J. Phys. Chem. B* **1997**, *101*, 5089.
6. Imran, A. B.; Seki, T.; Kataoka, T.; Kidowaki, M.; Ito, K.; and Takeoka, Y. *chem. Commun.*, **2008**, *41*, 5227-5229.
7. Okumura, Y.; Ito, K. *Adv. Mater.* **2001**, *13*, 485-487.
8. chapter 1
9. chapter 2
10. Taylor, L. D.; Cerankowski, L. D. *J. Polym. Sci.* **1975**, *13*, 2551.
11. a. Inomata, H.; Goto, S.; Otake, K.; Saito, S. *Langumir* **1992**, *8*, 687. b. Suzuki, A. *Adv. Polym. Sci.* **1993**, *110*, 199.
12. a. Inomata, H.; Goto, S.; Otake, K.; and Saito, S. *Langmuir* **1992**, *8*, 687-690. b. S. Sasaki and H. Maeda, *Phys. Rev.* **1996**, *E 54*, 2761. c. S. Sasaki, H. Kawasaki, and H. Maeda, *Macromolecules*. **1997**, *30*, 1847. d. M. Annaka, K. Motokawa, S. Sasaki, T. Nakahira, H. Kawasaki, H. Maeda, Y. Amo, and Y. Tominaga, *J. Chem. Phys.* **2000**, *113*, 5980.

13. a. T. Head-Gordon, J.M. Sorenson, A. Pertsemlidis, and R.M. Glaeser, *Biophys. J.* **1997**, 73, 2106. b. S. Sasaki, H. Kawasaki, and H. Maeda, *Macromolecules*. **1997**, 30, 1847.
14. Bai, G.; and Suzuki, A.; *Eur. Phys. J. E* **2004**, 14, 107-113.
15. Kawasaki, H.; Sasaki, S.; Maeda, H. *J. Phys. Chem. B*, **1997**, 101, 5089-5093.
16. Okumura, Y.; Ito, K. *Nippon Gomu Kyokaishi*. **2003**, 76, 31.
17. Ito, K. *Polym. J.* **2007**, 39, 489–499.
18. Haraguchi, K. and Li, H-J. *Angew. Chem. Int. Ed.* **2005**, 44, 6500 –6504.
19. a. Beltran, S.; Hooper, H. H.; Blanch, H. W. Prausnitz, J. M. *J. Chem. Phys.* **1990**, 92, 2061. b. Kawasaki, H.; Sasaki, S.; Maeda, H. *J. Phys. Chem B*. **1997**, 101, 4184 c. Kawasaki, H.; Sasaki, S.; Maeda, H. *J. Phys. Chem. B* **1997**, 101, 5090
20. Zhang, Y. Q.; Tanaka, T.; Shibayama, M. *Nature* **1992**, 360, 142-144.
21. a. Eloassaf, J. *J. Appl. Polym. Sci.* **1978**, 22, 873. b. Schild, H. G.; Tirrel, D. A. *Langmuir*. **1990**, 6, 1676. c. Inomata, H.; Goto, S.; Saito, S. *Langmuir*. **1992**, 8, 1030-1031

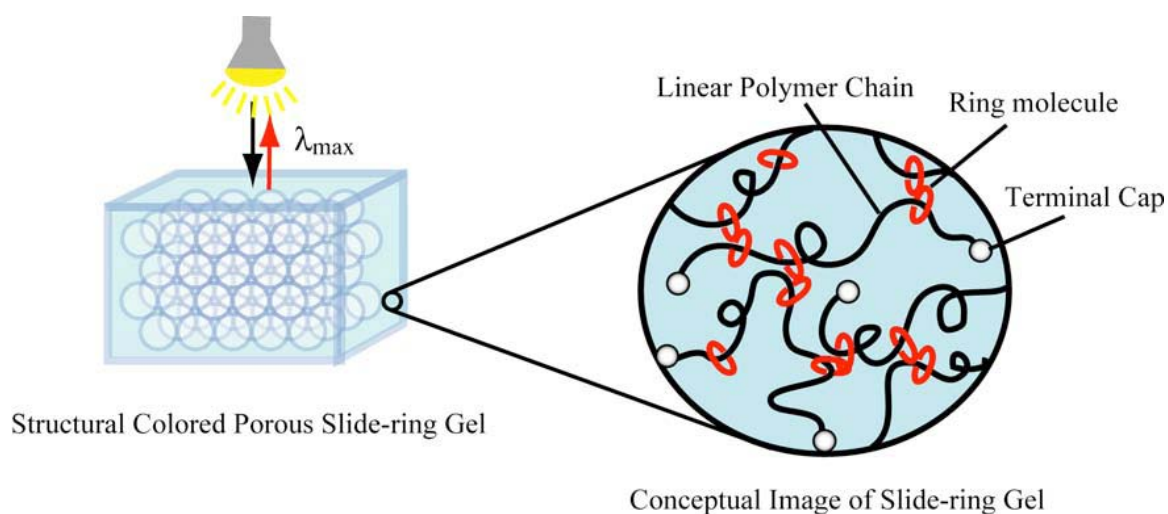
CHAPTER

5

Appendix: Chromic Slide-Ring Gel Based on Reflection from Photonic Bandgap

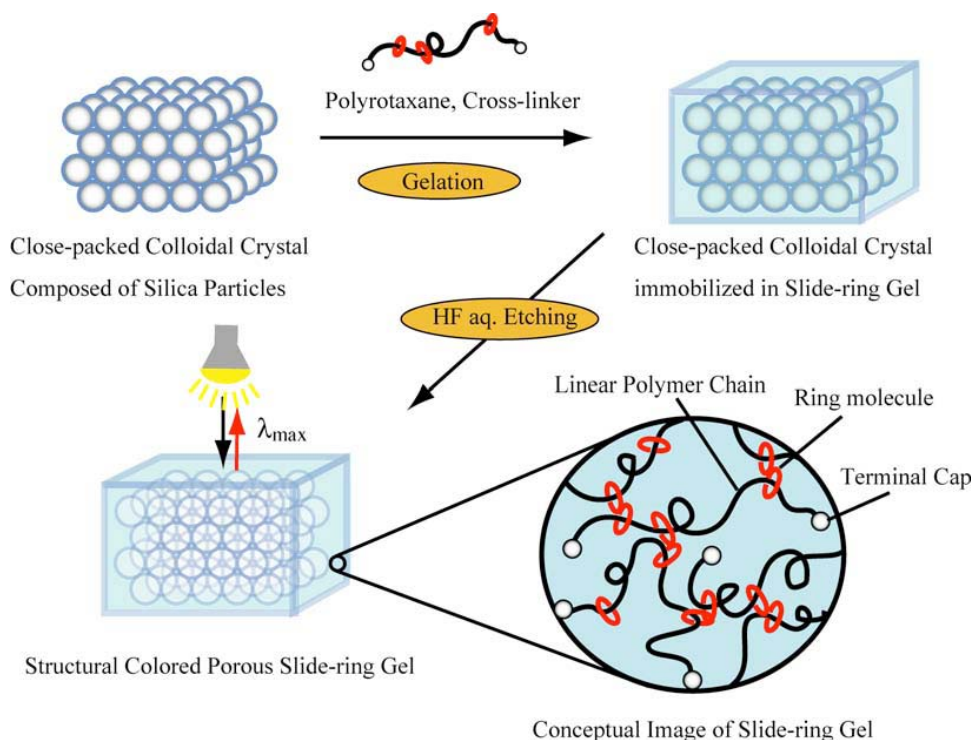
Abstract

Here chromic slide-ring gel consisting of polyrotaxane by using a close-packed colloidal crystal as a template has been reported. In the slide-ring gel, the polymer chains with bulky end groups are not covalently cross-linked like chemical gels nor do they interact attractively like physical gels, but are topologically interlocked by figure-of-eight cross-links. The slide-ring gel has freely movable cross-links, which have a pulley effect on tensile deformation. This effect improves the mechanical properties of polymer gels. In this work, this physically and mechanically optimized polymer gel was used to make stimuli-responsive photonic band gap materials. The gel exhibits solvatochromic behavior based on the change in structural color.

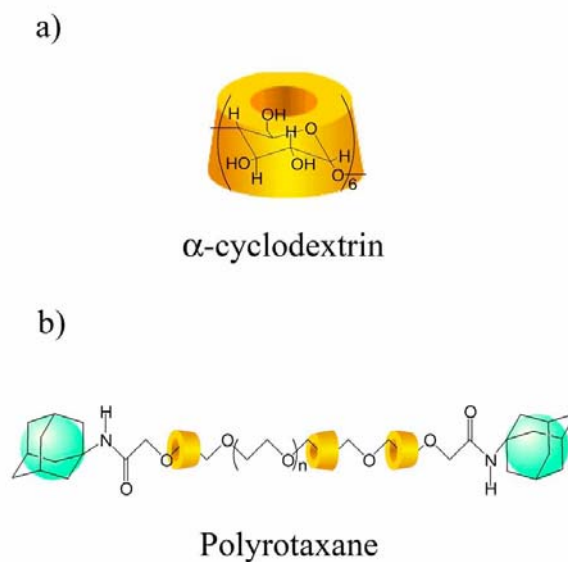


5.1. Introduction

Photonic band gap materials are the subject of intense research interest because of their potential use as sensors to detect chemical and biological species, active photonic crystals to control light propagation in response to various external perturbations, and dynamic optical switches for displays and smart windows.^{1,2} It is becoming increasingly clear that novel approaches to these applications demand smart soft materials with high-performance stimuli-responsivity. Polymer gels have the remarkable ability to respond to stimuli in a large variety of ways.³ Moreover, it is apparent that polymer gels have the distinction of being able to memorize or immobilize submicrometer- sized periodical fine structures in the network and hold the potential to be used as photonic band gap materials.⁴ Indeed, there have been a number of reports on the preparation of periodical structured polymer gels exhibiting a photonic band gap using templating techniques and self-organizing methods.⁴⁻¹⁴ As a result, research on active photonic band gap materials composed of polymer gels has recently increased, and this is attracting attention in a variety of fields. However, because traditional synthesis of polymer gels relies upon a free radical chain reaction between monomers and cross-linkers, these polymer gels have permanent and fixed spatial inhomogeneities¹⁵ and topological constraint on the subchains.¹⁶ This results in low deformability, low swellability, and low mechanical strength of the polymer gels, and these properties can be drawbacks for use in stimuli-responsive materials. For example, the polymer chains in the chemical cross-linked polymer gels will be cleaved gradually with repetitive alteration in the volume, due to the unequal stress exerted on the polymer chains.¹⁷ For this reason, it would be highly desirable to develop active photonic band gap materials for the above applications by



Scheme 5.1. Schematic procedure of the preparation of a porous slide-ring gel using a close-packed colloidal crystal as a template.



Scheme 5.2. Chemical structures of α -cyclodextrin (α -CD) and a polyrotaxane composed of α -CDs as ring molecules and a polyethyleneglycol as an axle linear polymer chain.

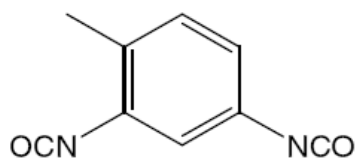
using physically and mechanically optimized polymer gels. Various approaches to avoiding these problems are currently under trial. One of them is based on a nanocomposite hydrogel composed of water-soluble polymer and water-swelling inorganic clay.¹⁸ This gel can deform to a large extent without any damage under bending, compression, torsion, and elongation. This mechanically improved property is attributed to the organic/ inorganic network structure in which exfoliated clay platelets act as multifunctional cross-linking units. Another hydrogel system is based on interpenetrating polymer networks that exhibit amazingly strong and tough mechanical behavior.¹⁹ The hydrogel cannot be sliced with a cutter nor broken down by a high compression. However, these hydrogels are inappropriate for making the intended polymer gels that show a photonic band gap, because the preparative conditions for obtaining structural colored porous gels are unfavorable. In devising a new strategy to address this issue, our attention was drawn to the utilization of “slide-ring gels” for making stimuli-responsive photonic band gap materials. Slide-ring gels can be prepared using polyrotaxane molecules consisting of terminal capped linear polymer chains that are threaded through ringlike molecules.²⁰⁻²² The network structure of the slide-ring gels can be obtained by the cross-linking reaction among the ringlike molecules on different polyrotaxane molecules. As the ringlike molecules can rotate and slide along the polymer chains, the length of the polymer chains in the network will be averaged, and the tension of the polymer chains can be equalized. This effect leads to improvement in the drawbacks that are observed in the traditional chemical cross-linked polymer gels. The application of the slide-ring gels for the fabrication of stimuli responsive photonic band gap materials could drive innovation in this field.

In this paper a new stimuli-responsive photonic band gap materials that is made of appropriate slide ring gels using a close-packed colloidal crystal as a template (Scheme 5.1.) has been described.

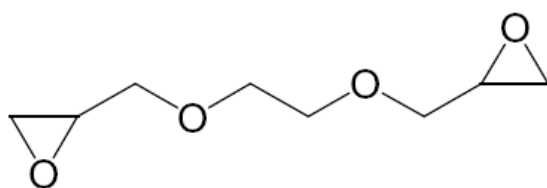
5.2. Experimental Section

5.2.1. Materials

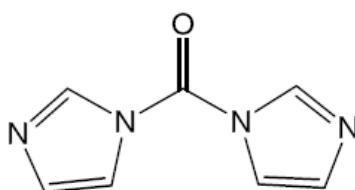
An aqueous suspension of sub-micrometer-sized silica particles (silica particles with a narrow particle size distribution, dispersed in water, Nippon Shokubai) was obtained and used to prepare close-packed colloidal crystals. The mean diameter of the particles used in this study was 300 nm. α -Cyclodextrin (α -CD), which was used for the ringlike molecule (Scheme 5.2.a.), was purchased from Nihon Shokuhin Kako Co. Ltd. (α -CD content >99%). Poly(ethylene glycol) 35000 (PEG 35000), having a hydroxyl content of 7.00×10^{-5} mol/g, corresponding to a number average molecular weight of 28600 (determined by titration of phthalic anhydride bound to OH groups), was purchased from Fluka. This macromolecule is used as an axis molecule for preparing a polyrotaxane. The free base form of 1-adamantanamine as a terminal cap was from ICN Biomedicals, Inc. The polyrotaxane, composed of a single chain of the PEG molecule, about 90-100 α -CDs (28% coverage of the PEG chain), and two terminal adamantane moieties (Scheme 5.2.b.), was synthesized. The detailed preparation of the polyrotaxane has previously been reported.^{23,24} A polyrotaxane that was essentially similar to the one we prepared in this study was also supplied by Advanced Softmaterials, Inc. (Tokyo, Japan) and was used to prepare slide-ring gels. 1,1'-Carbonyldiimidazole was purchased from Nacalai Tesque, Inc. (Kyoto, Japan). Ethylene glycol diglycidyl ether, cyanuric chloride, tolylene 2,4-diisocyanate, dibutyltin dilaurate, and anhydrous dimethyl



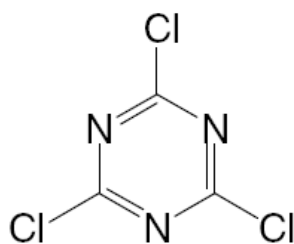
2,4-Toluene diisocyanate



ethylene glycol diglycidyl ether

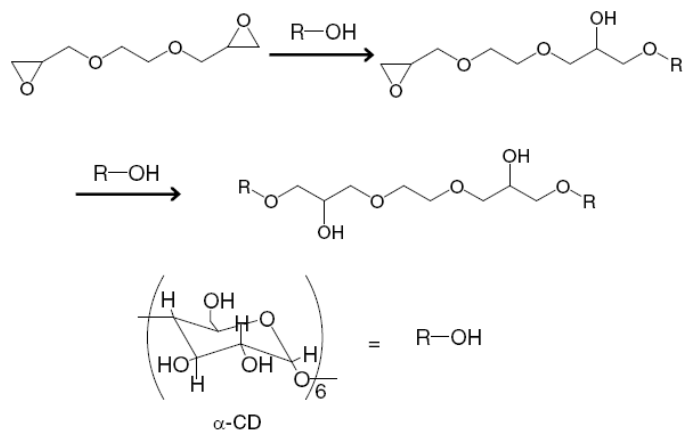


1,1'-carbonyldiimidazole

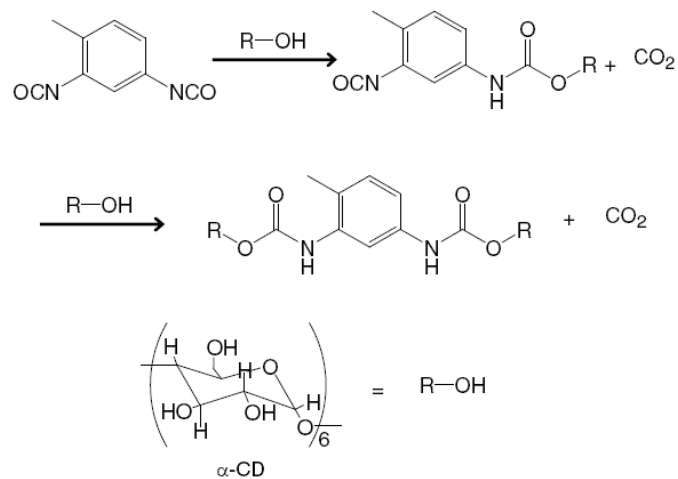


Cyanuric chloride

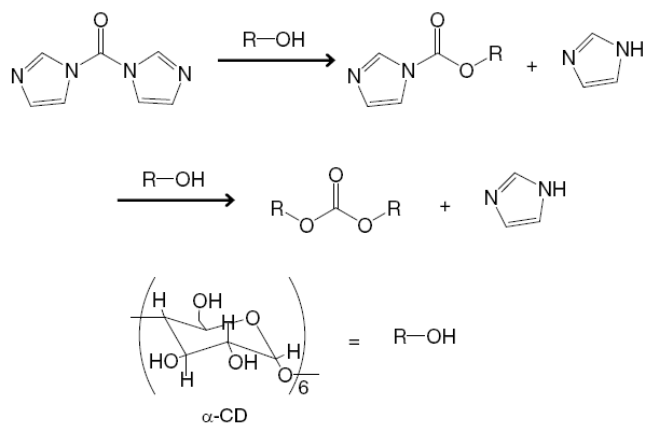
Chemical structures of cross-linkers



Schematic illustration of cross-linking reaction of ethylene glycol diglycidyl ether and $\alpha\text{-CD}$



Schematic illustration of cross-linking reaction between 1,4-bis(isocyanato)benzene and $\alpha\text{-CD}$



Schematic illustration of cross-linking reaction of 1,1'-carbonyldiimidazol and $\alpha\text{-CD}$

sulfoxide (DMSO) were obtained from Sigma-Aldrich Co. and used as received. *N*-Isopropylacrylamide (NIPA, Kohjin Co.) was purified by recrystallization from toluene/*n*-hexane. *N,N'*-Methylenebis(acrylamide) (BIS, Acros Organics) and α,α' -azoisobutyronitrile (AIBN, Kanto Chemical Co.) were reagent grade and used as received unless otherwise noted. Other chemicals were purchased from Wako Pure Chemical Industries, Ltd., and used without further purification. Milli-Q deionized water (Millipore) was used for all experiments. For the preparation of the close-packed colloidal crystals, the surface of a slide glass (76 mm \times 26 mm, Matsunami glass) was cleaned by ultrasonic treatment in a concentrated KOH ethanol solution. The slide glass was removed from the solution and was thoroughly rinsed with clean ethanol and Milli-Q deionized water.

5.2.2. Preparation of a Colloidal Crystal

A thick colloidal crystal was prepared by a solvent evaporation method using the silica colloidal suspension that was relatively concentrated compared with those used in earlier methods.^{25,26} The suspension of 20 wt % of the silica component was spread out on the surface-cleaned slide glass, which was placed in a thermostatic chamber at 90 °C. The water was gradually evaporated over 6 h. High-quality colloidal crystal was obtained with a thickness of about 0.5 mm. The evaluation of this thick colloidal crystal has previously been reported.¹⁴

5.2.3. Preparation of Gels

We examined the following chemicals as cross-linkers, having multiple reactive groups with hydroxyl groups of α -CD, to obtain the slide-ring gels under suitable conditions: ethylene glycol diglycidyl ether, tolylene 2,4-diisocyanate, cyanuric chloride, and 1,1'-carbonyldiimidazol. The polyrotaxane (25 mg) and an arbitrary amount of each

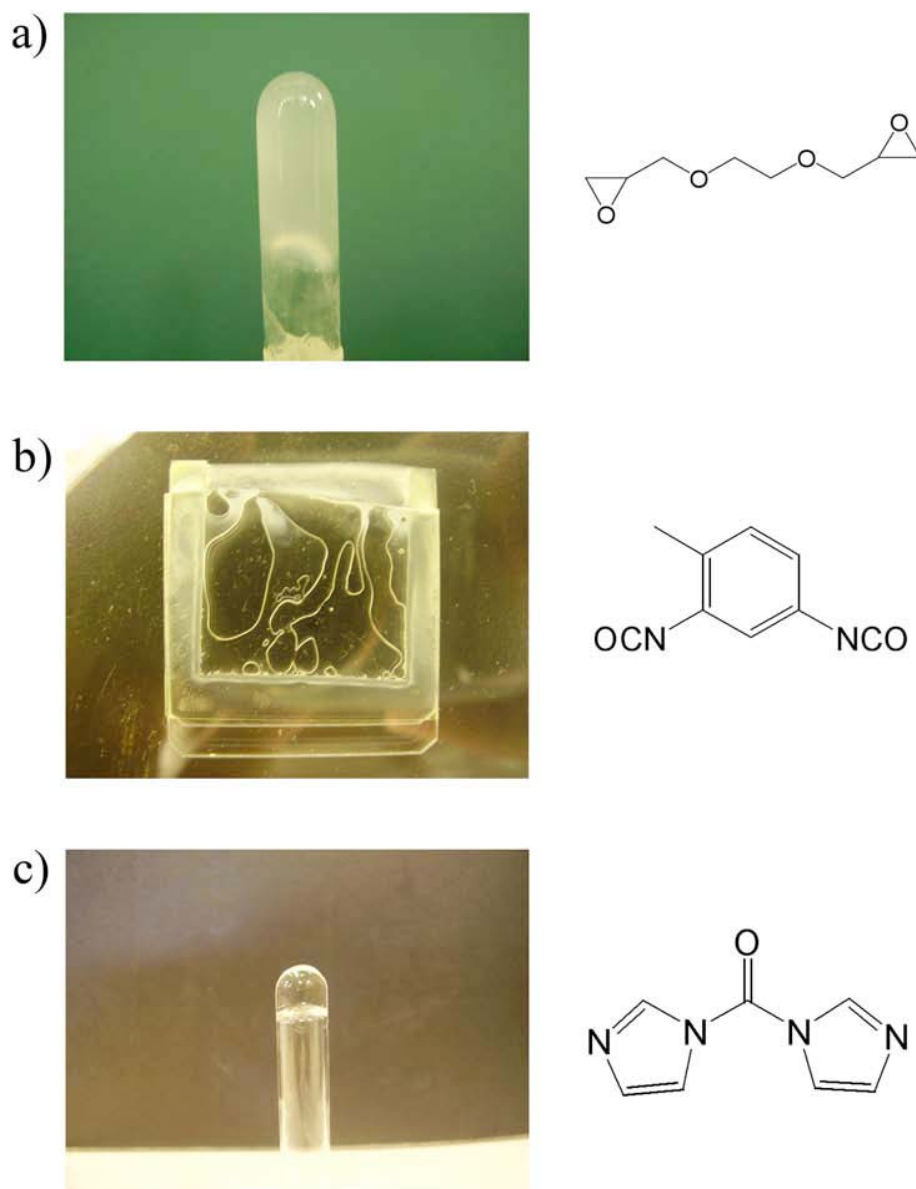


Figure 5.1. Photographs of slide-ring gels prepared by different cross-linkers. a) A squashy and opaque gel was prepared by using ethylene glycol diglycidyl ether as a cross-linker; b) A clear gel could be obtained by using tolylene 2,4-diisocyanate as a cross-linker, but bubble formation was observed; c) A clear gel was synthesized by using 1,1'-carbonyldiimidazol as a cross-linker.

candidate cross-linking agent were dissolved in 0.3 ml of anhydrous DMSO. In designing a controlled swelling degree of the gel, the amount of cross-linker was changed while that of the polyrotaxane was fixed. When tolylene 2,4- diisocyanate was used as a cross-linking agent, a slight amount of dibutyltin dilaurate was added as a catalyst in the reaction solution. The viscosities of all the pregel solutions were of the right consistency to be infiltrated into a close-packed colloidal crystal. To check the physical appearance of the gels obtained, the slab gels or rodlike gels were obtained in a flat cell composed of two glass plates and a Teflon spacer or a glass tube, respectively. To examine the swelling behaviors of the gels, tiny cylindrical-shaped gels were prepared in glass micropipettes with an internal diameter of 270 μm . The pregel solutions in these cells were polymerized at various temperatures for 24 to 120 h. The gels obtained were washed with DMSO to remove unreacted chemicals. The pregel solutions that turn into gels under the appropriate conditions for making structural colored porous gels were infiltrated into the interstitial regions of the colloidal crystal in a Petri dish, and the polymerizations were conducted under suitable conditions. Afterward, the resulting gels with involvement of the silica component were immersed in a 10 wt % HF aqueous solution for 1 week to remove the silica component. The porous gels obtained were washed carefully with a large amount of distilled water and DMSO to remove HF and other impurities. We confirmed that the polymer networks were chemically stable during the etching procedure by ^1H -NMR and by checking the degree of swelling of the gels. When the silica component is etched away, the remaining structures are porous gels consisting of a close-packed array of solvent spheres. Because of the direct templating of the close-packed colloidal crystal, the porous gels maintain the high crystalline quality of the colloidal crystal and exhibit structural color attributed to a photonic band. A series

of poly(NIPA) gel was prepared by free radical polymerization in which the concentration of NIPA monomer was kept constant at 2 M and that of the cross-linker, BIS, was varied from 20 to 100 mM. The NIPA, BIS, and 8.125 mM AIBN (initiator) were dissolved in anhydrous DMSO, and N₂ bubbling was passed through the pregel solution for 30 min. The pre gel solution infused to glass slides separated by Teflon spacers for the preparation of slab gels. Cylindrical gels were prepared using a micro-capillary tube with an inner diameter of 270 μ m. The gelation was carried out at 60 °C for 24 h. To remove the unreacted monomer and reaction residues, the gels were thoroughly washed with DMSO for 2 weeks.

5.2.4. Sample Characterizations

Photographs of the colloidal crystal and the gels were taken using a digital microscope (KEYENCE VH-8000).

The sphere size of the silica particle and the extent of ordering in the colloidal crystal were determined using a JEOL JSM-5600 scanning electron microscope (SEM) operating at 20 kV. The conductive coating on the surface of the colloidal crystal was applied by Au prior to the SEM observation.

The reflection spectra of the colloidal crystal and the porous gels were obtained using an Ocean Optics USB2000 fiber optic spectrometer. All spectra were monitored at normal incidence to the plane of the samples.

The swelling measurements of gels were carried out by monitoring the diameter of the cylindrical gels in a glass cell. The temperature in the cell was controlled by using a circulating water temperature control system. The cylindrical gels were cut into small pieces and put into various solvents. The equilibration time for swelling and shrinking depends on the solvent composition. The equilibrated swelling degree of each gel was measured under the various conditions. The kinetics

of the swelling of gels when the solvent composition was changed were observed as follows. A cylindrical gel immersed in water was dropped into another glass cell filled with a large amount of DMSO. This time-point was taken to be zero, and the change in the diameter of the cylindrical gel was observed with time.

The refractive index of the bulk gels and solvents was measured using a digital refractometer (ATAGO RX- 7000R).

The viscoelastic properties of the gels were measured with a Rheometric solids analyzer (RSA III of Rheometric Scientific, Inc.) equipped with one normal force transducer (1kFRT) that can detect normal forces up to 35 N (3500 g) and a motor having a frequency range from 6.28×10^{-6} to 502 rad s⁻¹, an amplitude range of ± 1.5 mm, response time <5 ms to 90% of the final value, and strain resolution of 0.00005 mm. For the purpose of measurement, (10 mm \times 10 mm) gel samples were cut after the gels reached equilibrium at room temperature, where the gels were 4 mm thick in the preparative state. Only the bulk-type slide-ring gels and the NIPA gels were used for this measurement, because structural colored porous gels cannot be obtained at that size. The swelling and deswelling of gels were maintained throughout the experiments by immersing the gels in the solvent used. To ensure that the sample was always under compression, 5% pre-strain was applied to the samples during the experiments. The data of storage (E') and loss (E'') moduli and $\tan \delta$ were analyzed in the frequency range of 0.05 to 50 rad/s with a 3% strain amplitude. The strain-controlled dynamic frequency sweep test was used as a test setup, and the selected 3% strain was in the region of the linear viscoelastic region of the sample. The temperatures in the sample chamber were controlled by an air oven equipped with an N₂ cooling unit.

5.3. Results and Discussion

5.3.1. Preparation of Slide-Ring Gels

Several requirements must be met when using a colloidal crystal to prepare polymer gels having a photonic band gap. First, pregel solutions must be infiltrated into the interstitial regions of the colloidal crystal without structural collapse of the crystal. The pregel solutions revealing extreme viscosity and low wettability upon the surface of the colloidal crystal are not adequate for preparing the polymer gels. Second, it is vital that the crystal structure remains stable during the gelation. A chemical reaction under an appropriate condition is preferred, such that the colloidal crystal can maintain its original structure. Finally, it is imperative that the polymer network is chemically stable for the etching liquids used. Cleavage of chemical bonds and hydrolysis of functional groups will affect the swelling behavior and mechanical properties of the polymer gel. In this work, the polyrotaxane comprised of a long chain PEG as an axis molecule and α -CD as a ringlike molecule was selected as the main structural component for the slide-ring gel. The presence of hydroxyl groups on α -CD allows for not only the formation of cross-linkage but also the incorporation of various functional groups to the polyrotaxane, leading to chemical tailoring of stimuli responsive gels. We examined the following four chemicals as cross-linkers to obtain the slide-ring gels: ethylene glycol diglycidyl ether, tolylene 2,4-diisocyanate, cyanuric chloride; and 1,1'-carbonyldiimidazol. In terms of the results, however, we could not identify the appropriate conditions for preparing structural colored porous gels except when using 1,1'-carbonyldiimidazol. Only squashy and opaque gels could be obtained when ethylene glycol diglycidyl ether was used as a cross-linker (Figure 5.1.a.). The opacity of the gels interferes with the structural color from the porous gels. Clear gels could be prepared by the reaction between tolylene 2,4-diisocyanate and

the polyrotaxane, but bubble formation was observed (Figure 5.1.b.). As the emergence of the bubble from the pregel solution in the colloidal crystal may cause destruction of the crystal structure, the reaction solution is an undesirable candidate for preparing the porous gels. The addition of cyanuric chloride into DMSO solution containing the polyrotaxane results in a risk of bumping and bubble formation,²⁰ the use of cyanuric chloride was rejected as unsuitable for the preparation of the slide-ring gel. In contrast, we could prepare a clear and homogeneous gel using 1,1'-carbonyldiimidazol under appropriate conditions for making the porous gels (Figure 5.1.c.).

5.3.2. *Properties of Slide-Ring Gels. Rheometric Analysis*

Dynamic mechanical analysis provides information on the gel strength expressed as viscosity or elasticity. For the ease of comparing the mechanical spectra between the slide-ring gels and chemically cross-linked poly(NIPA) gels, we used the slide ring gel obtained using 1,1'-carbonyldiimidazol and NIPA gel, which exhibit similar swelling ratios in DMSO. Figure 5.2.a. represents the frequency dependencies of E' and E'' in the strain controlled dynamic frequency sweep test of the NIPA gel and the slide-ring gel, respectively, in DMSO. For the NIPA gel, E' is considerably higher than E'' and both moduli do not depend on the test frequency, in the range between 0.05 and 50 rad/s. This result indicates that this NIPA gel represents typical characteristics of well-developed polymer networks. NIPA gels inherently have a large inhomogeneous structure due to the irregular distribution of the cross-links in the gel network. The cross-links fix the polymer chain and the gel cannot adjust its cross-link distribution or polymer length in the network structure under deformation. As a result, all of the stress is localized to short polymer chains, and gel networks cannot spread out the experienced tension. For this reason, the gel can only elastically

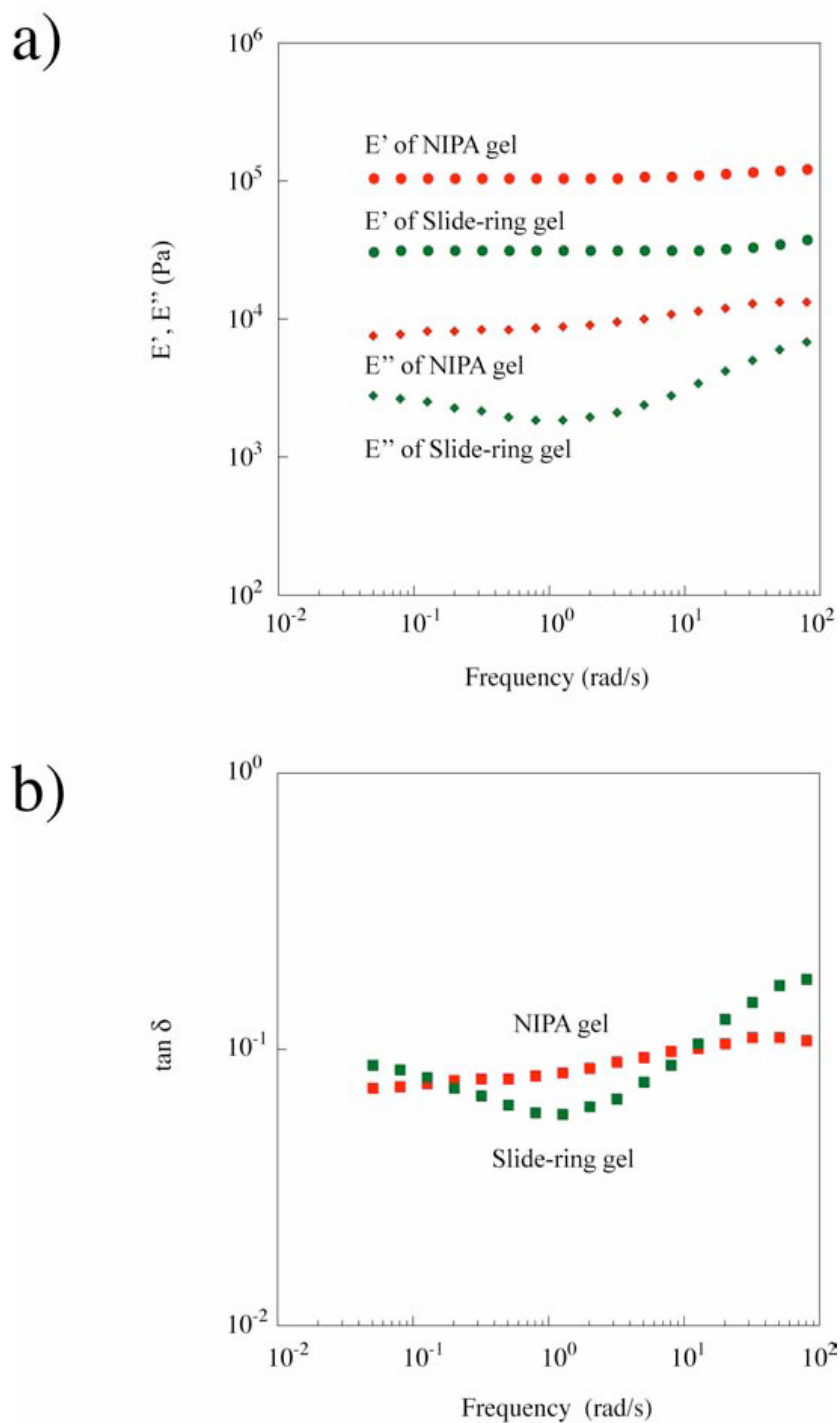


Figure 5.2. Dynamic frequency sweep test for a slide-ring gel and a chemical gel (NIPA gel). a) Frequency dependence of storage moduli and loss moduli of NIPA gel and the slide-ring gel by using 1,1'-carbonyldiimidazol as a cross-linker, in DMSO at 25° C. b) Frequency dependence of $\tan \delta$ of NIPA gel and the slide-ring gel by using 1,1'-carbonyldiimidazol as a cross-linker, in DMSO at 25 °C.

respond to the mechanical spectra and gives higher modulus values under applied frequency. The slide-ring gel obtained by using 1,1'-carbonyldiimidazol as a cross-linker displays high tensibility and softness. The values of both E' and E'' for the slide-ring gel are considerably smaller than those for the NIPA gel. This finding indicates that this slide-ring gel is softer than the NIPA gel. Figure 5.2.b. depicts the change of $\tan\delta$ ($\tan\delta = E''/E'$) values in the strain controlled dynamic frequency sweep test for the NIPA gel and the slide-ring gel in DMSO. Judging from the values of $\tan\delta \approx 0.1$, these gels are considered to exhibit elastic behavior. For the NIPA gel, the loss angle δ gradually decreases with decreases in frequency. On the other hand, the slide-ring gel shows a distinctive alteration of the loss tangent result due to the change in E'' in the frequency range. The relaxation of the sliding cross-links points occurs with ease at low frequencies but after some extent it again starts to increase. The excellent reproducibility of the results of the viscoelastic measurements of the slide-ring gel indicates that differences in the viscoelastic behavior from high to low frequencies do not correspond to damage of the gel networks. This viscoelastic behavior implies that the slide-ring gel is more liquid-like than the NIPA gel.²⁷ The softness must result from the inherent pulley effect of the slide-ring gel network. Additionally, as the two-dimensional small-angle neutron scattering patterns for uniaxially stretched slide-ring gel showed a normal butterfly pattern,²¹ we are convinced that the slide-ring gel is more liquid-like and that there exists a pulley effect in the gel. Thus, the use of this slide ring gel to prepare structural colored gel will be highly mechanically advantageous over chemically cross-linked poly- (NIPA) gel.

5.3.3. Equilibrium Swelling Degree of Slide-Ring Gel

In DMSO, the swelling ratios of the gels decreased with the increase in the amount of cross-linker, but these gels did not exhibit a dependence of volume on temperature from 20 °C to 45 °C (Figure 5.3.a.). D and D_0 are the diameters of the cylindrical gels in equilibrium states under certain conditions and in the reference state, respectively. Therefore, D/D_0 is defined as the equilibrium swelling degree of the gels. In this study, we used D_0 as the inner diameter of the glass micropipette used for the gel preparation. The volumes of these gels were found to be influenced by the solvent composition. Figure 5.3.b. shows the degrees of swelling of the gels plotted as a function of DMSO concentration in DMSO/water mixtures. The gels immersed in the mixtures of DMSO composition above 75% were swollen compared to the preparative states, but the swelling ratio gradually decreased with the increase in water content. At above a 40% H₂O composition, there was a reentrant phenomenon as the H₂O composition changed; the gel shrank and then swelled slightly again as the water kept being added. This reentrant phenomenon was observed in several gels and was considered to reflect the strong attractive interaction between water and the DMSO molecules that exclude the polymers.

5.3.4. Kinetics of Swelling Degree of Slide-Ring Gel

The kinetics of the swelling of the gels were observed with the abrupt environmental change. The swelling of the gel started immediately after the gel was taken from water and immersed in DMSO at room temperature. A typical time course of the swelling change is plotted in Figure 5.4. The gel exhibited rapid swelling at an early stage, followed by gradual shrinkage. This phenomenon is known to be a characteristic behavior of slidering gels.^{29, 30} We can interpret this phenomenon in the following ways. The change in the solvent compositions from water to DMSO expands the

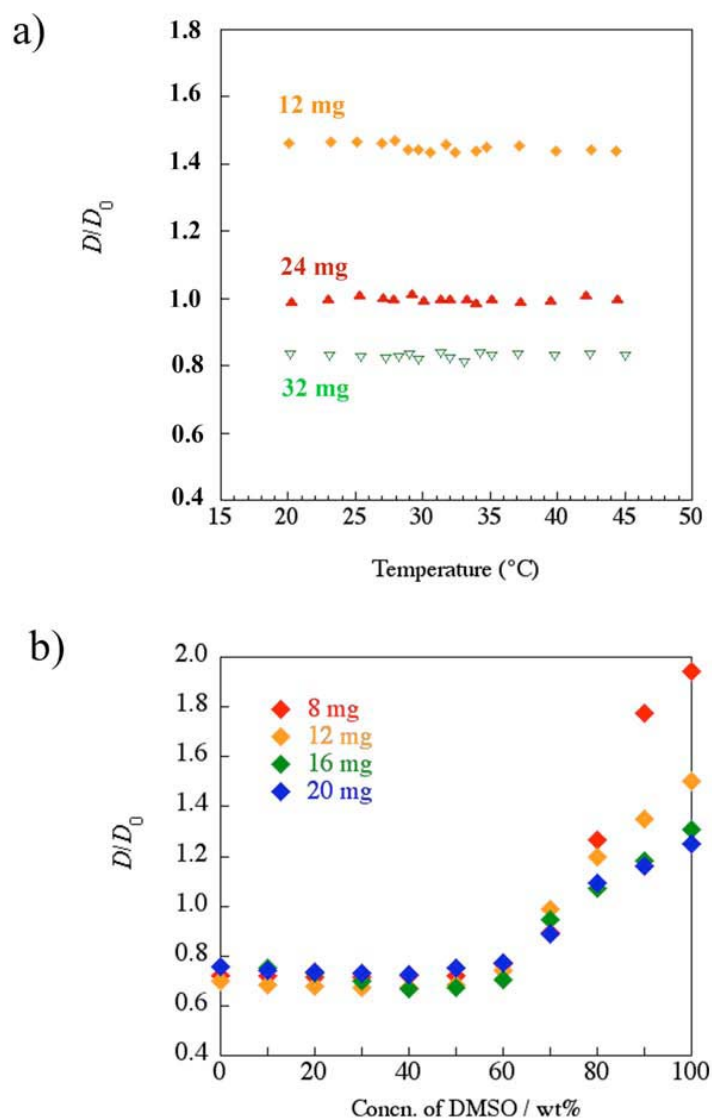


Figure 5.3. Degree of swelling of slide-ring gels prepared with different amounts of 1,1'-carbonyldiimidazole; a) in DMSO at several temperatures, and b) in DMSO aqueous solutions of various compositions at 25 ° C.

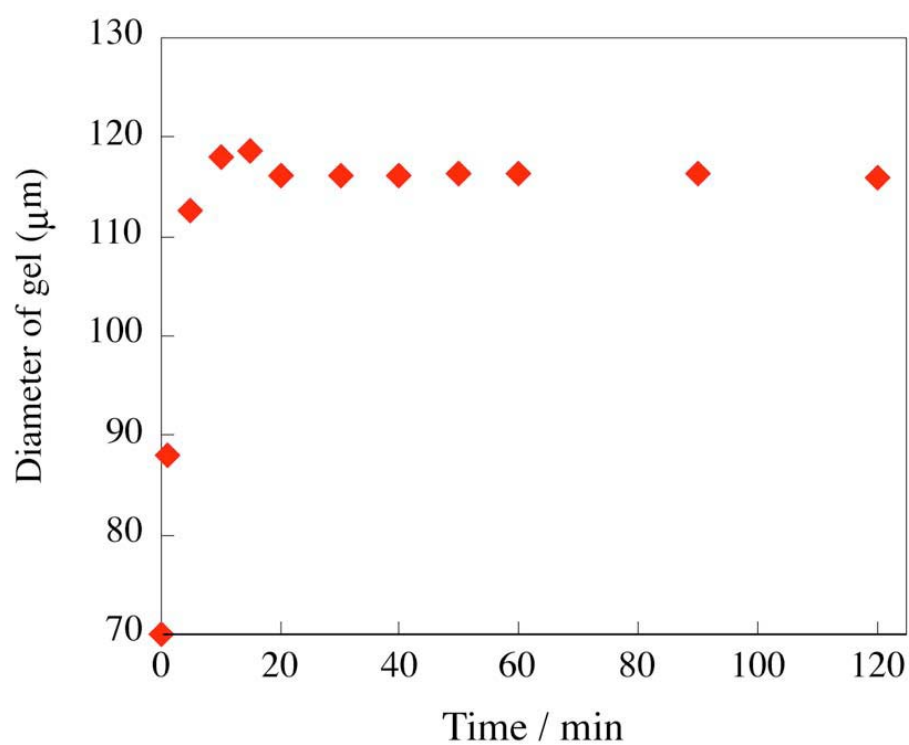


Figure 5.4. Typical time course of the diameter increase of the cylindrical slide-ring gel (this gel was prepared with 12 mg of 1,1'-carbonyldiimidazol) in response to a sudden change in solvent is plotted as a function of time at 25 ° C.

polymer network due to an attractive interaction between DMSO molecules and PEG chains. α -CD molecules then begin to aggregate,³¹ causing the repositioning of R-CD in the gel and slight gel shrinkage. This particular dynamic behavior of the swelling and shrinking processes seems to be closely related to the pulley effect.

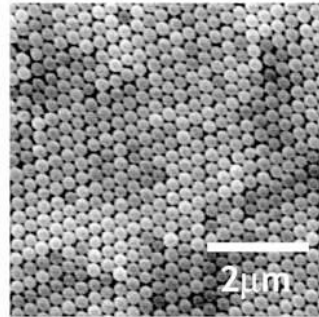
5.3.5. Properties of Colloidal Crystal

An SEM image of the surface of the colloidal crystal composed of 300 nm silica particles is shown in Figure 5.5.a. The silica spheres are organized into a close-packed arrangement with a long-range order in the lateral direction. This colloidal crystal exhibits monochromatic color caused by an interferential effect (Figure 5.5.b.). The appearance of the sample was observed when it was illuminated with white light at an angle normal to the planar surface of the crystal. The visual appearance of the crystal is a testament to the high crystalline quality. The reflection spectrum for the crystal is shown in Figure 5.5.c. The intensity maximum of the photonic-band λ_{max} of the crystal is located at 593 nm. We have reported that a face-centered cubic fcc structure is the most energetically stable, and this colloidal crystal is oriented with its (111) axis parallel to the glass substrate.¹⁴ Thus, the peak shown represents the selective reflection of a narrow band of wavelengths due to Bragg diffraction from the fcc (111) crystal. It follows that the silica spheres are organized into a close packed arrangement with a long-range order in both the lateral and normal directions in this crystal.

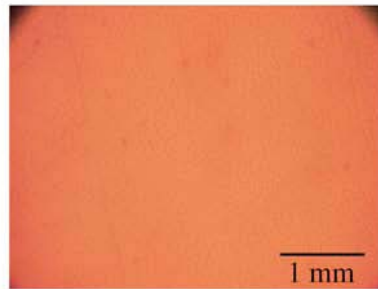
5.3.6. Properties of Structural Colored Slide-Ring Gel

Figure 5.6.a. shows a photograph of a rectangular piece of the structural colored porous gel. The porous gel, obtained by the close-packed colloidal crystal as a template, also exhibits brilliant structural color. Figure 5.6.b. shows the reflection spectra of the porous gel in a DMSO/water mixed solvent with different compositions.

a)



b)



c)

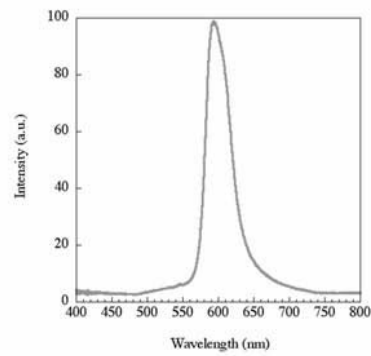


Figure 5.5. SEM image, optical microscope image, and reflection spectrum of a close-packed silica colloidal crystal composed of 300 nm-diameter silica particles.

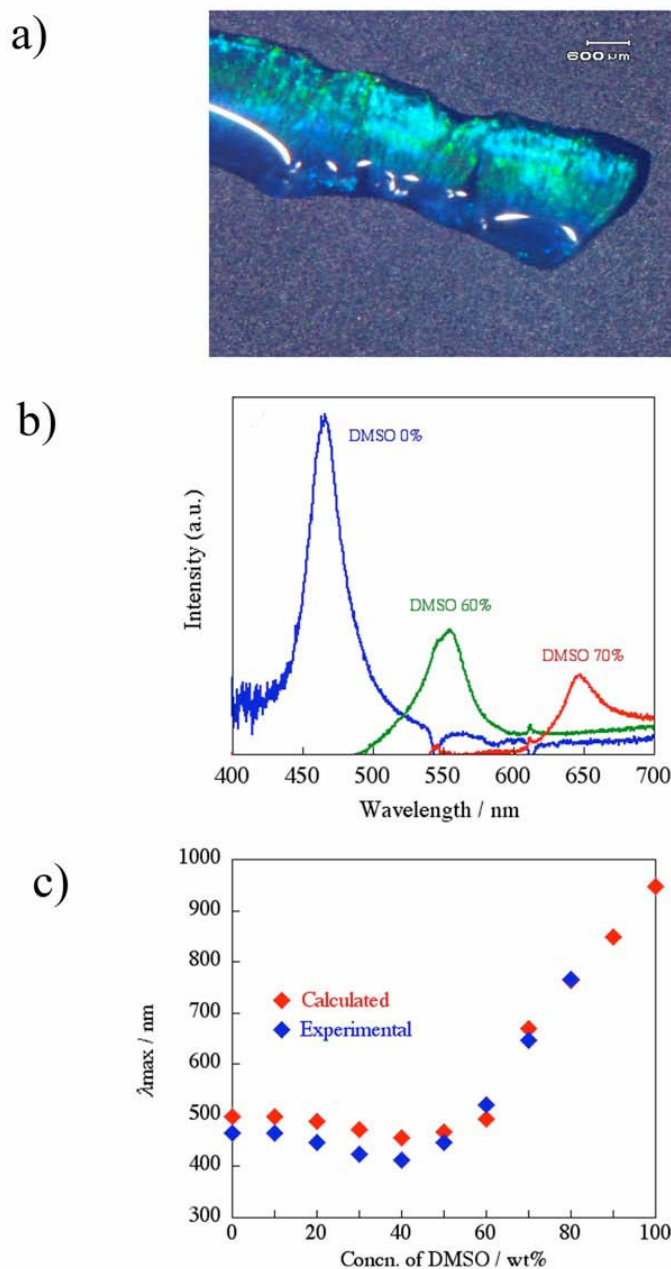


Figure 5.6. a) Photograph of a porous slide-ring gel swollen with water; b) Solvent composition dependence of reflection spectra for the porous slide-ring gel made by using colloidal crystals composed of silica particles with radii of 300 nm, at 25° C; c) Change in the position of λ_{max} of the reflection spectrum for the porous slide-ring gel with varying solvent compositions.

As the water composition was increased, the reflected peak wavelength shifted toward the shorter wavelength until the water composition reached 60%, but the peak position returned to the slightly higher wavelength when the water composition rose above 60% (Figure 5.6.c.). If the porous gel maintains the fine structure of the precursor colloidal crystal and the volume change is isotropic, the peak wavelength (λ_{\max}) can be estimated by the following eq,^{12,14}

$$\lambda_{\max} = 1.633 \{d(D/D_0)/m\} n_a \quad (1)$$

where d is the diameter of the silica spheres, and m is the order of the Bragg reflection. The value of n_a is calculated as a weighted sum of the refractive indices of the sphere portion and the gap portion:

$$n_a^2 = \sum n_i^2 \phi_i \quad (2)$$

Here ϕ_i is the volume fraction of each i portion. For the close packed structure, the ϕ values of the sphere portion and the intersphere portion are 0.74 and 0.26, respectively. It follows that this shift is due to a decrease in the lattice spacing of the crystal ($d(D/D_0)$) and/or to a change in the value of n_a . Thus, both the change in the lattice spacing and the value of n_a of the porous gel have to be considered to calculate the theoretical value of λ_{\max} when the solvent composition is varied. The refractive indices of the DMSO-water mixed solvents and the slide-ring gel in these mixed solvents are plotted as a function of the solvent compositions (Figure 5.7.). Both refractive indices increase almost linearly with the DMSO content. The solvent composition dependence of n_a of the porous slide-ring gel can be calculated by eq 2, assuming that the volume fraction of the gel portion is constant during the volume change. As shown in Figure 5.7., the change in n_a also increased linearly with the DMSO content. The amount of change in n_a for the porous gel was about 0.13 when the solvent composition was changed, while the change in the value of D/D_0 was

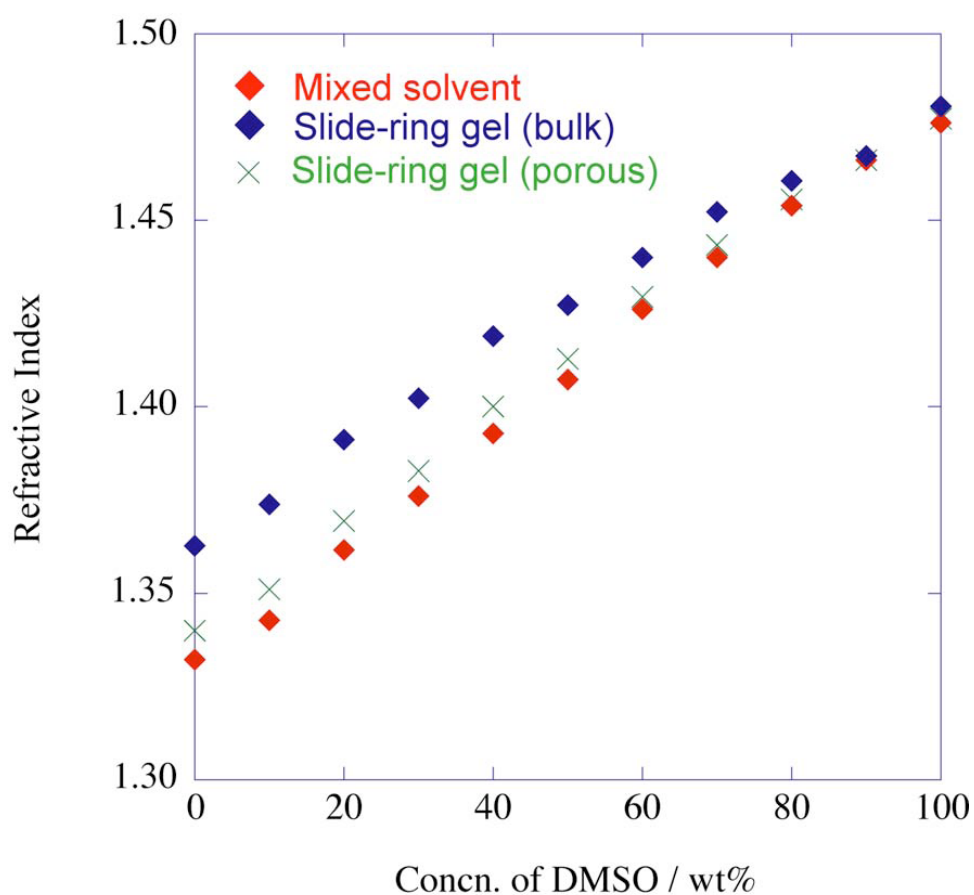


Figure 5.7. Refractive indices of DMSO-water mixed solvents, a bulk slide-ring gel, and a porous slide-ring gel in these solvents are plotted as a function of solvent composition.

almost a dozen times that of n_a . Therefore, the swelling ratio is dominant over λ_{\max} of the observed reflection spectrum for the porous gel. The positions of the peak wavelength, estimated by eq 1 using the experimentally obtained values of d , D/D_0 , and n_a , coincide with the spectroscopically determined values of λ_{\max} (Figure 5.6.c). This result provides evidence that the gel effectively templates against the colloidal crystal and preserves this imprinted fine structure even with the changes in volume and in the location of the crosslink- points.

5.4. Conclusion

In addition, as the structure of the polymer network can be modified by the incorporation of various functional groups, this system can shed light on the development of stimuli-responsive photonic band gap materials for use in future optical devices. Work is underway to promote such worthwhile applications of the gels.

References

- (1) *Photonic Crystals*; Busch, K., Löfkes, S., Wehrspohn, R. B., Föll, H., Eds.; Wiley-VCH: New York, **2004**.
- (2) *Nanochemistry-A Chemical Approach to Nanomaterials*; Ozin, G., Arsenault, A., Eds.; RSC Publishing: Cambridge, U.K., **2005**.
- (3) *Gels Handbook*; Kajiwara, K., Osada, Y., Eds.; Academic Press: San Diego, CA, **2000**.
- (4) Takeoka, Y.; Watanabe, M. *Langmuir* **2002**, *18*, 5977.
- (5) Liu, L.; Li, P.; Asher, A. *Nature (London)* **1998**, *397*, 141.
- (6) Lee, Y.-J.; Braun, P. V. *AdV. Mater.* **2003**, *15*, 563.
- (7) Fudouzi, H.; Xia, Y. N. *AdV. Mater.* **2003**, *15*, 892.
- (8) Arsenault, A. C.; Miguez, H.; Kitaev, V.; Ozin, G. A.; Manners, I. *AdV. Mater.* **2003**, *15*, 503.
- (9) Yoshinaga, K.; Fujiwara, K.; Mouri, E.; Ishii, M.; Nakamura, H. *Langmuir* **2005**, *21*, 4471.
- (10) Xia, J.; Ying, Y.; Foulger, S. H. *AdV. Mater.* **2005**, *17*, 2463.
- (11) Barry, R. A.; Wiltzius, P. *Langmuir* **2006**, *22*, 1369.
- (12) Takeoka, Y.; Watanabe, M. *Langmuir* **2003**, *19*, 9104.
- (13) Saito, H.; Takeoka, Y.; Watanabe, M. *Chem. Commun.* **2003**, 2126.
- (14) Takeoka, Y.; Seki, T. *Langmuir* **2006**, *22*, 10223.
- (15) Shibayama, M. *Macromol. Chem. Phys.* **1998**, *199*, 1.
- (16) Grossberg, A. Y.; Nechaev, S. K. N. *Macromolecules* **1991**, *24*, 2789.
- (17) Sato-Matsuo, E.; Tanaka, T. *Nature (London)* **1992**, *358*, 482.
- (18) Haraguchi, K.; Takehisa, T. *AdV. Mater.* **2002**, *14*, 1120.
- (19) Gong, J. P.; Katsuyama, Y.; Kurokawa, T.; Osada, Y. *AdV. Mater.* **2003**, *15*, 1155.

- (20) Okumura, Y.; Ito, K. *Adv. Mater.* **2001**, *13*, 485.
- (21) Karino, T.; Shibayama, M.; Ito, K. *Physica B* **2006**, 385-386, 692.
- (22) Oku, T.; Furusho, Y.; Takata, T. *Angew. Chem. Int. Ed. Engl.* **2004**, *43*, 966.
- (23) Araki, J.; Zhao, C.; Ito, K. *Macromolecules* **2005**, *38*, 7524.
- (24) Li, J.; Harada, A.; Kamachi, M. *Polym. J.* **1993**, *26*, 1019.
- (25) Jiang, P.; Bertone, J. F.; Hwang, K. S.; Colvin, V. L. *Chem. Mater.* **1999**, *11*, 2132.
- (26) Wong, S.; Kitaev, V.; Ozin, G. A. *J. Am. Chem. Soc.* **2003**, *125*, 15589.
- (27) Zhao, Y.; Cao, Y.; Yang, Y.; Wu, C. *Macromolecules* **2003**, *36*, 855.
- (28) Katayama, S.; Hirokawa, Y.; Tanaka, T.; *Macromolecules* **1984**, *17*, 2641.
- (29) Ito, K. *Proceedings of the International Symposium on Forefront of Nonlinear Science and Its Application to Material Science in the 21st Century*; Kyoto, Japan, **2005**, p 28.
- (30) Sakai, T.; Murayama, H.; Nagano, S.; Takeoka, Y.; Kidowaki, M.; Ito, K.; Seki, T. *Adv. Mater.* **2007**, *19*, 2023.
- (31) Karino, T.; Okumura, Y.; Ito, K.; Shibayama, M. *Macromolecules* **2004**, *37*, 6177.

CHAPTER

6

General conclusions and outlook

In this study, a facile and universal approach to introduce slide ring phenomena for varieties of polymer gels was presented to obtain highly mechanically stable and fast stimuli responsive polymer gels. Polyrotaxane is a supramolecule consists of a larger number of macrocycles. The macrocycles of the polyrotaxane can slide and rotate through the long polymer axle and the bulky end groups of the polyrotaxane prevent the dethreading of macrocycles. The study is focused on the use of polyrotaxanes as cross-linkers to prepare stimuli sensitive sliding polymer gels. A sparsely dispersed polyrotaxanes (PR), consisting of α -cyclodextrin or derivatives-rotors, which are threaded onto a long poly (ethylene glycol) axle (MW=35000) with an inclusion ratio of about 29% and are trapped by capping with bulky end groups 1-adamantanamine, was used as building blocks to make polyrotaxane cross-linkers. The hydroxyl groups of α -CDs were modified by isocyanate monomer, 2-Acryloyloxyethyl isocyanate through the formation of a stable carbamate bond to obtain the polyrotaxane-based hydrophobic and hydrophilic type cross-linkers, MPR and MHPR respectively.

Polymer gels are fabricated by using the MPR, with different modification ratios, as cross-linkers and thermo sensitive *N*-isopropylacrylamide (NIPA) as a monomer, which yielded transparent, very soft, flexible and mechanically improved rotaxane-NIPA gels, $R_{wi}N$ gels. The $R_{wi}N$ gels were found to have much smaller storage modulus, E' and loss modulus, E'' values at the whole frequency ranges. This indicates the soft nature of the $R_{wi}N$ gel networks. When the frequency is applied to the gel, the poly(NIPA) chains inside the gel network squeezes enough; but due to the sliding and rotating ability of the MPRs in the $R_{wi}N$ gel, the poly(NIPA) chains can gradually equalize its tension. In water, the gel exhibits sharp volume phase transition around the lower critical solution temperature (LCST) of poly(NIPA) chains. After a

temperature jump beyond the LCST, the cross-linked poly(NIPA) chains of typical poly(NIPA),TN gel forms a phase separated insoluble globular structure and shrinking of the gel volume proceed by going through deep unstable spinodal decomposition region. On the other hand, the movability of the cross-links of the $R_{wi}N$ gel may help to aggregate polymer networks to reach a complete collapsed state after a temperature jump. The micro and macro level spatial inhomogeneities and local stresses inside the $R_{wi}N$ polymer gels networks can automatically be homogenized and relaxed by the movement of the mobile cross-links points. The $R_{wi}N$ gels shrink by the growth of nucleation without going through any unstable spinodal decomposition mechanism and bringing about very fast shrinking rate. Although the gel is reached to an equilibrium shrunken state very quickly and isotropically but the hydrophobic aggregation of the water insoluble MPR gives the gel permanent opacity in the collapsed state in water.

To overcome this problem a hydrophilic polyrotaxane cross-linker, MHPR was synthesized by using hydroxypropyl modified polyrotaxane as a starting material. The hydrophilicity of the cross-linker, MHPR gives the transparency of the rotaxane-NIPA gels, $R_{ws}N$ gels in the swollen state at low temperatures and even in the collapsed state at high temperature. Use of MHPR restricts the formation of aggregated globules inside the gel networks. Hence the poly(NIPA) chains inside the $R_{ws}N$ gel can move or rotate freely through the long polymer axle. The gel also exhibits isotropic and very fast shrinking kinetics. An unusual swelling behavior is observed for the $R_{ws}N$ gel i.e. the increased hydrophilicity of the gel network does not affect on its volume phase transition temperature. The volume phase transitions of both hydrophilic and hydrophobic polyrotaxane based hydrogels remain same, only the swelling ratio of $R_{ws}N$ gel increases at lower temperature. An increase in the amount of cross-linkers or

increase in temperature results in increases in both storage moduli and loss moduli in water as well as in DMSO i.e. the softness or hardness of the RN gel may, therefore, be well controlled.

Although the gels prepared by MPR and MHPR as a cross-linker bring significant improvements in mechanical stability but none of the gel does not show appreciable tensile strength under deformation. A small amount of ionic groups (Sodium acrylate) was introduced in the hydrophilic rotaxane-NIPA gel as a next step. In the $R_{ws}N-S$ gel networks, the electrostatic repulsion between the ionic groups must increase the dispersity of the polymer chains attached to α -CD through the long PEG chains. The elongation at break of the $R_{ws}N-S$ gel is very high ca. 900 to 1200% strain. Interestingly the tensile strength of the gel is higher than the slide-ring gel and almost similar to the nanocomposite gel. The gel exhibits super absorbent property, it can absorb approximately 60,000 wt% water to its dried state. To the best of our knowledge this is the highest water uptake ratio exhibited by any polymeric materials.

Photonic band gap materials are the great interest of research due to their potential use as chemical or biological sensor, dynamic optical switches for displays etc. Since the slide-ring gel is soft and possesses higher mechanical strengths, so the use of this gel to prepare structural color gel will be highly beneficial over chemically cross-linked poly(NIPA) gel. Typical PNIPA, TN gels have spatial inhomogeneities which results in low deformability, swellability and mechanical strength. The polymer chains in the TN gels will be destroyed gradually with repetitive change in the volume. Hence a new stimuli-responsive photonic band gap material that is made of slide-ring gels using a close-packed colloidal crystal as a template has been prepared. The gel exhibits solvatochromic behavior based on the change in structural color.

The phenomenon of sliding gels may successfully be exploited for the development materials for diverse applications for example smart sensor, actuator, DDS, tissue engineering, bio-medical applications and consumer products (diaper, sanitary napkin) etc.

List of Publications

1. Imran, A. B., Seki, T., Kataoka, T., Kidowaki, M., Ito, K., Takeoka, Y.
“Fabrication of Mechanically Improved Hydrogels Using A Movable Cross-linker Based on Vinyl Modified Polyrotaxane”
Chemical Communications, 2008, 41, 5227-5229
2. Murayama, H., Imran, A. B., Nagano, S., Seki, T., Kidowaki, M., Ito, K., Takeoka, Y.
“Chromic Slide-Ring Gel based on Reflection from Photonic Bandgap”
Macromolecules, **41**, 1808-1814, 2008.
3. Imran, A. B., Seki, T., Kataoka, T., Kidowaki, M., Ito, K., Takeoka, Y.
Preparation of soft and mechanically improved hydrogels using a vinyl modified polyrotaxane as a Cross-linker. (*in preparation*)
4. Imran, A. B., Takeoka, Y., Seki, T.
Anomalous shrinking and swelling behavior of poly(NIPA) gels prepared by hydrophilic polyrotaxane based movable cross-linkers. (*in preparation*)
5. Imran, A. B., Takeoka, Y., Seki, T.
Comparative and contrastive studies of poly(NIPA) gels prepared by hydrophobic and hydrophilic polyrotaxane based cross-linkers. (*in preparation*)
6. Imran, A. B., Seki, T., Kidowaki, M., Ito, K., Takeoka, Y.
Synthesis of super absorbent and highly elastic novel polyelectrolyte gel using polyrotaxane based cross-linker. (*in preparation*)
7. Mohammad Harun-Ur-Rashid, Abu Bin Imran, Takahiro Seki, Yukikazu Takeoka, Masahiko Ishii and Hiroshi Nakamura
Template Synthesis for Stimuli-Responsive Angle Independent Structural Colored Smart Materials. *Transactions of the MRS-J* (*in press*)

List of some attended conferences

1. The 17th Polymer gel symposium, The society of polymer science, Tokyo, Japan .
January 18 (2006)
2. The 29th annual conference of Bangladesh Chemical Society, Bangladesh
Chemical Congress 2006, University of Dhaka, Dhaka, Bangladesh. March 9-11,
(2007)
3. The 56th polymer conference, The society of polymer science, Kyoto, Japan.
May 29-31 (2007)
4. GelSympo 2007, Polymer Gels: Fundamentals and functional control, The
University of Tokyo, Tokyo, Japan. August 6-8 (2007)
5. Global COE in Chemistry, Annual symposium 2008, Nagoya University, Nagoya,
Japan. June 11 (2008)
6. MRS fall meeting 2008, Material Research Society, Boston, Massachusetts, USA.
December 1-5 (2008)
7. 5th Yoshimasa Hirata Memorial Lecture and The 1st G-COE International
Symposium on Elucidation and Design of Materials and Molecular Functions, the
Chemical society of japan, Nagoya university, Nagoya, Japan. January 13-14
(2009)
8. The 20th Polymer gel symposium, The society of polymer science, Tokyo, Japan .
January 14-15 (2009).